MODELS FOR PROTEIN ASSEMBLY IN THE PRION DISEASES

by

Jon H. Come

B. S. Chemistry, Penn State University

(1985)

Submitted to the Department of
Chemistry in Partial Fulfillment of the
Requirements for the Degree of

DOCTOR OF PHILOSOPHY

at the

Massachusetts Institute of Technology

May 1994

Signature of Author _____
Department of Chemistry
May 13, 1994

Certified by _____
Peter T. Lansbury, Jr.
Associate Professor of Chemistry
Thesis Supervisor

Accepted by _____
Glenn A. Berchtold
Chairman, Departmental Committee on Graduate Students

This doctoral thesis has been examined by a Committee of the Department of Chemistry as follows:

Professor Daniel S. Kemp _____
Chairperson

Professor Peter T. Lansbury, Jr. _____
Thesis Supervisor

Professor Julius Rebek, Jr. _____
Department of Chemistry

Byron Caughey, Ph.D. _____
National Institute of Health

Models for Protein Assembly in the Prion Disease

by

Jon H. Come

Submitted to the Department of Chemistry
on May 13, 1994 in partial fulfillment of the
requirements for the Degree of Doctor of Philosophy

ABSTRACT

The transmissible spongiform encephalopathies (e.g. scrapie, Creutzfeldt-Jakob disease (CJD), and Gerstmann-Straüssler-Scheinker disease (GSS)) are neurodegenerative diseases characterized by abnormal brain pathology and the deposition of extracellular protein aggregate, which can be in the form of amyloid. These deposits consist predominately of a host-encoded protein, PrP. Scrapie can be transmitted via an infectious particle (prion) that seems to consist only of an insoluble, protease resistant form of PrP (PrP^{Sc}). PrP^{Sc} appears to be chemically, but not conformationally, identical to its cellular precursor (PrP^{C}). The prion converts host PrP^{C} into PrP^{Sc}. One possible replication mechanism assumes that PrP^{Sc} is an aggregate in which an alternative conformer of PrP is stabilized by intermolecular interactions. According to this mechanism, replication and infection involve the nucleation of polymerization. Peptides corresponding to PrP 118-133, 106-126, and 101-144 were synthesized along with a permuted sequence of PrP 118-133 denoted as Scr3. PrP 118-133 and PrP 106-126 formed amyloid fibrils. The kinetics of amyloid formation were found to follow a nucleation-dependent mechanism, in which there is a lag phase, where no fibril growth is seen, followed by a rapid growth phase; this behavior is similar to crystallization kinetics. The lag phase could be bypassed by the addition of a seed of preformed fibrils of the same peptide. This seeding was shown to be specific as unmatched fibrils did not act as seeds . A polymorphism which occurs at position 129 of PrP (valine or methionine) is non-pathogenic. However, the homozygous genotype predisposes individuals to sporadic CJD. Mixtures of peptides were studied corresponding to both variants. Homogeneous fibril formation was preferred suggesting that homozygous can more readily form assemblies of PrP. We have also studied the conversion of PrP^{C} to a PrP^{Sc}-like form in a cell-free system. Semipurified [^{35}S]PrP^{C} and unlabeled PrP^{Sc} were mixed together and the formation of protease-resistant radiolabeled material was seen over time.

Thesis Supervisor: Dr. Peter T. Lansbury, Jr.

Title: Associate Professor of Chemistry

Table of Contents

List of Figures

List of Tables

Acknowledgements

It took me 3 years of working in the "real" world to decide to go to graduate school—I'm glad I did. The past five years have been great for me both personally and professionally.

Peter Lansbury has been a terrific boss. He gives his students the freedom to pursue their own ideas (all the way to Montana if necessary) and is a constant source of enthusiasm, ideas, Red Sox statistics, and humorous quotes. Peter has always kept the interests of his students in mind when doing research—I hope I can do as well in the future.

My labmates have also contributed greatly to my life here. Kurt Halverson was a role model for me when I joined the lab with his wonderful ability to balance IM sports, beer drinking, fishing, cycling, and some efficiently done lab work. Joe Jarrett (along with being a possibly too obliging drinking buddy) was a tremendous help experimentally. The seemingly endless discussions of the mechanism of aggregation were amusing, aggravating, but, I think, ultimately useful. Of course, both in the lab and out, he was and is, dangerous Joe. Beth Berger is a good friend who was always ready to listen to my problems, particularly during that wacky first year. Kurt, Beth, and Joe shared, along with some long rides, the worst night sleep I've ever had. Maybe we should have staked the tents down.

Julia Hendrix was an amazing source of information on all subjects and one of the few people who understand my obscure references to TV shows.

Shimi Cohen-Anisfeld made life in the lab interesting with his unique point of view.

Jason McDevitt's insights at group meeting were appreciated almost as much as his speed in basketball.

Ted, the bay is yours now.

Irv and Todd, words cannot describe you, you have to be seen to be believed. I'll always remember Todd's discussion with Irv about chess, when Irv was bugging him to play and said, "but I don't want you to be distracted and lose", and Todd said to Irv, "I won't lose."

Brian, the hawk will never die.

I thank the new postdocs (Tosh, Cho, & Han) for adding some character(s) to the lab.

Paul Weinreb has happily accepted the task of proof-reading every document I wrote in the group. He and Ed Licitra have amply filled the beer drinking/softball gap caused by the departure of more stately ones.

Krista Rasmussen has put up cheerfully with my teasing about her cat calendar and her 15 friends named Heather.

Dave Kocisko has been a great collaborator and fishing buddy at Lansbury west. I thank him for making the last chapter of my thesis and interesting story. This is the year for the Browns, I'm sure of it.

The people at Rocky Mountain Labs were kind enough to welcome us into their labs and sometimes their homes. Byron Caughey was a great

collaborator, allowing me to take over his bench, and remaining optimistic regardless of how inconsistent my early results were. Byron is almost as low-key as our mutual friend, Paul Fraser, who took the x-ray diffraction of my peptide for me. Kathy Brown made space for me in her lab and her home. Sue Priola, Greg "the chapper" Raymond, Gil Katzenstein, Rich Bessen, and others helped experimentally and with their suggestions.

Many people outside the lab have made my time at MIT a lot of fun. Ivan Lorkovic was an interesting (if somewhat messy) housemate who never ceases to amaze and confuse me. I next moved in with Scott Jaynes who had to be taught the proper way to watch TV but took to it like a champion. Scoj was gone frequently (where was he sleeping?) but watched sports and played wiffleball when he was around and was there to lead us to a championship at IM football. He was replaced as a housemate by Kingsley Taft, who could always be counted on to go get ice cream and talk about chicks, sports, and even science. Scoj and King also had access to great vacation spots to escape from the constant pressure of ..... IM softball or something.

Heidi Erlacher and Annie Helgason were in my tutorial first year and have been there ever since to have a beer with and share the ups and downs of grad school. They were joined the next year by Jennifer Loebach who was always ready to see what the big city had to offer next.

The morning basketball game, started by Marty, Mike, Chris, and Kurt, and joined by Joe, Beth, Matt, Ray, Jason, Paul, Sandy, John, Ivan et al. kept me in shape and became a sacred ritual.

I thank my family for putting up with my busy schedule during these years. My parents have always supported me in whatever I've done, which has made it easier to pursue my interests wherever they take me. My father has nurtured the scientist in me since we wrote "How to Divide" together when I was 7 years old. Thanks Mom and Dad.

Finally, of all the good things that have happened to me in grad school, by far the best was meeting Sandy. Thanks for your confidence in me. Coming home to you is the best part of the day.

List of Abbreviations

Ac	acetyl
AD	Alzheimer's disease
APP	amyloid precursor protein
Boc	*t*-butoxycarbonyl
BOP	benzotriazol-1-yl-oxy-*tris*-(dimethylamino)phosphonium hexafluorophosphate
BSE	bovine spongiform encephalopathy
CAS	Chemical Abstract Service
CD	Circular dichroism
CJD	Creutzfeldt-Jakob disease
CR	Congo red
CSF	cerebrospinal fluid
DIEA	diisopropylethylamine
DMF	dimethylformamide
DMS	dimethylsulfide
DMSO	dimethylsulfoxide
EM	electron microscopy
FABMS	fast atom bombardment mass spectrometry
FFI	fatal familial insomnia
Fmoc	fluorenylmethoxycarbonyl
FTIR	Fourier-transform infrared spectroscopy
GPI	glycosyl phosphotidylinositol
GSS	Gerstmann-Straüssler-Schenker disease
HFIP	hexafluoro-2-propanol
HPLC	high pressure liquid chromatography
LDMS	laser desorption mass spectrometry
MBHA	methylbenzhydrylamine
MNB	mouse neuroblastoma
NMR	nuclear magnetic resonance
ORF	open reading frame
PDMS	plasma desorption mass spectrometry
PIPLC	phosphatidylinositol-specific phospholipase C
PK	proteinase K
PRNP	gene for PrP
PrP	prion protein
PrP^{Sc}	scrapie associated prion protein
PrP^{C}	cellular prion protein
RPHPLC	reverse phase high pressure liquid chromatography
SAF	scrapie associated fibrils
SDS-PAGE	sodium dodecyl sulfate polyacrylamide gel electrophoresis
TFA	trifluoroacetic acid
TFE	trifluoroethanol
TFMSA	trifluoromethanesulfonic acid
TSE	transmissible spongiform encephalopathy

Chapter 1

The Transmissible Spongiform Encephalopathies

The transmissible spongiform encephalopathies (TSE), or prion diseases are neurodegenerative diseases affecting both animals and humans and are unique in being transmissible, genetic, and sporadic diseases. Human TSE's include Creutzfeldt-Jakob disease (CJD), Gerstmann-Straüssler-Schenker syndrome (GSS), fatal familial insomnia (FFI), and kuru. Animal forms of TSE's include scrapie in sheep, bovine spongiform encephalopathy in cattle, transmissible mink encephalopathy, and chronic wasting disease of captive mule deer.

CJD is characterized by dementia, ataxia, and spongiform degeneration in the brain. The onset of CJD is usually late in life, or in the case of infection, months to years after exposure. Infection with CJD is usually caused by exposure during a medical procedure. Many cases of transmissible CJD have been caused by infected instruments used in neurological or ocular procedures, partly because of the extreme resistance of the infectious agent to the generally employed disinfection procedures that kill most other microbials. Contaminated human-derived products have also caused transmissible CJD. A large outbreak has recently occurred that was caused by contaminated cadaver-derived human growth hormone. Recombinant

sources of hormone have eliminated further infection. GSS is a familial variant of CJD, usually characterized by the formation of proteinaceous deposits known as amyloid plaques along with dementia and spongiform changes. FFI is a subacute condition with untreatable insomnia, dysautonomia, and severe selective atrophy of thalamic nuclei. Spongy degeneration is less prevalent in FFI than CJD. Kuru afflicted a small population in the highland region of New Guinea, and was the leading cause of death among women and younger individuals. It has been virtually eliminated by the cessation of ritualistic cannibalism among these people.[1]

The most studied animal forms of TSE's are scrapie in sheep and goats, and bovine spongiform encephalopathy (BSE) or "mad cow disease" in cattle and dairy cows. Both of these diseases are still significant veternary problems. Until recently, the policy in the United States in regards to scrapie was to destroy all animals in a flock with an afflicted individual. This severe action limited the exposure of healthy sheep to infected animals, pastures, and housing, and reduced the incidence of scrapie in the United States. BSE has been a crippling problem in the British cattle industry, with the incidence of BSE only recently beginning to level off. The outbreak was apparently caused by feed contaminated with infective material from sheep or other cattle. Changes in the rendering process appear to have stopped further exposure to infectious agent. Although no known case of human TSE infection has resulted from consumption of contaminated meat, many still will not eat British cattle products.

Early Studies of the Scrapie Agent

TSE's have peculiar traits which set them apart from most other diseases and were defined as slow infections by Sigurdsson, who put forth the

concept of slow infections based upon studies of four chronic diseases that appeared in Icelandic sheep during the 1930's.[2] Slow infections have attributes of both acute and chronic diseases, which define the ends of a continuum. For the acute case, after infection the disease rapidly approaches a crisis. At this point a resolution occurs, the host either fighting off the infection or dying. Chronic diseases, on the other hand, are lingering illnesses, going into remission, possibly for extended periods, and then reoccurring. Slow diseases have characteristics of both; they have a long period after infection with no symptoms, similar to chronic diseases, but are then followed by a rapid disease course, similar to acute diseases. Scrapie and several other diseases fit this definition of slow infections.

Later, Hadlow was the first to suggest a connection between TSE's in different species, pointing out the similarity between scrapie and kuru based on the pathology they shared.[3] Gadjusek, Gibbs, and Alpers completed the connection by transmitting kuru to chimpanzees in 1965[4] and later by transmitting CJD to animals.[5, 6] Scrapie, CJD, and GSS have all been transmitted to rodents, after long incubation times, by inoculation of brain extracts from afflicted individuals. Extracts from the brains of these rodents can subsequently infect, via intercerebral injection, other animals of the same species with a much shorter incubation time. This species barrier has been observed for many infections across species, and it may explain the lack of correlation between the incidence of scrapie and the incidence of CJD.

The transmission to rodents, first accomplished in mice by Chandler,[7] greatly improved the ability to study these diseases and purify the infectious agent. Nevertheless, the bioassay for the infectious agent still required serial dilutions of the samples and the housing and monitoring of mice for about one year. The development of a Syrian golden hamster line[8, 9] with a much

shorter incubation period than the mouse lines (60 days vs. approx. 200 days) greatly improved the assay. Further improvements resulted from the use of incubation time to the onset of illness rather than death as an endpoint.[10]

Early in the study of scrapie, the unusual properties of the infectious agent led investigators to speculate on its nature. Because of its resistance to heat and to treatment with acetylethyleneimine, Stamp et al. suggested that it appeared "most unlikely that the factor could be nucleo-protein in nature".[11] Based upon studies of the agent's resistance to ionizing radiation at 254 nm, Alper et al. proposed, "scrapie is most unlikely to depend on nucleic acid moiety for its replicative ability".[12] They could not determine from those experiments whether or not a protein was involved in the pathogen. Every other pathogen known (e.g. bacteria, viruses) required nucleic acid to replicate. The apparent lack of nucleic acid in the scrapie agent has continued to be a great source of controversy.

A self-replicating protein was considered by many to be inconsistent with the basic tenets of molecular biology. In 1967, J.S. Griffith, a mathematician at Bedford College in London, suggested three ways in which a protein-only TSE agent might be possible without altering the dominant paradigm.[13] In one scenario, the protein of interest, although encoded for in the genome, is not produced normally, has no required function, and is harmful to the host if produced. If it should also induce its own production, infection with this protein would upregulate synthesis of itself causing the production of more harmful protein. This proposal was proven false when the protein involved was shown to be a host protein, produced in afflicted and unaffected individuals.[14, 15, 16] A second mechanism, which Griffith thought less likely, involved the immune system but is also inconsistent with later experimental data. The third scenario Griffith proposed still

deserves attention. In this mechanism, the infectious protein acts as a seed to convert a normal protein (or normal state of a protein) to an abnormal protein (or abnormal state of the same protein). The infectious protein only causes this transformation in a multimeric state, which the normal protein cannot access without catalysis. The conversion is analogous to the idea that "a gas can only condense on nuclei already present". This mechanism will be discussed in detail in the last chapter of this thesis.

Purification of a Protein from the Infectious Agent

An important breakthrough in determining the nature of the infectious agent in scrapie was the isolation of a protein from semi-purified preparations of the agent from rodents. Prusiner and coworkers purified the agent by low-speed centrifugation, precipitation from ethylene glycol and ammonium sulfate, enzymatic digestion, and sedimentation through a sucrose gradient[17] The amount or titer of the infectious agent in various fractions was assayed for by infectivity in rodents, and a 100- to 1000-fold enrichment in terms of protein was accomplished. Fractions enriched in infectious titers contained as the major constituent a 27 to 30 kDa protein, designated PrP. It was suggested this protein was necessary, and possibly sufficient, for infectivity; this proposal is still not accepted by all researchers in this field. The presence of this protein was seen by other workers. Diringer et al. showed a correlation between infectivity, the presence of fibrils, and a similar 26 kDa protein.[18] They believed these fibrils were identical to the scrapie associated filaments (SAF) seen by Merz and coworkers in brain extracts from scrapie infected animals.[19]

An N-terminal sequence of the 27-30 kDa protein was determined after purification of the agent by denaturing in sodium dodecyl sulfate and size

exclusion HPLC.[20] From this sequence, a hamster cDNA library was prepared and the sequence determined.[14] The protein was found in both normal and infected brains. Southern blotting revealed a gene with the same restriction pattern in normal and infected brain. The mRNA level was also similar in both normal and scrapie-infected hamster brain samples.[16] Finally, antisera against PrP from infected brain reacted with a protein from both scrapie-infected, and to a lesser extent, normal brain. Subsequently, the mouse[15] and human[21, 22] sequence were determined (see Figure 1.1) and found to be highly homologous. No significant homology was found to any other known proteins.

PrP is a normal host-produced protein, designated PrP^{C} (for cellular form), and appears to be covalently identical to the protein found in the infectious agent, designated PrP^{Sc} (for scrapie form).[23] The open reading frame of the PrP gene encodes for 254 amino acids. The protein comprises the following domains (see Figure 1.2): a 22 amino acid signal peptide cleaved during biosynthesis,[24, 25] a stretch of five octapeptide and two hexapeptide repeats rich in Gly and Pro, a stretch of hydrophobic amino acids similar to a transmembrane sequence, a possible amphipathic helix, and a hydrophobic sequence which is cleaved with the addition of a glycosyl phosphatidylinositol (GPI) anchor to Ser231.[26] Arg25 and Arg37 in PrP^{Sc}, and at least Arg25 in PrP^{C} appear to be modified as judged by difficulties encountered in sequencing.[25, 27] Both isoforms contain a disulfide bridge between Cys179 and Cys214[25] and asparagine-linked glycosylation at Asn181 and Asn197.[28] PrP is highly cationic with a net positive charge of 18 at pH 7.4 and 9 at pH 5.0. This positive charge resides predominately in the N-terminus with residues 23-140 having 18 positively charged residues and no negatively charged ones at neutral conditions. Residues 141-231 contain 13

Figure 1.1 The sequence of prion protein (PrP). SHaPrP, syrian hamster PrP; MoPrP, mouse PrP; Hu PrP, human PrP; Hu Var., variations in the human sequence. Variations include: (1) disease causing incorporation of extra octapeptide repeats, (2) Pro to Leu at codon 102 found in GSS, (3) Ala to Val at codon 117 found in cases of GSS, (4) natural polymorphism at position 129, (5) Asp to Asn at 178 linked to CJD and FFI, and (6) Glu to Lys at codon 200 linked to CJD in Libyan Jews. Other modifications are in italics. The Arg at position 25 and 37 are modified. There is a disulfide between Cys 179 and Cys 214. Glycosylation occurs at Asn 181 and Asn 197. Protease cleavage in PrP^{Sc} occurs at about residue 90.

```
                                10                  20                  30
SHaPrP MAN- -Lsy W IL aLFVAmWtDvGLCKK*R*PKPG-GWN
MoPrP           G       T
HuPrP           GC  M V       T   S L
Hu Var
                   40                  50                  60
SHaPrP TGGS*R*YPGQGSPGGNRYPPQGGGtWGQPHGGGWG
MoPrP
HuPrP                                              G
Hu Var                                    (^1)
          70                  80                  90
SHaPrP QPHGGgWGQPHGGgWGQPHGGGWGQGGGTHnQ
MoPrP        S                   S
HuPrP                                                  S
Hu Var
        100                 110                 120                 130
SHaPrP WNKpSKPKTNmKHmAGAAaAGAVVGGLGGYmLGS
MoPrP                   L       V
HuPrP
Hu Var       L(2)                           V(3)                    V(4)
                  140                 150                 160
SHaPrP AMSRPmmHFGnDwEDRYYRENMnRYPNQVYYRPv
MoPrP             I                         Y
HuPrP          I  I       S  Y              H                     M
Hu Var
          170                 180                 190                 200
SHaPrP DqYnNQNNFVHd*C*V*N*ITIKQHTVTTTTKGE*N*FTeTD
MoPrP      S
HuPrP   E  S
Hu Var                      N(5)                                    K(6)
                210                 220                 230
SHaPrP iKiMERVVEQM*C*tTQYqkESQAYYdgRRSS-avLFSS
MoPrP V M                   V                           S T
Hu PrP V M                  I       ER          -Q      M
Hu Var
        240             250
SHaPrP PPVILLISFLIFLmVG
MoPrP                   I
HuPrP                   I
Hu Var
```

Figure 1.2 Schematic of PrP. **A**) Full-length PrP encompassing entire ORF. SP, signal peptide; GP repeats, a set of five octapeptide; TM, a transmembrane-like sequence; AH, possible amphipathis helix; SS hydrophobic C-terminal sequence cleaved with the attachment of a GPI anchor. **B**) PrP after posttranslational processing. X, modified Arg25 & Arg 37 residues; Sug, glycosylated Asn181 & Asn197; SS, disulfide between Cys179 & Cys214; GPI, glycosylphosphotidylinositol anchor attached at Ser 231. **C**) PrP^{Sc} after proteinase K treatment (cleavege around residue 90).

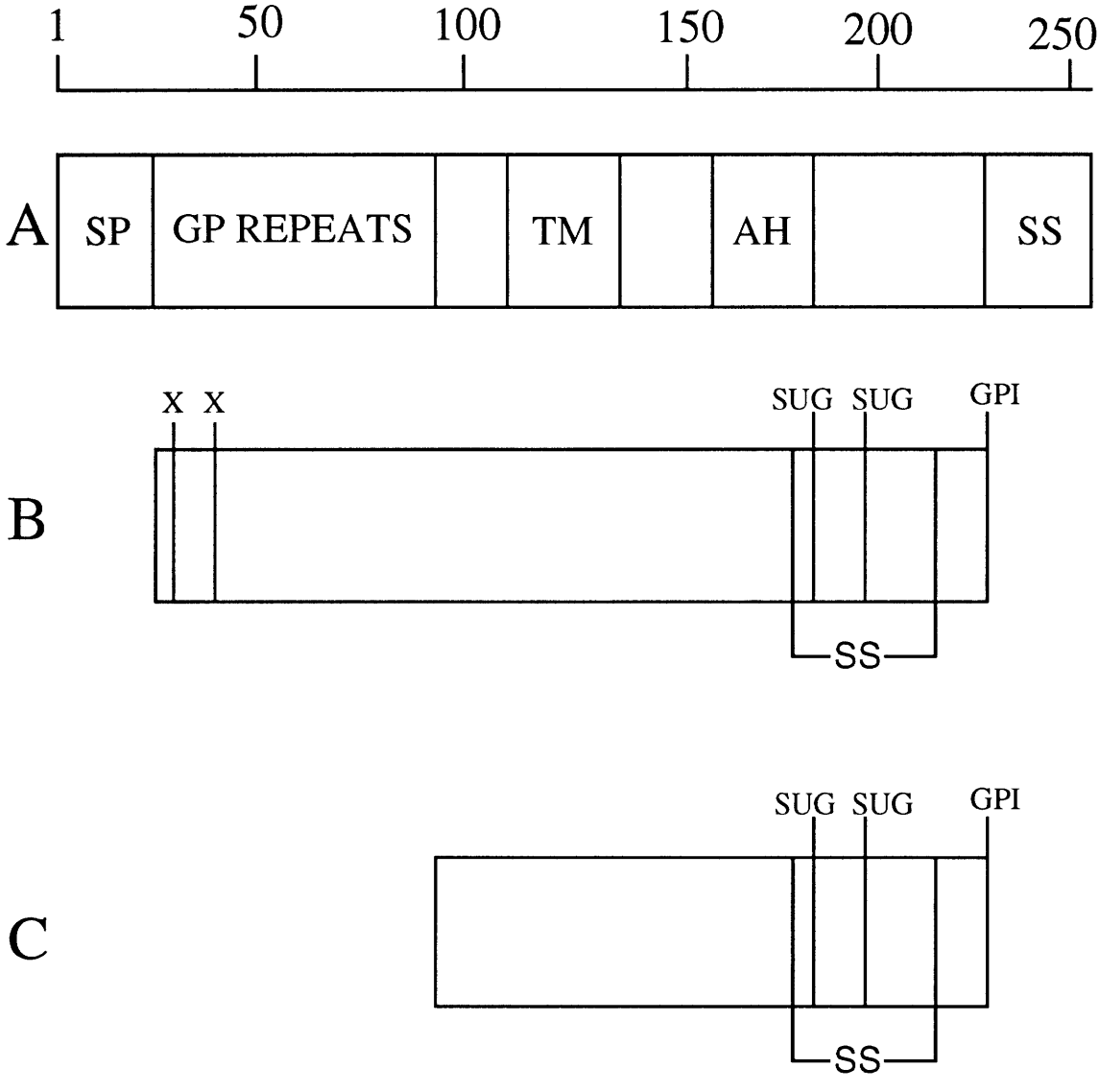

positively and 13 negatively charged residues. The localization of the charge to the N-terminus may partially cause the greater proteinase sensitivity of this region.

Differences between Host- and Agent-Derived PrP

Although there are no known covalent differences between PrP^C and PrP^{Sc}, several other properties distinguish the two isoforms. PrP^C is substantially more soluble than PrP^{Sc}, and a corresponding difference in the centrifugation properties can be seen. The two isoforms differ in their sensitivity to protease digestion also. PrP^C is completely digested by proteinase K (PK) under conditions where PrP^{Sc} is only partially degraded. Treatment of PrP^{Sc} with PK removes approximately 67 amino acids from the N-terminus, although no change in infectivity titers is observed. PK treatment seems to be necessary for the formation of amyloid fibrils of PrP^{Sc} as visualized by electron microscopy.[29] A similar truncation of PrP^{Sc} may occur in infected animals as the lifetime of PrP^{Sc} is quite long, whereas PrP^C is turned over rapidly with a half life of a few hours.[30] The glycosylation (at Asn181 and Asn 197) causes an apparent heterogeneity in the molecular weight of PrP (in both isoforms) as measured by sodium dodecyl sulfate (SDS) polyacrylamide gel electrophoresis (PAGE). In PrP^{Sc}, part of this heterogeneity disappears with PK treatment. Regardless, the glycosylation does not appear to be required for conversion of PrP^C to PrP^{Sc} in scrapie infected cells.[31]

The two isoforms also differ conformationally, as shown by Fourier transform infrared (FTIR) spectroscopy. Caughey and coworkers determined that PrP^{Sc} has approximately 50% β-structure with intense absorbances in the FTIR spectra at 1627, 1636, and 1657 cm^{-1}.[32] Prusiner later was able to purify

sufficient quantities of PrP^C for FTIR analysis and found it composed of predominately helix/turn/random coil structures with a large absorbance centered at approximately 1660 cm^{-1}.[33] This data suggests a conformational change is involved in the conversion of PrP^C to PrP^{Sc}. The greater β-sheet content of PrP^{Sc} is consistent with data on inclusion body formation where higher β-sheet content correlates with the less soluble isoform.[34]

The nature of the infectious agent is still a subject of heated debate. Although preparations of the scrapie agent are enriched in PrP^{Sc}, some investigators have claimed that PrP^{Sc} is not a part of the agent but a pathogenic product which copurifies with the infectious agent.[35] There is substantial evidence that PrP^{Sc} is required for infectivity.[36] The agent is also resistant to many conditions expected to destroy nucleic acids such as nuclease treatment and irradiation at 254 nm, which would be expected to destroy conventional viruses. This evidence does not prove absolutely that nucleic acids or other molecules are not required. Unfortunately, the conditions found to date to solubilize the agent for high resolution purification, also destroy the infectivity. Until purified and completely characterized components can be assembled into the infectious agent, the nature of the agent will remain controversial.

Biosynthesis of PrP^C and PrP^{Sc}

PrP^{Sc} is derived from a portion of the PrP produced by the cell. Although the function of PrP is unknown, many details of its biosynthesis of PrP^C and PrP^{Sc} have been elucidated. The highest concentration of PrP mRNA is found in neurons[16, 37] and does not increase over the course of infection.[14] The higher level of expression in the brain may be part of the reason this organ is affected.

Mouse neuroblastoma cells are the simplest system to date that can convert PrP^C to PrP^{Sc} and produce infectious agent. This system has provided insights to the location of the conversion of PrP^C to PrP^{Sc}. Studies of PrP^C and PrP^{Sc} formation in scrapie-infected (sc+) murine neuroblastoma cells exhibited differences in the biosynthesis of these two isoforms.[30] Pulse-chase metabolic labeling with [^{35}S] methionine showed a peak in concentration of PrP^C after 2 hours with a half-life of about 4 hours. PrP^{Sc} labeling, on the other hand, continued to increase up to 45 hours later with half-maximal labeling after 6 hours and no evidence of turnover. PrP^C is labeled 2 mins. after the addition of [^{35}S]methionine, while PrP^{Sc} is not labeled until after 60 mins. This lag corresponds approximately to the time required for translocation of PrP^C to the cell surface. Treatment of these cells with phosphatidylinositol-specific phospholipase C (PIPLC) released PrP^C from the cell and inhibited PrP^{Sc} formation. The amount of PrP^{Sc} produced was found to be about 3% of the PrP^C. Taken together, this evidence suggests PrP^{Sc} is made from a small percentage of PrP^C after PrP^C is brought to the cell surface and anchored by GPI to the membrane. It is not yet clear if the conversion of PrP^C to PrP^{Sc} is more prevalent in particular populations of PrP^C.

Because the conversion occurs after PrP reaches the surface, it is believed to occur in the endosomal pathway.[30, 38] The conversion however, appears to occur before PrP^C reaches the lysosomes. The study of the effect of lysosomotropic amines support this proposal. Lysosomotropic amines do not inhibit the formation of PrP^{Sc}, but they do block the digestion of the N-terminal 90 amino acids of PrP^{Sc}. Lysosomotropic amines do not however, alter the digestion of PrP^C, which suggests PrP^C is degraded before reaching

the lysosomes.[39] In addition, kinetic studies indicate that PrP^{Sc} is formed before exposure to lysosomal proteases.[40]

Genetic Studies of PrP

Several mutations in the PrP gene (PRNP) have been linked with GSS and CJD (see Figure 1.1). PRNP is found on the short arm of human chromosome 20 and the homologous region of mouse chromosome 2.[22, 41] The entire open reading frame of the PRNP gene[14, 42] is found in a single exon. A cytosine to thymine substitution in the second position of codon 102 causes a proline to leucine change, which segregates with GSS in more than one family.[43, 44] Another mutation found in patients with dementing GSS is an alanine to valine substitution at codon 117.[45, 46] A mutation at codon 200 (Glu to Lys) has been linked to CJD in Libyan Jews.[47] Also, the insertion of several addition octapeptide repeats has been found to segregate with GSS.

The change of aspartic acid to asparagine at codon 178 causes a prion protein disease with the phenotype determined by the amino acid at position 129 (Met or Val).[48] This polymorphism at position 129 occurs throughout the human population and neither Met nor Val at position 129 appears to segregate with the disease. The amino acid at position 129, however, does affect the phenotype of the disease when coupled with the mutation at position 178. The Met 129, Asn 178 allele segregated with FFI, while the Val 129, Asn 178 allele segregated with familial CJD. This polymorphism at 129 is also of interest because people with sporadic CJD are more likely to be homozygous, for either Met or Val, than heterozygous at this position (discussed in Chapter 4).[49]

The existence of several different strains of scrapie[50, 51] with different characteristics and clinical signs has been one of the strongest arguments for

the requirement of an infectious agent of a viral-like nature with its own genome. When scrapie in sheep was passaged to goats, either a scratching or a drowsy syndrome was observed, which remained constant in subsequent passages.[51] Multiple strains have been studied in mice as well, with differences seen in incubation time, the severity and distribution of pathological changes, the heat inactivation properties, and in other properties. Different strains can be seen and passaged in a single inbred mouse line. Also, different mouse lines may respond differently (e.g. different incubation times) to the same strain because of changes in a gene closely linked to PRNP, which may be PRNP itself.[52, 53] Many strains maintain their characteristics through several passages while others appear to be less stable.

Transgenic Animals

Transgenic (Tg) studies in rodents have partly elucidated how changes in PrP influence prion diseases. In one study[54], the Syrian hamster (SHa) PRNP gene, which encodes for a protein differing at 16 residues (see Figure 1.1) from mouse PrP (MoPrP), was placed into mice (Tg (SHaPrP) mice). These mice did not become spontaneously ill. Their response to infection was determined next. Normally, mice are resistant to infection with SHa scrapie, but the Tg (SHaPrP) mice were very susceptible with incubation times comparable to hamsters. When these transgenic mice, which now produced both MoPrP and SHaPrP, were infected with SHa scrapie, they only produced $SHaPrP^{Sc}$; no $MoPrP^{Sc}$ was found using MoPrP specific antibodies.[55] That is, the nature of the PrP^{Sc} formed in these mice was determined by source of the inoculuum. The tropism (as judged by which species could be infected) of the agent produced was also determined. The transgenic mice were infected with

either SHa or mouse scrapie, and portions of their brains were subsequently injected into other normal hamsters and mice. In all cases, the species susceptibility was determined by the original inoculuum. If the transgenic mice were infected with mouse scrapie, samples from their brains could infect mice and not hamsters; if they were infected with SHa scrapie, samples from their brains could infect hamsters and not mice.

Tg mice were also produced that have a proline to leucine mutation at position 101; the analogous 102 mutation in humans segregates with GSS.[55] These mice developed a neurodegenerative disease without inoculation with infectious agent. However, the pathology was different from that observed in humans with the analogous mutation and could not be effectively transmitted to other mice, which leads one to question the relevance to scrapie. This difference in pathology may be due to other differences between the mouse and human sequences that interact with position 101. Transgenic systems are fraught with possible complications, and one has to be careful in interpreting the results. For example, recent studies have shown that overproduction of PrP in transgenic animals can lead to a neurological disorder that is not scrapie.[56]

In perhaps the most dramatic transgenic study, Charles Weissman and coworkers produced a line of mice having no functional PRNP gene.[57] These "knockout" mice appeared to suffer no ill effects from the removal of this gene. Remarkably, a protein so highly conserved across species is not required for survival. Possibly, redundancy built into the system compensates for the removal of this protein, or its importance may only become apparent in a situation to which the laboratory mice are not exposed.

The mice with no PRNP gene were impervious to infection with scrapie.[58] Could the infectious agent replicate in these mice without causing

scrapie, and subsequently be passed on to other normal mice? To answer this question, mice were sacrificed at intervals after exposure to scrapie and homogenates from their brains were injected into the brains of additional normal mice. No infectivity was found in these samples with the exception of a small titer at early time points, probably due to residual inoculuum. There are a couple of caveats, however. A small number of animals did get ill after a long interval. Contamination was suspected in these cases, and infection has not been observed in additional experiments. Also in these experiments, the handling of the samples was somewhat different than the generally employed procedures. The brain samples used to test infectivity were heated to 80°C before injection, presumably to kill other pathogens. This treatment normally would not disable the scrapie agent but is not usually done in experiments of this kind. If the absence of PrP reduced the heat-resistance of the agent but did not eliminate its production, this heat treatment would be misleading. That is, the agent may still be replicating without PrP, but not be as stable. Despite these reservations, these experiments are some of the strongest evidence to date for a protein-only infectious agent.

Inhibitors of Scrapie Infection

No therapy for the TSE's exists. Certain molecules have been shown to inhibit the formation of PrP^{Sc} in scrapie-infected cell lines and have a prophylactic effect in animals subsequently exposed to scrapie. Congo Red and sulfated polyanions greatly inhibit the build-up of PrP^{Sc} in scrapie-infected mouse neuroblastoma cells.[59, 60, 61] Diringer and Ehlers have shown that mice given three applicaions of polyanion pentosanpolysulphate two

months before injection were protected from scrapie infection.[62] To date, nothing has been shown to reverse the effects of scrapie infection.

Studies of PrP^{Sc} Outside the Cell

The next important step in understanding the nature of the TSE's is the formation of infectious agent outside the machinery of the cell from purified components. If the conversion of PrP^{C} to PrP^{Sc} is sufficient for infectivity, conditions causing this transformation are necessary to elucidate the mechanism and to prove it does not require genetic information. Prusiner and coworkers have addressed this question by attempting to renature PrP^{Sc}.[63] In these experiments, PrP^{Sc} was treated with denaturants, generally chaotrophic salts such as guanidine thiocyanate or urea. The denaturant was then diluted or removed by dialysis, and the protein was later assayed for infectivity. Infectivity did not return under the conditions used.

Can anything be learned by studying shortened forms of PrP? The brains of certain patients with GSS contain truncated forms of PrP. The plaques in a family known as the Indiana kindred contain an 11kD fragment of PrP stretching from about codon 58 to codon 150.[64] An amber mutation (Tyr^{145} to stop) was found in a patient who had a dementing illness with PrP plaques.[65] In this patient, the plaques only contain the truncated version of PrP, although mRNA for both full-length and truncated PrP could be detected. It has also recently been shown that truncated forms of PrP can form PrP^{Sc} in cell culture.[66] Mutants were made where amino acids 23-88 were deleted; Other mutants were made where Ser 231, to which the GPI anchor is attached, was replaced by a stop codon. Both of these shortened forms could be converted to PrP^{Sc}. The ability of these truncated plaques to cause illness in animals has not yet been reported, however, the formation of

PrP^{Sc} in shortened sequences has encouraged studies with peptides to try an elucidate the mechanism of conversion of PrP^{C} to PrP^{Sc}. We have studied the mechanism of polymerization of peptides derived from the PrP sequence. The formation of ordered assemblies from peptides derived from the PrP sequence is discussed in Chapters 2-4. This assembly was shown to follow nucleation-dependent kinetics. We applied this knowledge to the task of renaturing the entire protein and converting PrP^{C} to PrP^{Sc} outside the cell (see Chapter 5).

REFERENCES FOR CHAPTER 1

(1) Gajdusek, D. C.; *Science* **1977**, *197*, 943.
(2) Sigurdsson, B.; *Br. Vet. J.* **1954**, *110*, 341.
(3) Hadlow, W. J.; *Lancet* **1959**, *1959-II*, 289.
(4) Gajdusek, D. C.; Gibbs, C. J.; Alpers, M.; *Nature* **1966**, *209*, 794.
(5) Gibbs, C. J.; *Science* **1968**, *161*, 388.
(6) Gibbs, C. J.; Gajdusek, D. C.; *Science* **1973**, *182*, 67.
(7) Chandler, R. L.; *Lancet* **1961**, *1961-I*, 1378.
(8) Kimberlin, R. H.; Walker, C. A.; *J. Gen. Virology* **1977**, *34*, 295.
(9) Marsh, R. F.; Kimberlin, R. H.; *J. Infect. Disease* **1975**, *131*, 104.
(10) Prusiner, S. B.; Groth, D. F.; Cochran, S. P.; Masiarz, F. R.; McKinley, M. P.; Martinez, H. M.; *Biochem.* **1980**, *19*, 4883.
(11) Stamp, J. T.; Brotherston, J. G.; Zlotnik, I.; Mackay, J. M. K.; Smith, W.; *J. Comp. Path.* **1959**, *69*, 268.
(12) Alper, T.; Haig, D. A.; Clarke, M. C.; *Biochem. Biophys. Res. Comm.* **1966**, *22*, 278.
(13) Griffith, J. S.; *Nature* **1967**, *215*, 1043.
(14) Oesch, B.; Westaway, D.; Wälchli, M.; McKinley, M. P.; Kent, S. B. H.; Aebersold, R.; Barry, R. A.; Tempst, P.; Teplow, B. B.; Hood, L. E.; Prusiner, S. B.; Weissmann, C.; *Cell* **1985**, *40*, 735.
(15) Locht, C.; Chesebro, B.; Race, R.; Keith, J. M.; *Proc. Natl. Acad. Sci. USA* **1986**, *83*, 6372.
(16) Chesebro, B.; Race, R.; Wehrly, K.; Nishio, J.; Bloom, M.; Lechner, D.; Bergstrom, S.; Robbins, K.; Mayer, L.; Keith, J. M.; Garon, C.; Haase, A.; *Nature* **1985**, *315*, 331.
(17) Bolton, D. C.; McKinley, M. P.; Prusiner, S. B.; *Science* **1982**, *218*, 1309.
(18) Diringer, H.; Gelderblom, H.; Hilmert, H.; Özel, M.; Edelbluth, C.; Kimberlin, R. H.; *Nature* **1983**, *306*, 476.
(19) Merz, P. A.; Somerville, R. A.; Wisniewski, H. M.; Manuelidis, L.; Manuelidis, E. E.; *Nature* **1983**, *306*, 474.
(20) Prusiner, S. B.; Groth, D. F.; Bolton, D. C.; Kent, S. B.; Hood, L. E.; *Cell* **1984**, *38*, 127.
(21) Kretzschmar, H. A.; Stowring, L. E.; Westaway, D.; Stubblebine, W. H.; Prusiner, S. B.; DeArmond, S. J.; *DNA* **1986**, *5*, 315.
(22) Liao, Y.-C. J.; Lebo, R. V.; Clawson, G. A.; Smuckler, E. A.; *Science* **1986**, *233*, 364.
(23) Stahl, N.; Baldwin, M. A.; Teplow, D. B.; Hood, L.; Gibson, B. W.; Burlingame, A. L.; Prusiner, S. B.; *Biochem.* **1993**, *32*, 1991.
(24) Hope, J.; Morton, L. J. D.; Farquhar, C. F.; Multhaup, G.; Beyreuther, K.; Kimberlin, R. H.; *The EMBO J.* **1986**, *5*, 2591.
(25) Turk, E.; Teplow, S. B.; Hood, L. E.; Prusiner, S. B.; *Eur. J. Biochem.* **1988**, *176*, 21.
(26) Stahl, N.; Borchelt, D. R.; Hsiao, K. K.; Prusiner, S. B.; *Cell* **1987**, *51*, 229.
(27) Hope, J.; Multhaup, G.; Reekie, L. J. D.; Kimberlin, R. H.; Beyreuther, K.; *Eur. J. Biochem.* **1988**, *172*, 271.

(28) Haraguichi, T.; Fisher, S.; Olofsson, S.; Endo, T.; Groth, D.; Tarentino, A.; Borchelt, D.; Teplow, D.; Hood, L.; Burlingame, A.; Lycke, E.; Kobata, A.; Prusiner, S. B.; *Arch. Biochem. Biophys.* **1989**, *274*, 1.
(29) McKinley, M. P.; Meyer, R. K.; Kenaga, L.; Rahbar, F.; Cotter, R.; Serban, A.; Prusiner, S. B.; *J. Virology* **1991**, *65*, 1340.
(30) Caughey, B.; Raymond, G. J.; *J. Biol. Chem.* **1991**, *266*, 18217.
(31) Taraboulos, A.; Rogers, M.; Borchelt, D. R.; McKinley, M. P.; Scott, M.; Serban, D.; Prusiner, S. B.; *Proc. Natl. Acad. Sci. USA* **1990**, *87*, 8262.
(32) Caughey, B. W.; Dong, A.; Bhat, K. S.; Ernst, D.; Hayes, S. F.; Caughey, W. S.; *Biochemistry* **1991**, *30*, 7672.
(33) Pan, K.-M.; Baldwin, M.; Nguyen, J.; Gasset, M.; Serban, A.; Groth, D.; Mehlhorn, I.; Huang, Z.; Fletterick, R. J.; Cohen, F. E.; Prusiner, S. B.; *Proc. Natl. Acad. Sci. USA* **1993**, *90*, 10962.
(34) Mitraki, A.; King, J.; *Bio/Technology* **1989**, *7*, 690.
(35) Manuelidis, E. E.; Manuelidis, L.; *Proc. Natl. Acad. Sci. USA* **1993**, *90*, 7724.
(36) Prusiner, S. B.; *Science* **1991**, *252*, 1515.
(37) Kretzschmar, H. A.; Prusiner, S. B.; Stowring, L. E.; DeArmond, S. J.; *Am. J. Pathology* **1986**, *122*, 1.
(38) Borchelt, D. R.; Taraboulos, A.; Prusiner, S. B.; *J. Biol. Chem.* **1992**, *267*, 16188.
(39) Caughey, B.; Raymond, G. J.; Ernst, D.; Race, R. E.; *J. Virol.* **1991**, *65*, 6597.
(40) Taraboulos, A.; Raeber, A.; Borchelt, D.; McKinley, M. P.; Prusiner, S. B.; *FASEB J.* **1991**, *5*, A1177.
(41) Sparkes, R. S.; Simon, M.; Cohn, V. H.; Fournier, R. E. K.; Lem, J.; Klisak, I.; Heinzmann, C.; Blatt, C.; Lucero, M.; Mohandas, T.; DeArmond, S. J.; Westaway, D.; Prusiner, S. B.; Weiner, L. P.; *Proc. Natl. Acad. Sci. USA* **1986**, *83*, 7358.
(42) Basler, K.; Oesch, B.; Scott, M.; Westaway, D.; Wälchli, M.; Groth, D. F.; McKinley, M. P.; Prusiner, S. B.; Weissmann, C.; *Cell* **1986**, *46*, 417.
(43) Hsiao, K.; Baker, H. F.; Crow, T. J.; Poulter, M.; Owen, F.; Terwilliger, J. D.; Westaway, D.; Ott, J.; Prusiner, S. B.; *Nature* **1989**, *338*, 342.
(44) Doh-ura, K.; Tateishi, J.; Sasaki, H.; Kitamoto, T.; Sakaki, Y.; *Biochem. Biophys. Res. Comm.* **1989**, *163*, 974.
(45) Nochlin, D.; Sumi, S. M.; Bird, T. D.; Snow, A. D.; Leventhal, C. M.; Beyreuther, K.; Masters, C. L.; *Neurology* **1989**, *39*, 910.
(46) Hsiao, K. K.; Cass, C.; Schellenberg, G. D.; Bird, T.; Devine-Gage, E.; Wisniewski, H.; Prusiner, S. B.; *Neurol.ogy***1991**, *41*, 681.
(47) Goldfarb, L.; Korczyn, A.; Brown, P.; Chapman, J.; Gajdusek, D. C.; *Lancet* **1990**, *2*, 637.
(48) Goldfarb, L. G.; Peterson, R. B.; Tabaton, M.; Brown, P.; LeBlanc, A. C.; Montagna, P.; Cortelli, P.; Julien, J.; Vital, C.; Pendelbury, W. W.; Halta, M.; Willis, P. R.; Hauw, J. J.; McKeever, P. E.; Monari, L.; Schrank, B.; Swergold, G. D.; Autillo-Gambetti, L.; Gajdusek, D. C.; Lugaresi, E.; Gambetti, P.; *Science* **1992**, *258*, 806.

(49) Palmer, M. S.; Dryden, A. J.; Hughes, J. T.; Collinge, J.; *Nature* **1991**, *352*, 340.
(50) Carp, R. I.; Kascak, R. J.; Wisniewski, H. M.; Merz, P. A.; Rubenstein, R.; Bendheim, P.; Bolton, D.; *Alzheimer Dise. Assoc. Disorders* **1989**, *3*, 79.
(51) Bruce, M. E.; Fraser, H. in *Transmissible Spongiform Encephalopathies: Scrapie, BSE and Related Disorders*; Chesebro, B. W.; Springer-Verlag, Berlin-Heidelberg, **1991**; pp 125.
(52) Carlson, G. A.; Kingsbury, D. T.; Goodman, P. A.; Coleman, S.; Marshall, S. T.; DeArmond, S.; Westaway, D.; Prusiner, S. B.; *Cell* **1986**, *46*, 503.
(53) Westaway, D.; Goodman, P. A.; Mirenda, C. A.; McKinley, M. P.; Carlson, G. A.; Prusiner, S. B.; *Cell* **1987**, *51*, 651.
(54) Prusiner, S. B.; Scott, M.; Foster, D.; Pan, K.-M.; Groth, D.; Mirenda, C.; Torchia, M.; Yang, S.-L.; Serban, D.; Carlson, G. A.; Hoppe, P. C.; Westaway, D.; DeArmond, S. J.; *Cell* **1990**, *63*, 673.
(55) Scott, M.; Foster, D.; Mirenda, C.; Serban, D.; Coufal, F.; Walchli, M.; Torchia, M.; Groth, D.; Carlson, G.; DeArmond, S. J.; Westaway, D.; Prusiner, S. B.; *Cell* **1989**, *59*, 847.
(56) Westaway, D.; DeArmond, S. J.; Cayetano-Canlas, J.; Groth, D.; Foster, D.; Yang, S.-L.; Torchia, M.; Carlson, G. A.; Prusiner, S. B.; *Cell* **1994**, *76*, 117.
(57) Büeler, H.; Fischer, M.; Lang, Y.; Bluethmann, H.; Lipp, H.-P.; DeArmond, S. J.; Prusiner, S. B.; Aguet, M.; Weissmann, C.; *Nature* **1992**, *356*, 577.
(58) Bueler, H.; Aguzzi, A.; Sailer, A.; Greiner, R.-A.; Autenried, P.; Aguet, M.; Weissmann, C.; *Cell* **1993**, *73*, 1339.
(59) Caughey, B.; Raymond, G. J.; *J. Virol.* **1993**, *67*, 643.
(60) Caughey, B.; Race, R. E.; *J. Neurochem.* **1992**, *59*, 768.
(61) Caughey, B.; Ernst, D.; Race, R. E.; *J. Virol.* **1993**, *67*, 6270.
(62) Diringer, H.; Ehlers, B.; *J. Gen. Virol.* **1991**, *72*, 457.
(63) Prusiner, S. B.; Groth, D.; Serban, A.; Stahl, N.; Gabizon, R.; *Proc. Natl. Acad. Sci. USA* **1993**, *90*, 2793.
(64) Tagliavini, F.; Prelli, F.; Ghiso, J.; Bugiani, O.; Serban, D.; Prusiner, S. B.; Farlow, M. R.; Ghetti, B.; Frangione, B.; *EMBO J* **1991**, *10*, 513.
(65) Kitamoto, T.; Iizuka, R.; Tateishi, J.; *Biochem. Biophys. Res. Comm.* **1993**, *192*, 525.
(66) Rogers, M.; Yehiely, F.; Scott, M.; Prusiner, S. B.; *Proc. Natl. Acad. Sci. USA* **1993**, *90*, 3182.

Chapter 2

Amyloid Formation by Peptides Derived from the PrP Sequence

We hoped to learn something about how PrP might undergo the transformation from PrP^{C} to PrP^{Sc} by studying a less complex system, namely peptides derived from the PrP sequence. Several peptides from a highly conserved region of PrP were synthesized and studied. The solubility of the peptides, and their ability to form amyloid fibrils was determined. The structures of these peptides were also studied using Fourier-transform-infrared spectroscopy (FTIR). These studies will be discussed in this chapter.

We initially became interested in the PrP sequence through studies of the β-amyloid protein of Alzheimer's disease (AD). Kurt Halverson, a graduate student in the Lansbury lab, noticed the periodic spacing of glycine every fourth residue in the hydrophobic C-terminus of the β-amyloid protein. A search of the protein data base for sequences of the form $(GXXX)_n$, where $n \geq 3$ and X is a hydrophobic amino acid other than proline, revealed eighty sequences. Polyglycine and $(GXGX)_n$ were eliminated, and the relatively hydrophobic sequences (hydropathy ≥1.4) were selected. Twenty-seven sequences remained including β-amyloid protein (res.29-40), the *E. coli* OsmB gene product, and PrP (res. 118-131). PrP caught our attention because, like the

β-amyloid protein, it is an amyloid forming protein found in a neurodegenerative disease.

Table 2.1 Comparison of the sequence of PrP and the β-protein. Gly every fourth residue is shown underlined in bold.

β-protein (res. 25-42)	**G**SNK**G** A I I **G**LMV**G**GVVIA
PrP (res. 116-133)	AAA**G**AVV**G**GLG **G**YML**G**SA

Many diseases are characterized by amyloid depostion

Amyloid plaques are found in many cases of TSE's, in particular GSS, although their presence does not correlate as well with disease as in Alzheimer's disease (AD).[1] In some cases purification of PrP^{Sc}, including detergent extraction and limited proteolysis, is necessary for amyloid formation.[2, 3] Although staining is not evident in many cases of TSE's, the presence of protein deposits is suggested by the ability to purify the insoluble PrP^{Sc} from infected brains. Presumably, if PrP^{Sc} is present in the brain, it is not soluble. In cases where deposits are not seen by staining, either the formation of stainable deposits requires concentration of the protein, or the deposits which may already be present lack something required for staining.

To date, there are more than twenty diseases characterized by amyloid deposition, systemically or in specific organs.[4, 5, 6, 7] These amyloid plaques, which are generally surrounded by damaged tissue, can be studied in a post-mortem examination only, and little is known in detail about their structure or mechanism of formation. The amyloid-forming proteins are different for each disease and contain no obvious similarity other than their insolubility. Rudolph Virchow gave these deposits the name amyloid because their staining characteristics with sulfuric acid/ iodine indicated they might contain carbohydrate.[8] Chemical analysis of amyloid by Freidreich and

Kekulé showed it to be proteinaceous[9], but the term amyloid persists to this day. Amyloid deposits frequently have associated proteoglycans such as heparin, which may have caused the staining exhibited. Glenner and coworkers first identified a specific protein involved in an amyloid disease when they determined the amyloid protein in fatal systemic amyloidosis is a fragment of the immunoglobulin light chain.[10, 11] More than 15 other proteins have since been identified in amyloid-forming diseases (see Table 2.2).

Table 2.2 Some of the proteins forming amyloid in humans and the difference between the normal and amyloidogenic form. P: shortened by proteolysis; M: amino acid difference because of mutation; C: conformational change. Adapted from references 4-7.

Location	Precursor	Cause	Amyloid Protein
Systemic	Immunoglobulin (23kD)	P	Immunoglobulin(5-23kD)
Systemic	Apolipoprotein-SAA(12kD)	P	Apo-SAA (8kD)
Systemic	Apolipoprotein-AI (26kD)	M,P	Apo-AI (9-11 kD)
Systemic	Transthyretin (14kD)	M,P,C	ATTR (5-14 kD)
Systemic	Lysozyme (15kD)	M	Lysozyme (15 kD)
Pancreas	Pro-IAPP (9kD)	P	IAPP (4kD)
Thyroid	Calcitonin (14kD)	P	Calcitonin (6kD)
Muscular	β-2-microglobulin (12kD)	C (?)	β-2-microglobulin (12kD)
Brain	βAPP (110-135kD)	P,M	β protein (4 kD)
Brain	Cystatin C (13kD)	M	Cystatin C (12kD)
Brain	PrP cellular (30-35 kD)	C	PrP-scrapie (27-35 kD)

Generally, the amyloid forming proteins are fragments of precursor proteins. In some instances, these fragments are abnormally produced because of a defective proteolysis step, possibly caused by a mutation in the precursor protein. Other factors may cause normally produced proteins or protein fragments to form amyloid deposits, as may be the case in AD.

In AD, the amyloid forming protein is a fragment of a protein named the amyloid precursor protein (APP). This fragment (β1-40) is found in the cerebrospinal fluid of healthy individuals[12] and in the plaques, along with longer fragments, particularly C-terminally extended peptides.[13, 14, 15] These longer fragments can increase the rate of aggregation of β1-40 *in vitro*.[16] Mutations in APP that segregate with AD occur on either side of the β-Amyloid protein. One pair of mutations near the N-terminus of the β-Amyloid protein causes an increased production of β1-40 in cell culture.[17, 18] Another set of mutations, near the C-terminus, but outside of the β-amyloid protein (corresponding to position 46) have no effect on the amount of β1-40 produced in cell culture, but they may affect the cleavage site and increase the production of longer fragments.[18] These longer fragments may then cause the precipitation of normally produced β1-40.

Another mechanism for amyloid formation may involve improperly folded protein. Conformational changes may play a role in amyloid formation in β-2-microglobulin. Patients with amyloid composed of this protein may also have a higher *in vivo* protein concentration which leads to aggregation. Possibly, the conformational change is an effect of aggregation and does not cause amyloid formation. Differently folded species are implicated in inclusion body formation, which may be an analogous process. As discussed in Chapter 1, the amyloid protein in the prion diseases is known to be different conformationally than its precursor.

The following criteria are generally used to define amyloid:[8] insoluble deposits that (1) are straight unbranched fibrils as visualized by electron microscopy (EM), (2) stain with the dye congo red showing apple-green birefringence, and (3) have an x-ray fiber diffraction pattern consistent with a cross β-fibril. Glenner found bands corresponding to 4.75Å and 9.8Å using x-ray diffraction of non-oriented and mechanically oriented samples of systemic amyloid derived from the immunoglobulin light chain.[19] The β-strands were perpendicular to the fibril axis in the oriented samples. Glenner also studied amyloid deposits using infrared spectroscopy, using both dried plaques in KBr pellets, and films made from 50% formic acid.[20] The spectra had significant absorption at ~1630 cm^{-1} indicative of antiparallel β-sheets. Based on this data, he proposed that the structure of this amyloid was similar to the structure proposed by Linus Pauling for the silk proteins[21, 22] depicted in Figure 2.1. Other amyloids studied subsequently fit this low resolution model.

In this model the protein chains are extended and anti-parallel to the adjacent chains which forms an anti-parallel β-sheet. These sheets stack on top of each other. The distance between chains in the anti-parallel β-sheet is 4.7 Å., and the distance between two sheets is between 5-10 Å. The fibrils grow in the direction of the hydrogen bonding, perpendicular to the direction of the sheet stacking. The third dimension is determined by how the chains overlap or lie adjacent to one another. If there is no overlap, that is if the chains all line up with each other, this dimension will be the length of the extended chain. This distance may be longer if the chains overlap like the bricks in a brick wall. In this model the detailed interactions of the side chains are not specified, only the hydrogen-bonding is shown in detail. However the generally hydrophobic side-chain interactions are likely to be a

Figure 2.1
Pauling's model of a cross β fibril

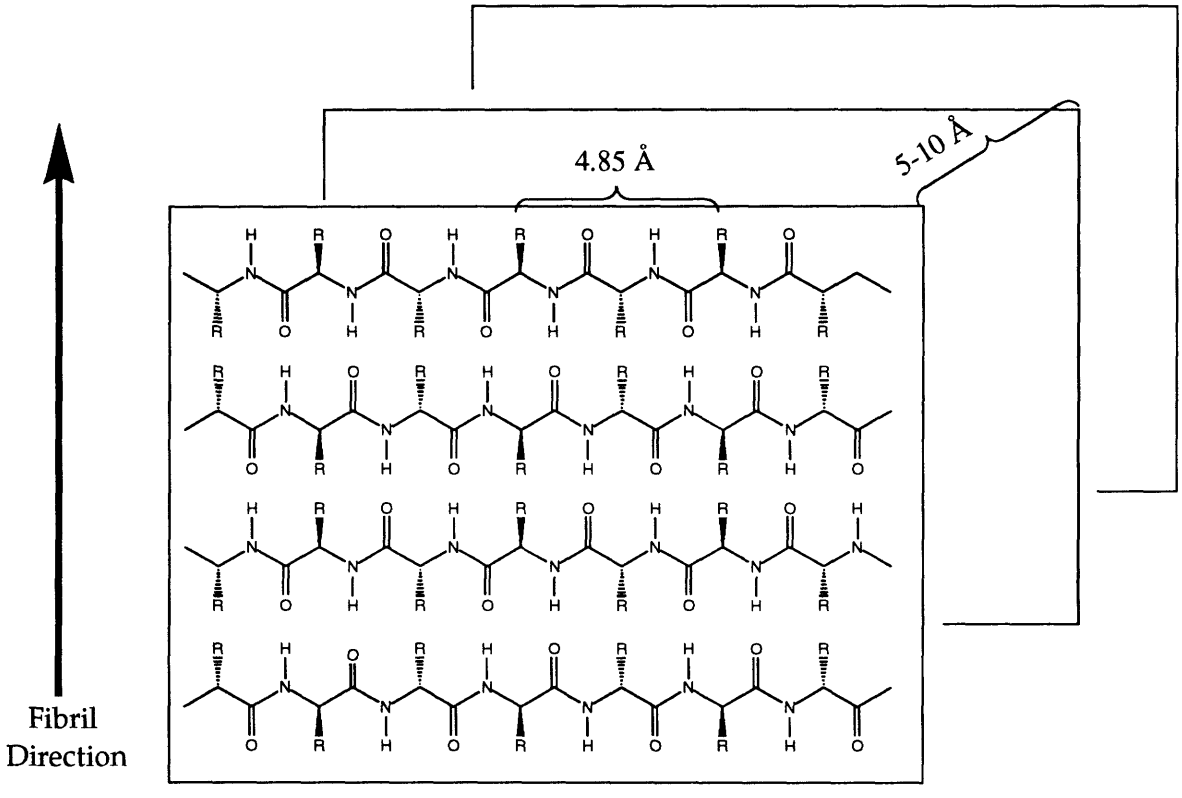

Figure 2.2
Congo Red, the histochemical dye used to stain amyloid

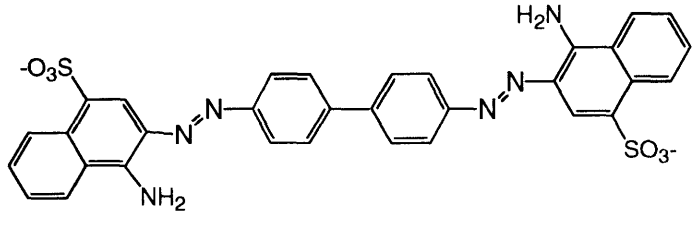

large part of the driving force for the formation of these fibrils. Also regions of the protein may be in other secondary structures, since non-repeating structures will not be seen in the diffraction pattern.

There is a similarity between the process of protein aggregation or inclusion body formation *in vitro* (important to those interested in the overproduction of protein in recombinant organisms) and the formation of amyloid within living tissue.[23] In protein refolding experiments *in vitro*, a low level of denaturant can cause inclusion body formation, suggesting that the partial unfolding of these proteins under these conditions facilitates the aggregation process. For example, tryptophanase, forms highly insoluble aggregates at 3M urea, but folds properly when a 8M urea solution is rapidly diluted.[24] Transthyretin is least soluble at intermediate denaturant concentrations suggesting a partially denatured structure is required for its abnormal polymerization.[25] Similarly, unfolding of proteins *in vivo* may facilitate amyloid formation in some cases.

Peptide models of PrP

Simultaneous with this research, other workers have shown that peptides derived from the PrP sequence can form amyloid fibrils. Tagliavini et al. made peptides corresponding to PrP residues 57-64, 89-106, 106-126, and 127-147.[26] The latter two formed amyloid fibrils as determined by EM, x-ray diffraction, and congo red staining. They also determined that the peptide corresponding to PrP 106-126 was neurotoxic and protease-resistant.[27, 28] The neurotoxicity was tested by exposing primary rat hippocampal neurons to micromolar amounts of the peptide. At this concentration, the peptide polymerized into amyloid fibrils. This insolubility likely contributes to the

protease resistance and may also be responsible for the neurotoxicity. It may be that the formation of insoluble protein deposits is generally detrimental.

Gasset et. al synthesized peptides from regions they predicted would be α-helices, corresponding to residues 109-122, 113-127, 178-191, 202-218.[29] These peptides all formed amyloid and exhibited β-sheet structure by FTIR. Undoubtably, conditions exist where these peptides (or almost any 12-16 residue peptide) could exhibit helical structure also. They found AGAAAAGA (PrP113-120) to be the most amyloidogenic peptide. This sequence is conserved across all species for which the PrP sequence is known.

Goldfarb et. al synthesized peptides corresponding to PrP mutations known to cause CJD including PrP195-213 Glu 200 (native) or Lys 200 (mutation), PrP 169-185 Asp 178 (native) or Asn 178 (mutation), and PrP 119-137 Met or Val 129 (a nonpathogenic polymorphism).[30] They found the mutant sequences to be more fibrillogenic and morphologically different as judged by the appearance and number of fibrils seen by electron microscopy. They also tested the effect of adding PrP 119-137 in with PrP 169-185 because the amino acid at position 129 affects the phenotype of the disease caused by the mutation of position 178 in humans (see Chapter 4). In their hands, PrP 119-137 did not form fibrils by itself or affect the fibril formation by the other peptides.

Solubility of peptides derived from the PrP sequence

The region of PrP from approximately codon 113 to codon 135 is highly conserved across different species and contains a hydrophobic, glycine-rich sequence. This region is likely to be protected from solvent in the normally folded protein, and exposure of this sequence may allow the protein to polymerize. To study the polymerization process, peptides have been

synthesized corresponding to PrP 106-126, PrP 118-133, and PrP 101-144 using standard Fmoc or t-Boc chemistry (see Table 2.3). PrP 118-133 with both variants at position 129 were made along with peptides substituting Gly and Pro at position 129. PrP 106-126 Val 117 which corresponds to a disease-causing PrP mutation in humans was also made.[31, 32] In addition, a peptide was synthesized where the amino acids in the central region were scrambled (Scr3) in order to change the spacing of glycine from every fourth to every third amino acid while maintaining the same amino acid composition.

The first property measured was the solubility of these peptides. Whether the peptide was in solution was defined operationally as the ability to pass through a 0.22 μm filter. One potential problem with this measurement is that small "soluble" oligomers can pass through the filter.

Table 2.3. Synthetic peptides derived from PrP sequences and variants. Shown in bold are residues which differ from the normal human sequence except for in PrP 101-144 mouse where the bold residues are the differences with the Syrian hamster sequence.

PrP 118-133 Met 129	AcHN-AGAVVGGLGGY**M**LGSA-$CONH_2$
PrP 118-133 Val 129	AcHN-AGAVVGGLGGY**V**LGSA-$CONH_2$
PrP 118-133 Pro 129	AcHN-AGAVVGGLGGY**P**LGSA-$CONH_2$
PrP118-133 Gly 129	AcHN-AGAVVGGLGGY**G**LGSA-$CONH_2$
Scr3	AcHN-AGAV**GVLGGYG**MLGSA-$CONH_2$
PrP 106-126	AcHN-KTNMKHMAGAAAAGAVVGGLG-$CONH_2$
PrP 106-126 A117V	AcHN-KTNMKHMAGAA**V**AGAVVGGLG-$CONH_2$
PrP 101-144 (mouse)	H_2N-KPSKPKTN**L**KH**V**AGAAAAGAVVGGLGG YMLGSAMSRPM**I**HFND-COOH

Based on studies on the mechanism of fibril formation in these and other peptides (see Chapter 3), the population of low molecular weight oligomers is probably small and will not greatly effect the measurement. The solubility determination was done in two different ways: from soluble peptide to precipitate and from precipitate back into solution. Both methods should result in the same number provided there is no kinetic barrier to precipitation or dissolution.

In the first method, a supersaturated solution of peptide in buffer is made and then allowed to precipitate from solution over time with stirring. The suspension was filtered and the amount of soluble peptide determined by amino acid analysis, standard protein assay, or in the case of radiolabeled peptide, scintillation counting. The solubility determined in this manner was 15-25 μM for PrP118-133 with Met or Val at position 129, and also 15-25 μM for the scrambled sequence Scr3. The peptides with proline (3 mM) or glycine (0.5mM) at position 129 were substantially more soluble in buffer than were the native sequences. The effect of proline may be because of its known tendency to break up extended structures.[33] The Gly 129 peptide was approximately 20 fold more soluble than either the Met 129 or Val 129 peptides. The change in hydrophobicity may in part account for this difference, however, it also suggests this position is important in the formation of the fibrils. The importance of this position was further elucidated by studying the interactions of the Met 129 and Val 129 peptides (see Chapter 4). The solubilities determined in this manner are dependent on concentration; less concentrated solutions contain less soluble peptide after precipitation. The results from the solubility determination in the opposite direction discussed below are consistent with this observation.

In order to determine the solubility after dissolution, radiolabeled fibrils were formed under the same conditions as fibrils formed in the forward direction. These fibrils were centrifuged and the supernatant decanted. Fresh buffer was added to these fibrils and aliquots were filtered at different time points. The solubility determined in this manner was 7.4±0.4 μM for PrP118-133 Met and 4.4±0.3 μM for PrP118-133 Val. The final concentration of peptide in this case, both soluble and precipitate, is approximately 30 μM or 10% of the concentration of peptide used to measure solubility in the forward direction. The concentration dependence of the solubility may account for the difference in the solubility measurement in the different directions. The solubility of small molecules does not vary with the concentration of the precipitate. However, the solubility appears to vary with concentration with the peptides studied here. Possibly the time needed to reach equilibrium is just much longer. Another explanation is that the morphology of the fibrils changes with concentration altering the solubility.

Amyloid formation by peptides derived from the PrP sequence

Do these peptides fit the definition of amyloid? Yes (except for PrP 101-144). The first criteria is the appearance of the peptides when viewed under an electron microscope. All the peptides studied, except PrP 101-144, appeared as straight, unbranched fibrils with a diameter ranging from 10-20 nm. Fibrils from PrP 118-133 Met 129, PrP 118-133 Val 129, and Scr 3 are shown in Figure 2.3. The fibrils composed of PrP 118-133 Met or Val are indistinguishable from each other. In those samples the fibrils are attached side to side in most cases. In the sample of Scr 3 the fibrils appear as solitary rods and are on average longer. Two other preparations of fibrils are shown in Figure 2.4. These fibrils were prepared from either a 10% DMSO solution in buffer

(panels A & C) or at pH2 in buffer (panels B & D). The fibrils from the DMSO solution are shorter than the ones in Figure 2.3. Fibrils were also formed from PrP 106-126 and PrP 106-126 Val 117 (see Figure 2.5). The fibrils from the native sequence appear to be more sheet-like than the fibrils from the mutant sequence, which appear as rods.

Varying lengths of fibrils were seen in different samples along with varying tendencies towards fibril-fibril or "clumping" interactions. There were also differences in the shape of the fibrils (rods vs. sheets) in different samples. These differences did not seem to be sequence dependent. Slight differences in sample preparation appear to be the cause. All of the peptides studied (except PrP 101-144) fit the definition of amyloid fibrils and were similar in morphology to naturally-derived samples. It is unknown whether any of these differences seen have any *in vivo* significance.

Table 2.4. Solubility and amyloid formation of PrP peptides.

Peptide	Soubility (dissolution)	Solubility (precipitation)	Amyloid-Forming?
PrP 118-133 Met 129	7.4 μM	25-30 μM	yes
PrP 118-133 Val 129	4.4 μM	25-30 μM	yes
PrP 118-133 Pro 129	ND	> 3 mM	no
PrP118-133 Gly 129	ND	500 μM	no
Scr3	ND	25-30 μM	yes

The second criteria is the ability to stain in a birefringent manner with Congo Red (see Figure 2.2 for structure). Films of PrP 118-133 Met 129, PrP 118-133 Val 129, and Scr 3 all stained with Congo Red to give pinkish-red

Figure 2.3 Electron micrographs of fibrils at 60K magnification. A. PrP 118-133 Met 129. B. PrP 118-133 Val 129. C. Scr3. Fibrils were formed from supersaturated solutions in PBS pH 7.4. Black bar represents 100 nm in all panels.

Figure 2.4 Electron micrographs of fibrils. A.PrP 118-133 Met 129 from 10% DMSO at 60K magnification. B. PrP 118-133 Met 129 from PBS pH 2 at 50K magnification. C. Scr3 from 10% DMSO at 60K magnification. D. Scr3 from PBS pH 2 at 50K magnification.

Figure 2.5 Electron micrographs of fibrils at 60K magnification. A. PrP106-126. B. PrP106-126 Val 117. Fibrils were formed from supersaturated solutions in PBS pH 7.4. Black bar represents 100 nm in both panels.

Figure 2.6 X-ray diffraction pattern of unoriented PrP118-133 Met 129 fibrils.

Figure 2.3

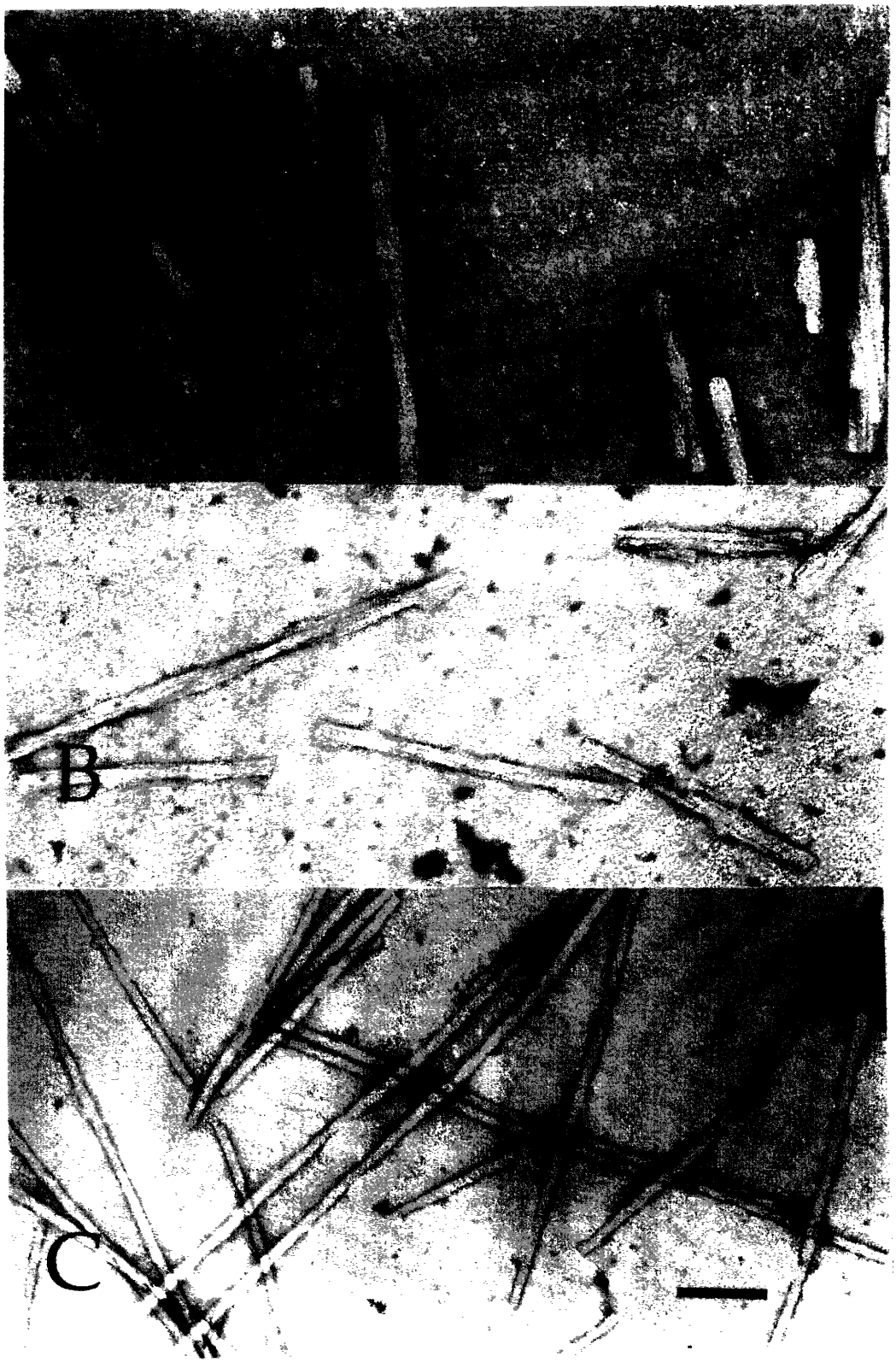

Figure 2.4

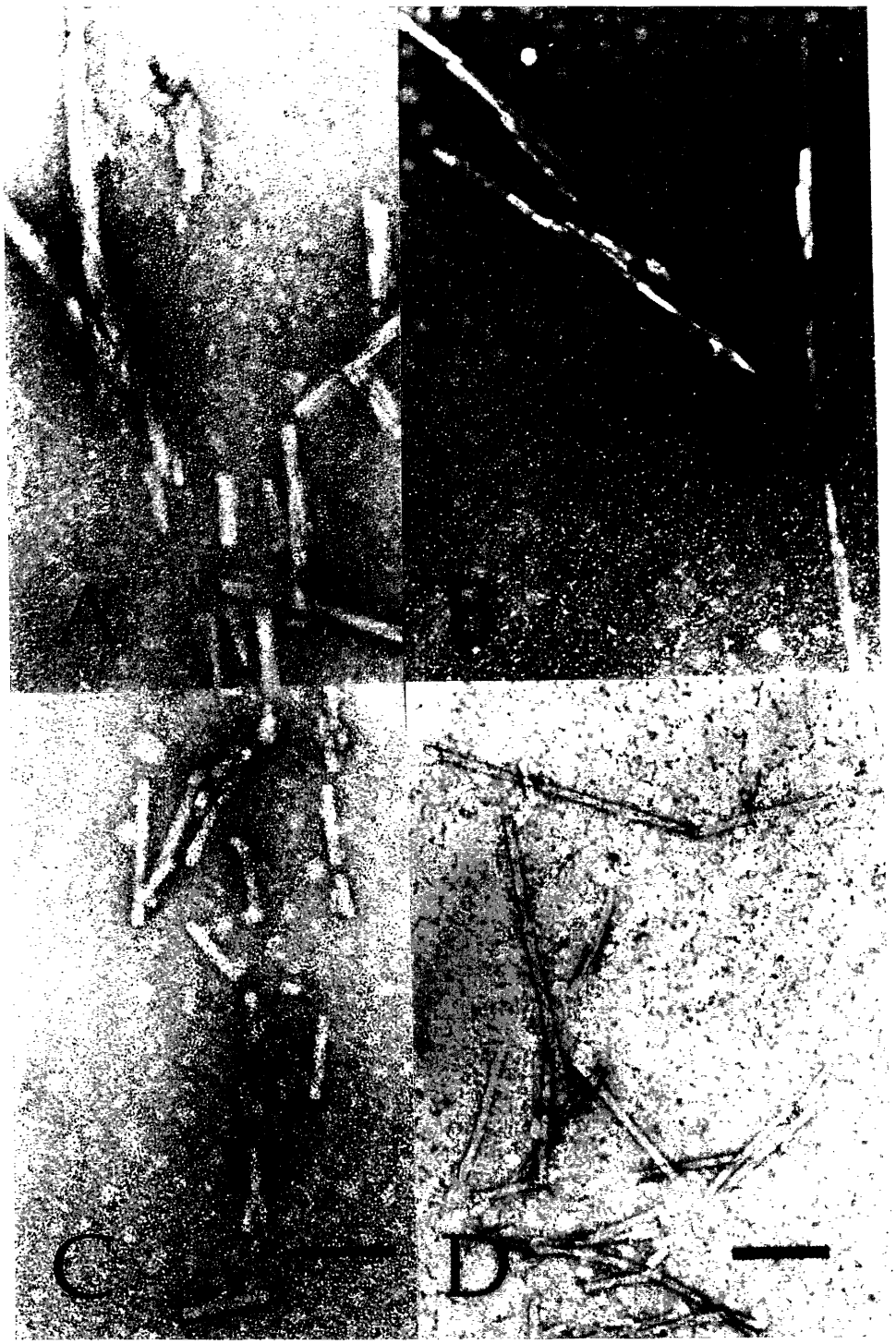

Figure 2.5

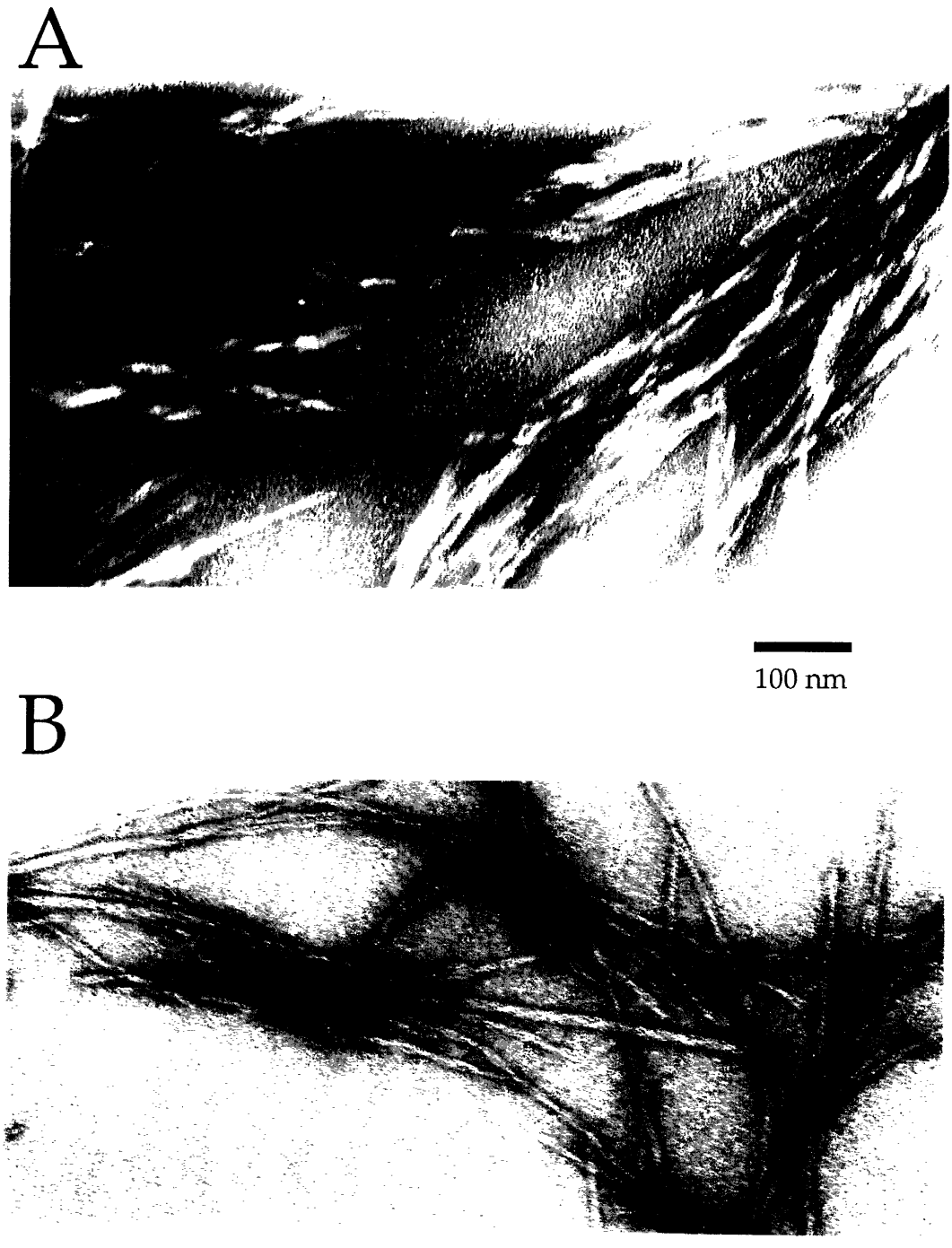

Figure 2.6. Fiber diffraction pattern of fibrils composed of PrP 118-133 Met 129

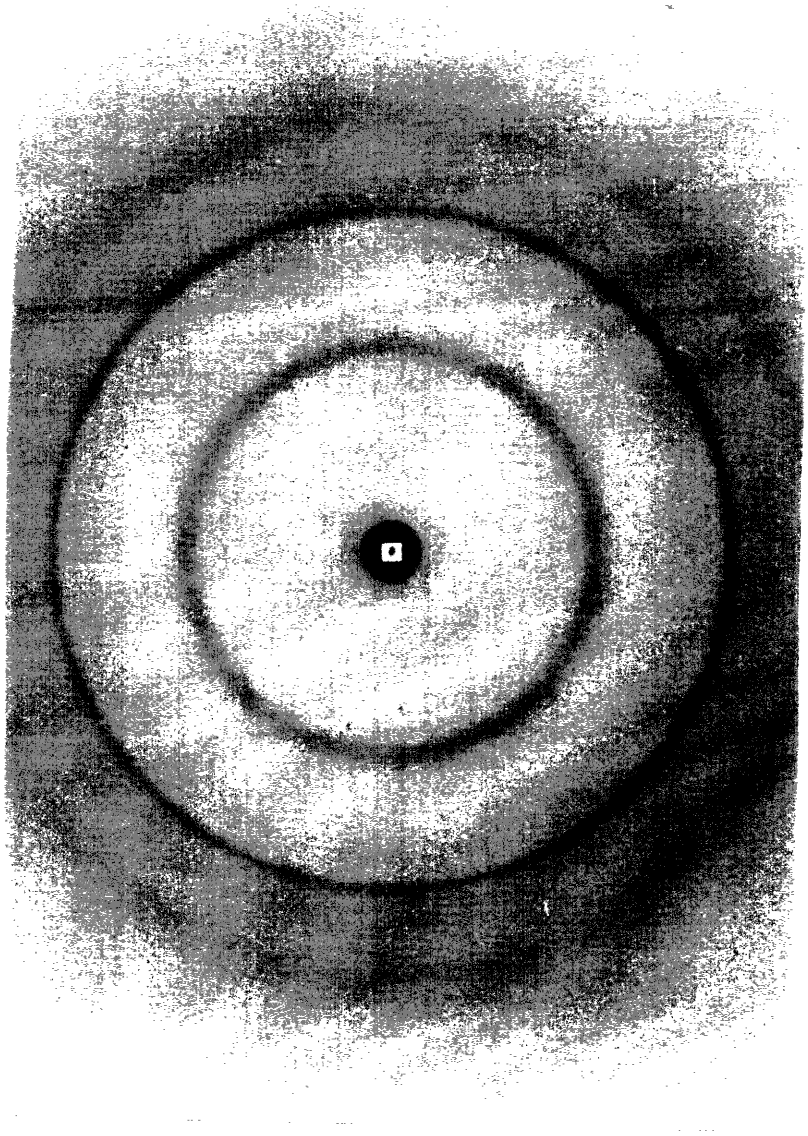

films. Staining was more effective if fibrils were formed in the presence of Congo Red. These films appeared apple-green when viewed under polarized light. PrP 118-133 Gly 129 and PrP118-133 Pro 129 were soluble at the concentration tested, and therefore, fibrils did not form to be stained with Congo Red. The exact nature in which Congo Red binds to amyloid fibrils is unknown. Cooper has postulated that Congo Red binds by intercalating into the hydrophobic space between sheets, holding the molecules in an ordered array.[34] Binding in this manner would appear to have a large disruptive effect on the fibrillar structure. It is not clear that the fibril could accommodate Congo Red in this way. Although Congo Red is a useful histological tool for staining tissue sections, it may not be a good tool for classifying protein structures because little is known about the specific requirements for binding.

The third criteria is an x-ray diffraction pattern consistent with a cross β-fibril. The x-ray diffraction pattern of oriented fibrils of PrP 118-133 Met 129 was taken by Paul Fraser and is shown in Figure 2.6. The outer ring corresponds to a spacing of 4.7Å, consistent with the chain-chain spacing in an antiparallel β-sheet. The inner band corresponds to a repetitive spacing of 7.4 Å. This distance probably corresponds to the distance between two β-sheets, similar to the 9.8 Å distance Glenner measured for the systemic amyloid, though slightly shorter. The tighter packing may be because of the high percentage of glycine residues in this sequence. Glycine allows the side chains of residues on adjacent strands to occupy the space that the side chain of non-glycine residues would occupy.

Structural features of peptides derived from the PrP sequence

The structure of PrP 118-133 Met 129 and Scr 3 was in solution was

Figure 2.7 CD spectra at 100 mM peptide in o, water, □, 35% HFIP/water, and •,100% HFIP. Panel A PrP118-133 Met 129. Panel B Scr 3.

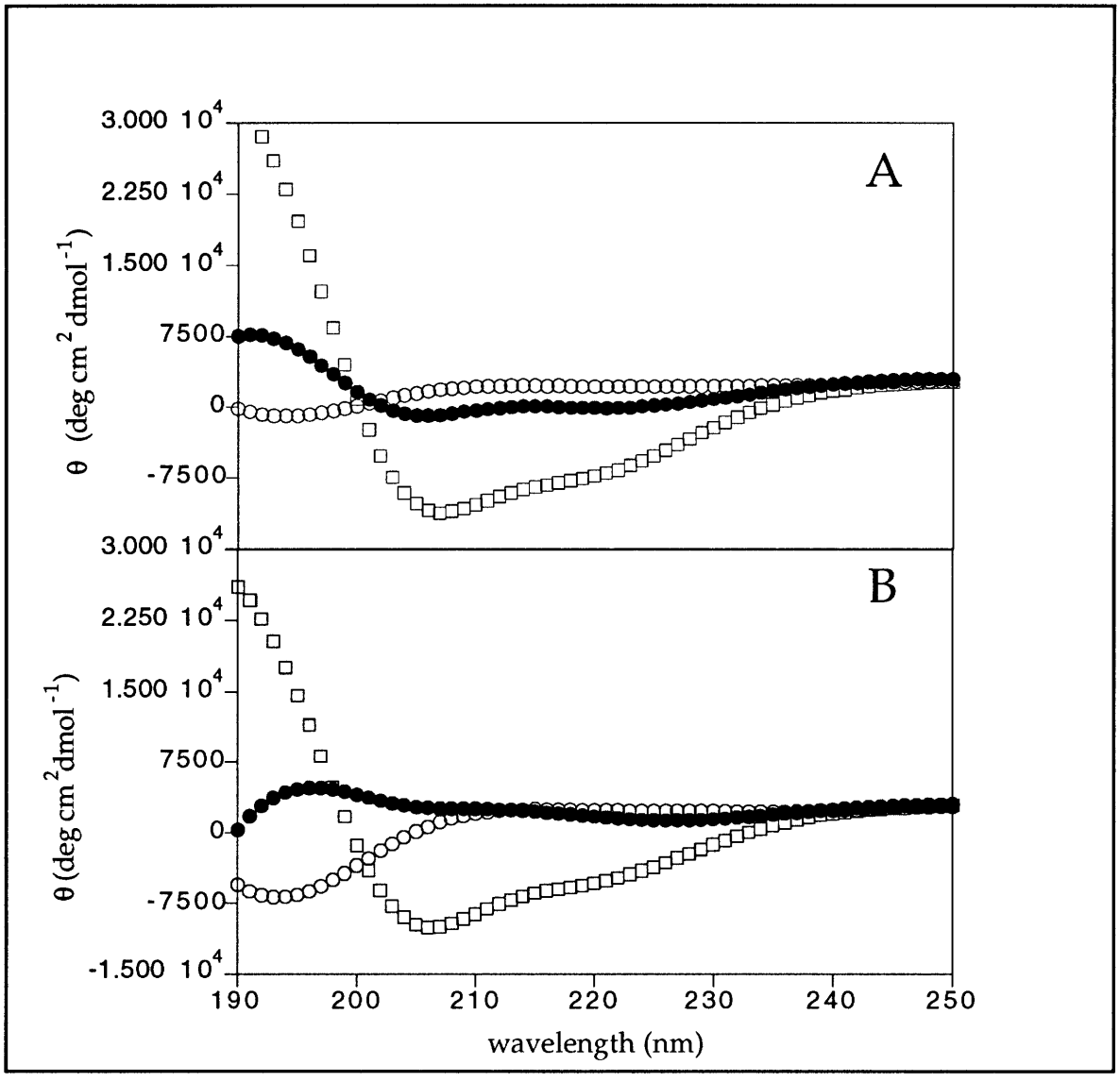

studied by circular dichroism. Both peptides had little structure in water. The helical content of both peptides increase with the addition of organic solvents such as HFIP or TFE. The CD spectra of PrP 118-133 Met 129 and Scr 3 are shown in Figure 2.7. The spectra are similar, particularly in mixtures of HFIP and water. The helical content was at a maximum at approximately 35 % HFIP and was 20 % for both peptides as calculated by the method of Morrisett et al.[35]

The fibrils composed of PrP peptides were also studied by FTIR. The FTIR of PrP^C and PrP^{Sc} have been shown to contain substantially different populations of secondary structures. Fibrils were formed from peptides corresponding to different regions of PrP to help elucidate which regions of the protein are important, and what conditions are necessary, for the conversion of PrP^C to PrP^{Sc}. Fibrils were formed of each of these peptides and dried onto CaF_2 plates. Several differences are apparent as shown in Figure 2.8.

The FTIR spectra of PrP 106-126 contains a strong absorption at ~1630 cm^{-1}, indicative of the highly coupled structure of an antiparallel β-sheet. There is a smaller absorption at ~1660 cm^{-1} arising from random coil/ helix/ turn structures which are not as easily differentiated by FTIR.

The spectra of PrP 118-133 Met 129, PrP 118-133 Val 129, and Scr3 were indistinguishable. The spectra of these peptides also showed a strong absorption at 1630 cm-1, but a greater intensity of absorptions in other regions, indicating a variety of conformations in these peptides. Apparently the scrambling of the residues in the central region did not change the conformational preferences substantially. However, because the FTIR data only describes the whole population of secondary structures, differences in the orientation of specific residues cannot be determined. There are differences in the surface presented in these fibrils as shown by the nucleation experiments in Chapter 3. These peptides could have the same populations of secondary structures, but because of the difference in sequence, the exact structures are likely to be different.

The FTIR spectra of PrP 101-144, which spans both PrP 118-133 and PrP 106-126 with additional residues on either side, had the strongest absorption

Figure 2.8 FTIR spectra of fibrils composed of PrP derived peptides dried onto CaF_2 plates. A. PrP 118-133 Met 129. B. PrP 106-126. C. PrP101-144. Fibrils were formed from buffer (100 mM NaCl, 10 mM phosphate, pH 7.4 and all spectra are smoothed equivalently.

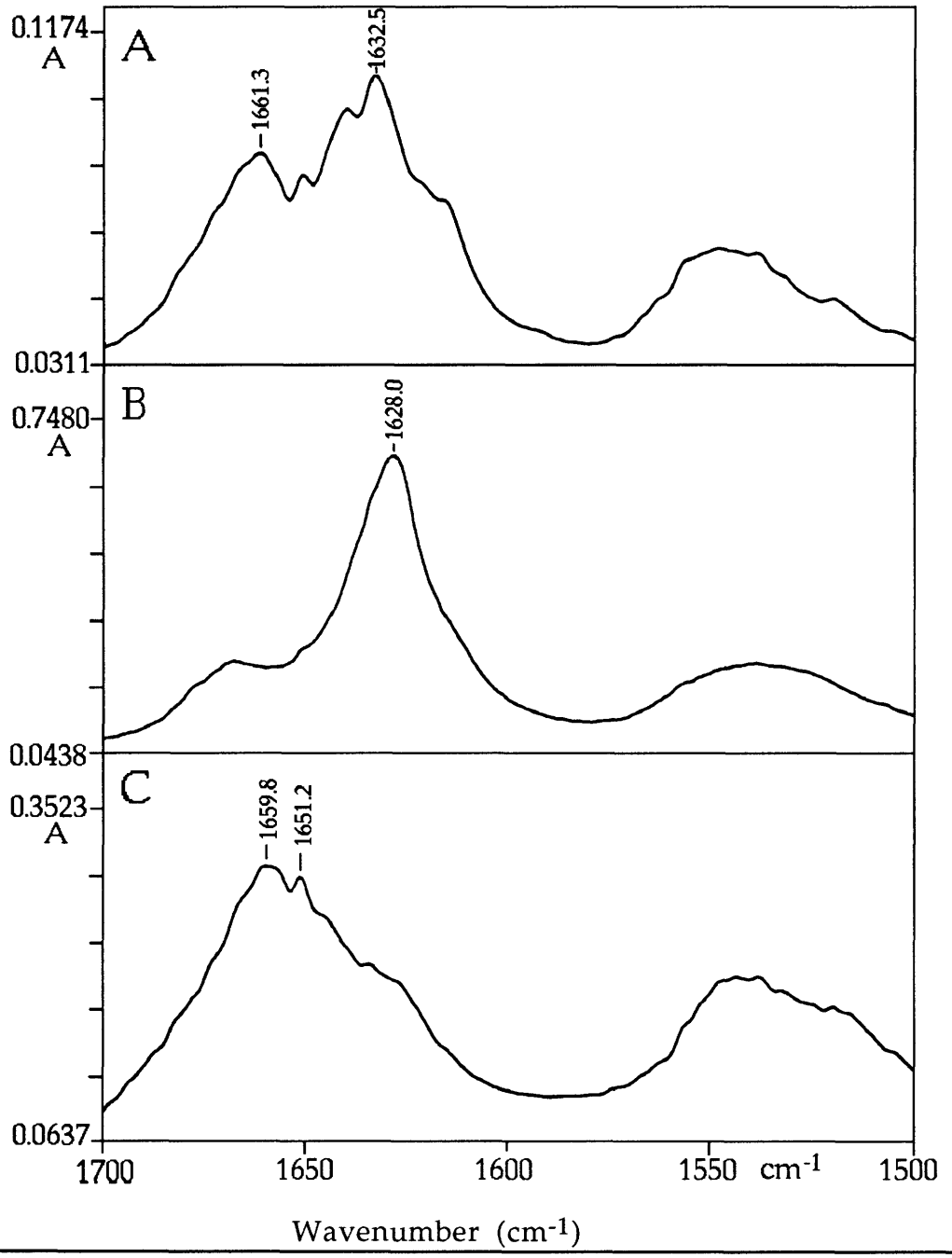

at approximately 1660 cm^{-1}, with little absorption in the region indicative of antiparallel β-sheets. Apparently the addition of residues flanking 106-133 cause the peptide to adopt other conformations. This peptide was significantly more soluble in distilled H_2O than buffer and also more soluble at pH 4.7 than pH 7.4. Fibrils were formed under different conditions to see if fibrils with more β-sheet structure could be produced under certain conditions and give some insight into the conditions necessary for *in vivo* protein assembly. None of the conditions attempted (100 mM NaCl,10 mM phosphate, pH7.4; 100 mM NaCl, 10 mM glycine, pH 9.7; 1M NaCl, 10 mM phosphate, pH 7.4, and 100 mM NaCl, 10 mM phosphate, 2 eq. heparin, pH 7.4) altered the FTIR spectra of the resulting fibrils.

From these FTIR studies, it appears that the region from residues 106-126 has the greatest tendency toward β-structures. This region is very hydrophobic and consists in part of a run of alanine residues (AGAAAAGA). This alanine-rich portion has been implicated by others as being very fibrillogenic.[29] and contains residue 117 which is mutated to valine in some cases of GSS.

EXPERIMENTAL

Peptide Synthesis

The peptides were made using either t-Boc/benzyl or Fmoc/Boc chemistry. In the t-Boc protocol, the Boc group was removed by treatment with 50% trifluoroacetic acid in methylene chloride for 15 min.. The resin was then washed three times each with CH_2Cl_2, DMF, CH_2Cl_2, and DMF. The couplings were done for about 1 hr. in DMF with 3 equiv. of incoming t-Boc protected amino acid, 3 equiv. of BOP, and 5 equiv. of DIEA. The completeness of the coupling was determined by a Kaiser test and double

couplings were done as necessary. In the Fmoc protocol, the Fmoc group was removed by treatment with 50% piperidine in DMF for 15 min.. The resin was washed 3 times each with DMF, CH_2Cl_2 and DMF. The couplings were done as in the case of the Boc protocol except that 0.5 equiv. of HOBt was added. In both cases the resin was acetylated after coupling by treatment with 5 equiv. Ac_2O, and 5 equiv. of DIEA in CH_2Cl_2 for 15 min.. The N-terminus was acetylated with 10 equiv. Ac_2O and 5 equiv. DIEA in CH_2Cl_2 for at least 4 hrs. and monitored by Kaiser test. All peptides were characterized (except PrP101-144) by isocratic RPHPLC, AAA, and mass spectra.

Reagent K for Fmoc protocol cleavage: 82.5 % trifluoroacetic acid, 5% phenol, 5 % H2O, 2.5% ethanedithiol, and 5 % thioanisole.

Ac-PrP118-133-NH_2-Met 129. AVVGGLGGY(2,6DiClBzl)MLGS(Bzl)A-MBHA resin. The synthesis was started with 1.92g (0.39 mmol/g) Boc-Ala-MBHA resin. Couplings were done as described above to give 3.61g of dried resin.
AAA resin S 0.4 (1), G 6.9 (6), A 3.2 (3), Y 0.96 (1), V2* (2), M 0.8 (1), L 2.2 (2).

Cleavage, deprotection, purification. The peptide resin (1.55g) was treated with 30 mL HF, 1.6 mL thioanisole, and 1.6 mL m-cresol at 0°C for 1 hour. After removal of the HF, the residue was taken up in TFA, filtered, and washed with more TFA. After evaporation of most of the TFA, the remainder was precipitated from Et_2O, spun down and dried to 540 mg crude peptide. A portion of this (100 mg) was purified by reverse-phase HPLC, on a C_4 column using as eluents (CH_3CN + 0.1 % TFA) and (H2O + 0.1 % TFA) on a gradient (85/15 to 65/35) to give 239 mg, 0.17 mmol, pure peptide. This extrapolates to a 42% yield based on Boc-Ala-resin.
FABMS (Harvard) MNa^+ 1442. AAA Ser 1.1 (1), Gly 6.0 (6), Ala* 3.0 (3), Tyr 0.9 (1), Val 1.5(2), Met 0.8 (1), Leu 1.9 (2).

Ac-PrP118-133-NH_2-Met 129. 2.0 g (0.4 mmol/g), 0.8 mmol of Rink amide- methylbenzhydrylamine resin was used in an Fmoc synthesis. The couplings were done as described above. The resin was dried to 2.89 g and 2.5 g was used in the cleavage reaction. The dried resin was taken up in 50 mL reagent K. and stirred under nitrogen at room temperature for 2 hrs. The reaction was filtered through a sintered glass funnel, the filtrate was concentrated to an oil, and 150 mL of cold Et_2O was added. A white precipitate formed and the suspension was centrifuged, washed with Et_2O 2 more times and the solid dried to 0.81 g. This was purified by reverse-phase HPLC, on a C_4 column using as eluents (CH_3CN + 0.1 % TFA) and (H2O + 0.1 % TFA) on a gradient (85/15 to 65/35) to give 239 mg, 0.17 mmol, pure peptide in 21% yield. PDMS MH^+ 1420. AAA Ser 1.0 (1), Gly 5.9 (6), Ala 3* (3), Tyr 1.0 (1), Val 1.5 (2), Met 0.7 (1), Leu 2.0 (2).

Ac-PrP118-133-NH_2 Val 129. Synthesis accomplished as above using 2.0 g of Rink amide-methylbenzhydrylamine resin in an Fmoc synthesis which was dried to 2.4 g ; 2.2 g was cleaved and worked up as above. This gave 1.12 g of crude peptide. A portion (350 mg) was purified by RPHPLC (same system as above) to give 94 mg (27 % yield). PDMS MH+ 1388. AAA Ser 1.0 (1), Gly 5.9 (6), Ala 2.8 (3),Tyr 0.8 (1), Val 2.1(3), Leu 2* (2)

Ac-AGAVGVLGGYGMLGSA-NH_2. 2.0 g, 1 mmol of 4-(2'-,4'-Dimethoxyphenyl-fmoc-aminomethyl)-phenoxy resin (0.5 mmol/g) was used in an Fmoc synthesis. The couplings were done as above. The resin was dried to 2.7 g and 1.3 g was cleaved with reagent K as described above to give 0.53g of crude peptide. A portion (100 mg) was purified by RPHPLC (same gradient as above) to give 37 mg of pure peptide in 14 % yield. PDMS MH+ 1420. AAA Ser 1.0 (1), Gly 6.0 (6), Ala 3* (3),Tyr 1.0 (1), Val 1.9 (2), Met 0.8 (1), Leu 2.0 (2).

$^3H_3CC(O)NH$-PrP118-133 Met 129. To 6.0 mg, 4.3 μmol H_2NPrP118-133 Met 129, 40 μL (0.4mCi) of a 0.102M solution of $^3H_3C(O)ONa$ (10mCi/mL. 97.7 mCi/mmol) in EtOH was added. The EtOH was removed with a stream of nitrogen, and 10 equiv. BOP, 2 equiv. DIEA were added in 0.2 mL DMF. This solution/suspension was stirred for 90 min. at which point 1 mg of cold sodium acetate was added. After 3 hrs. 0.5 mL H_2O was added and the reaction shaken for 14 hrs. The suspension was centrifuged and the pellet washed twice with H_2O. HFIP was added to bring the total volume to approximately 0.5 mL. The PDMS gave MH+ 1420, MNa+ 1433. Scintillation counting of a small aliquot gave a specific activity of 38mCi/ mmol. This solution was added to cold peptide for experiments requiring radiolabeled peptide.

$^3H_3CC(O)NH$-PrP118-133 Val 129. Synthesized using the procedure described above for PrP118-133 Met 129. The specific activity of the final solution was 46 mCi/mmol.

Mouse PrP101-144. 1.0 g MBHA resin was used in a t-Boc synthesis. The side-chain protecting groups were as follows: Lys-Cl-Z, Thr benzyl, His-benzyloxymethyl, Tyr-2,6 dichlorobenzyl, Ser-benzyl, Arg-MTS, Asp-cyclohexyl. Double couplings were required at positions 138, 136, 121, 104, 101. A triple coupling was done at Asn 108 with the third coupling using HOBt and DIC. The resin was dried to 3.7 g and the cleavage was done on 1.2 g using a low-high HF procedure described below. The resin was first treated at 0°C for 2 hr. with a mixture of 13 mL dimethyl sulfide (DMS), 4 mL p-cresol, and 5 mL anhydrous HF. The HF and DMS were removed *in vacuo*, after which 20 mL additional HF was added. After stirring for 1 hr. the HF was removed *in vacuo* at less than 10° C and the residue kept *in vacuo* overnight. The residue was then taken up in 25 mL TFA and filtered into 300 mL of cold

Et_2O. The remaining resin was washed with 2 portions each of 5 mL of TFA into the Et_2O. The resulting Et_2O suspension was centrifuged and the pellet washed 2 times with Et_2O. The pellet was then dried to 860 mg of a beige solid. Initial attempt at purification by RPHPLC were not fruitful. The peptide was purified using a Waters ultrastyragel-HT 10^3 Å size exclusion column run in HFIP.[36] 100 mg of crude material yielded 15 mg of a white powder. LDMS MH+ 4359 (calc. 4365). AAA Ala 7.0 (7), Asx 3.1(3), Phe 1.1 (1) Gly 7.9 (8), His 1.8 (2), Ile 0.7 (1), Lys 3.6 (4), Leu 3.0 (3), Met 2.6 (3), , Pro 3* (3), Arg 1.1 (1), Ser 2.8 (3), Thr 0.9 (1), Val 2.3 (3), Tyr 0.9 (1).

Ac-PrP106-126. This peptide was synthesized by Carmen Barnes on Rink amide resin. Couplings were done as described above. The cleavage was as described above for PrP118-133 Met to give 0.8 g of crude peptide. This was slightly soluble in DMSO and 200 mg was prepped (C4, eluents as above, 80/20 to 55/45) to yield 39 mg of pure peptide as a white powder. PDMS MH+ 1955.

Ac-PrP106-126 Val 117. This peptide was synthesized by Carmen Barnes on Rink amide resin. Couplings were done as described above. The cleavage was as described above for PrP118-133 Met to give 1.0 g of crude peptide. This was slightly soluble in DMSO and 200 mg was prepped (as above) to yield 28 mg of pure peptide as a white powder. PDMS MH+1983.

Electron microscopy

Fibrils for electron microscopy were either taken from kinetic assay experiments (see chapter 3 and 4) or were prepared as described below for the FTIR samples. Aliquots of suspended fibrils were placed onto carbon-coated copper grids and let sit for 1-5 min. These were washed with H2O, and then stained with a 2 % uranyl acetate solution. Electron micrographs (EMs) were

taken on a JOEL 1200 CX electron microscope operating at 80 kV, at a magnification of 60,000X.

Congo red staining

Samples were prepared by drying fibrils onto glass microscope plates. These plates were dipped into a solution of 1 mM Congo Red, 100 mM NaCl, 10 mM phosphate, pH 7.4, and then rinsed in distilled water. Samples were also prepared by forming fibrils in the presence of the same Congo Red solution. Samples were viewed with a Wild Leitz M3Z light microscope equipped with a polarizing stage to determine birefringence.

FTIR of fibrils.

Fibrils for FTIR were prepared by the addition of a concentrated DMSO solution to buffer. This solution was stirred for several hours to days and then centrifuged. The pellet was washed twice with H_2O and the wet fibrils were spread evenly onto a CaF_2 plate with the end of a pipet and dried *in vacuo*. The spectra were taken on a Perkin-Elmer series 1600 FTIR spectrometer at 2.0 cm^{-1} resolution. The interferograms from 64 scans were averaged. The spectra were smoothed, as noted, to improve signal to noise. Peak positions were determined with the aid of second derivative analysis.

Protein Sequence Search

The CAS Online protein sequence database was searched for proteins containing the $(GXXX)_n$ where $n \geq 3$, and x is any uncharged residue other than proline (G, A, V, I, L, F, W, T, Y, S, or M). Eighty sequences matched this criteria. Sequences containing polyglycine or (GX)n repeats (silk proteins) were eliminated. The remaining sequences were narrowed down to those

which were hydrophobic (hydropathy ≥ 1.4) and which contained residues often found in β-sheets over α-helices (P_β-$P_\alpha \geq 0.17$). Twenty-seven sequences remained, including the β-amyloid protein and PrP.

REFERENCES FOR CHAPTER 2

(1) Prusiner, S. B.; *Annu. Rev. Microbiol.* **1989**, *43*, 345.
(2) Prusiner, S. B.; McKinley, M. P.; Bowman, K. A.; Bolton, D. C.; Bendheim, P. E.; Groth, D. F.; Glenner, G. G.; *Cell* **1983**, *35*, 349.
(3) McKinley, M. P.; Meyer, R. K.; Kenaga, L.; Rahbar, F.; Cotter, R.; Serban, A.; Prusiner, S. B.; *J. Virology* **1991**, *65*, 1340.
(4) Sipe, J.; *Annu. Rev. Biochem.* **1992**, *61*, 947.
(5) Stone, M. J.; *Blood* **1990**, *75*, 531.
(6) Pepys, M. B.; Hawkins, P. N.; Booth, D. R.; Vigushin, D. M.; Tennent, G. A.; Soutar, A. K.; Totty, N.; Nguyen, O.; Blake, C. C. F.; Terry, C. J.; Feest, T. G.; Zalin, A. M.; Hsuan, J. J.; *Nature* **1993**, *362*, 553.
(7) Halverson, K., The Molecular Determinants of Amyloid Deposition on Alzheimer's Disease, *Ph.D. Thesis, Massachusetts Institute of Technology,* **1992.**
(8) Glenner, G. G.; *N. Engl. J. Med* **1980**, *302*, 1333.
(9) Friedreich, N.; Kekule, A.; *Virchows Arch.* **1859**, *16*, 50.
(10) Glenner, G.; Harada, M.; Isersky, C.; Cuatrecasas, P.; Page, D.; Keiser, H.; *Biochem. Biophys. Res. Comm.* **1970**, *41*, 1013.
(11) Glenner, G. G.; Terry, W.; Harada, M.; Isersky, C.; Page, D.; *Science* **1971**, *172*, 1150.
(12) Seubert, P.; Vigo-Pelfrey, C.; Esch, F.; Lee, M.; Dovey, H.; Davis, D.; Sinha, S.; Schlossmacher, M.; Whaley, J.; Swindlehurst, C.; McCormack, R.; Wolfert, R.; Selkoe, D.; Lieberberg, I.; Schenck, D.; *Nature* **1992**, *359*, 325.
(13) Miller, D.; Papayannopoulos, I.; Styles, J.; Bobin, S.; Lin, Y.; Biemann, K.; Iqbal, K.; *Arch. Biochem. Biophys.* **1993**, *301*, 41.
(14) Mori, H.; Takio, K.; Ogawara, M.; Selkoe, D.; *J. Biol. Chem.* **1992**, *267*, 17082.
(15) Glenner, G.; Wong, C.; *Biochem. Biophys. Res. Comm.* **1984**, *120*, 885.
(16) Jarrett, J. T.; Berger, E. P.; Lansbury Jr., P. T.; *Biochem.* **1993**, *32*, 4693.
(17) Citron, M.; Oltersdorf, T.; Haass, C.; McConlogue, L.; Hung, A. Y.; Seubert, P.; Vigo-Pelfrey, C.; Lieberburg, I.; Selkoe, D. J.; *Nature* **1992**, *360*, 672.
(18) Cai, X. D.; Golde, T. E.; Younkin, S. G.; *Science* **1993**, *259*, 514.
(19) Eanes, E. D.; Glenner, G. G.; *J. Histochem. Cytochem.* **1968**, *16*, 673.
(20) Termaine, J. D.; Eanes, E. D.; Ein, D.; Glenner, G. G.; *Biopolymers* **1972**, *11*, 1103.
(21) Marsh, R. E.; Corey, R. B.; Pauling, L.; *Acta Cryst.* **1955**, *8*, 710.
(22) Marsh, R. E.; Corey, R. B.; Pauling, L.; *Biochim. Biophys. Acta* **1955**, *16*, 1.
(23) Mitraki, A.; King, J.; *Bio/Technology* **1989**, *7*, 690.
(24) London, J.; Skryzynia, C.; Goldberg, M.; *Eur. J. Biochem.* **1974**, *47*, 409.
(25) Colon, W.; Kelly, J. W.; *Biochemistry* **1992**, *31*, 8654.

(26) Tagliavini, F.; Prelli, F.; Verga, L.; Giaccone, G.; Sarma, R.; Gorevic, P.; Ghetti, B.; Passerini, F.; Ghibaudi, E.; Forloni, G.; Salmona, M.; Bugiani, O.; Frangione, B.; *Proc. Natl. Acad. Sci. USA* **1993**, *90*, 9678.
(27) Selvaggini, C.; De Giora, L.; Cantu, L.; Ghibaudi, E.; Diomede, L.; Passerini, F.; Forloni, G.; Bugiani, O.; Tagliavini, F.; Salmona, M.; *Biochem. Biophys. Res. Comm.* **1993**, *194*, 1380.
(28) Forloni, G.; Angeretti, N.; Chiesa, R.; Monzani, E.; Salmona, M.; Bugliani, O.; Tagliavini, F.; *Nature* **1993**, *362*, 543.
(29) Gasset, M.; Baldwin, M. A.; Lloyd, D. H.; Gabriel, J.-M.; Holtzman, D. M.; Cohen, F.; Fletterick, R.; Prusiner, S. B.; *Proc. Natl. Acad. Sci. USA* **1992**, *90*, 10940.
(30) Goldfarb, L. G.; Brown, P.; Haltia, M.; Ghiso, J.; Frangione, B.; Gajdusek, D. C.; *Proc. Natl. Acad. Sci. USA* **1993**, *90*, 4451.
(31) Nochlin, D.; Sumi, S. M.; Bird, T. D.; Snow, A. D.; Leventhal, C. M.; Beyreuther, K.; Masters, C. L.; *Neurology* **1989**, *39*, 910.
(32) Hsiao, K. K.; Cass, C.; Schellenberg, G. D.; Bird, T.; Devine-Gage, E.; Wisniewski, H.; Prusiner, S. B.; *Neurol.* **1991**, *41*, 681.
(33) Chou, P. Y.; Fasman, G. D.; *Biochemistry* **1974**, *13*, 222.
(34) Cooper, J.; *Lab. Invest.* **1974**, *31*, 232.
(35) Morrisett, J. D.; David, J. J. K.; Pownall, H. J.; Grotto Jr, A. M.; *Biochemisrty* **1973**, *12*, 1290.
(36) Hendrix, J.; Halverson, K.; Lansbury Jr., P. T.; *J. Am. Chem. Soc.* **1992**, *114*, 7940.

Chapter 3
Kinetics of Fibril Formation in PrP-Derived Peptides

Having established that peptides derived from the PrP sequence can form amyloid fibrils, we studied the kinetics of this process to elucidate its mechanism. This chapter will discuss experiments on the kinetics of fibril formation and possible mechanistic consequences. The kinetics were measured by forming supersaturated solutions of peptide and measuring the formation of amyloid fibrils over time. Fibril formation followed nucleation-dependent kinetics, which are characterized by a significant period of no measurable fibril formation, followed by relatively rapid growth. The nucleation phase of this polymerization can be bypassed by the addition of previously formed fibrils. This nucleation, or "seeding", process involves specific interactions as shown by the inability of related peptides to nucleate the growth of fibrils in solutions of each other. The *in vivo* consequences of a nucleation-dependent mechanism are discussed.

Mechanisms for Protein Polymerization

Three possible mechanisms have been suggested for protein polymerization: simple growth, exponential, or nucleation-controlled (see Figure 3.1).[1]

In simple or isodesmic growth, the addition of each monomer is favorable to the same extent. That is, the free energy is negative and of similar magnitude for each added monomer regardless of the size of the aggregate. Larger aggregates are favored, but smaller ones are populated according to a Boltzmann distribution, particularly at early times. An example is polymerization involving covalent bonds, such as polyethylene.

Exponential growth is an example of positive cooperativity, that is the addition of each monomer is more favorable than the addition of the preceding monomer. The free energy change is negative for the addition of each monomer and larger in magnitude as the aggregate size increases One explanation for exponential growth is that larger aggregates have more

Figure 3.1 Free energy dependence on aggregate size for three mechanisms for growth of polymers: simple, exponential, and nucleation-controlled. Adapted from reference 1.

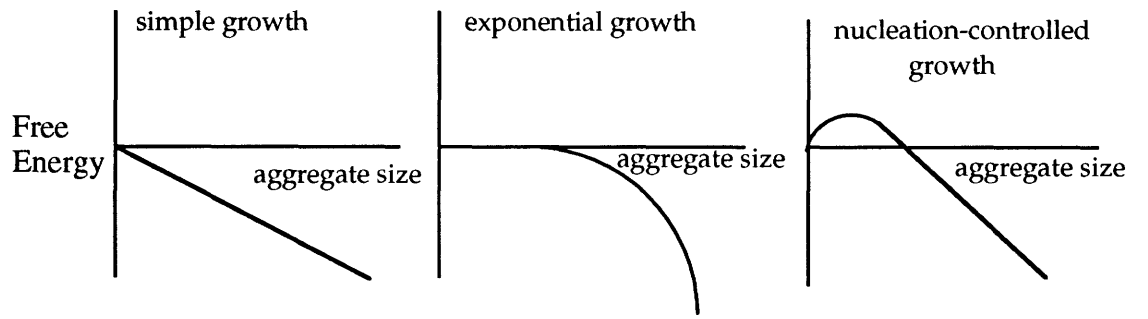

surfaces for additional monomers to attach to than smaller ones do. As the aggregate grows, the rate of growth increases because of the increase in sites for monomer attachment.

The aggregation of the peptides discussed here is an example, along with protein and small molecule crystallization, of the third mechanism, nucleation-controlled polymerization. There are two phases in a nucleation-dependent polymerization (see Figure 3.2), the nucleation phase (or lag time)

and the growth phase. The nucleation phase is a result of the unfavorable initial equilibria. Monomer addition is favorable enthalpically because of the formation of hydrophobic contacts, electrostatic interactions, and hydrogen bonds between the monomer and the aggregate.[2] However, the formation of these contacts fixes the monomer in a particular conformation and is therefore disfavored entropically. In the initial steps of a nucleation-dependent polymer assembly, the gain in enthalpy upon dimerization or addition of monomer to the oligomer does not outweigh the loss of entropy of the monomer. The addition of more monomers continues to be unfavorable until an oligomer of sufficient size is formed which allows enough contacts between monomer and aggregate to make monomer

Figure 3.2 Theoretical diagram of fibril formation following a nucleation-dependent mechanism.

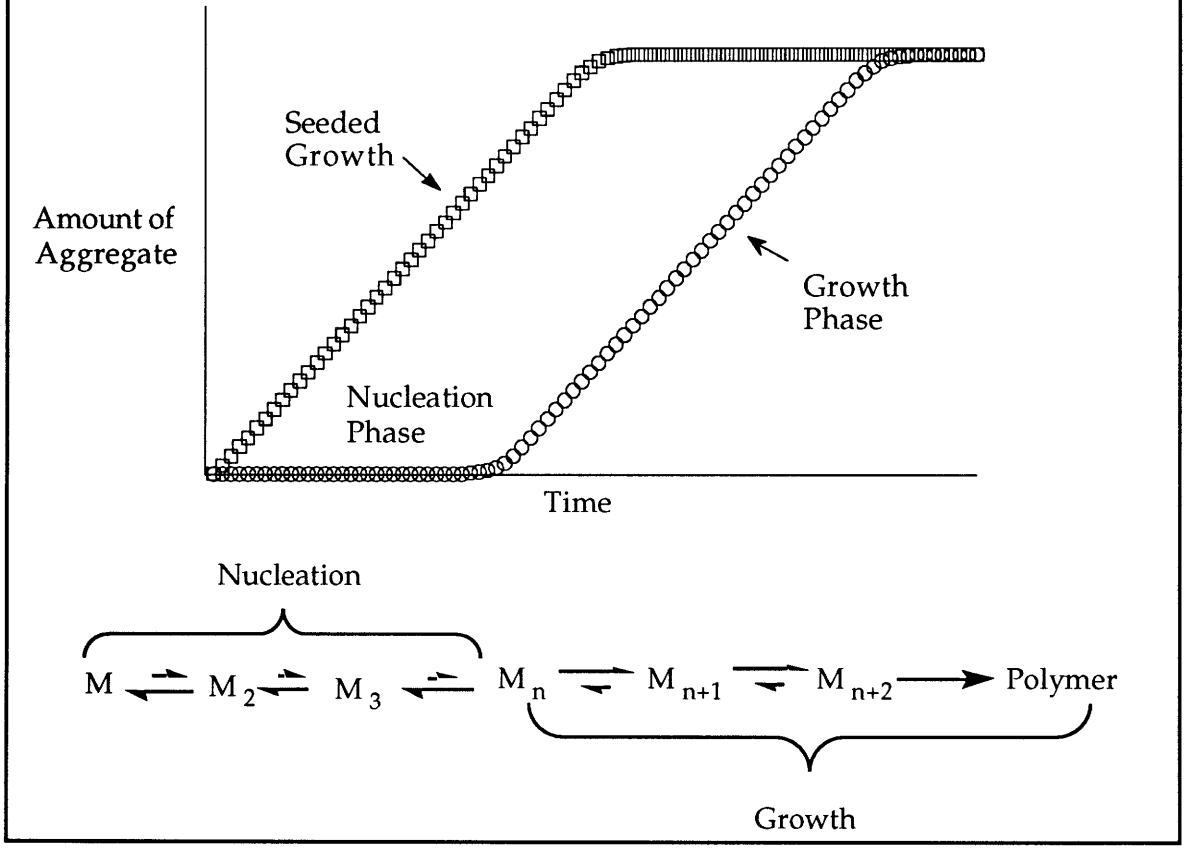

addition favorable. This oligomer is the high point in energy and is defined as the nucleus. After nucleus formation the addition of monomer is favorable and the growth phase begins. While the monomer suffers similar entropic losses as in the earlier stages of assembly, additional (negative) enthalpic terms account for the negative free energy. The growth continues until thermodynamic equilibrium (the solubility of the peptide or protein) is reached.

In this mechanism, the free energy for adding monomers is positive, until the nucleus is reached, which is by definition the high point in free energy. Oligomers smaller than the nucleus are unstable and no appreciable population of these intermediates (dimers, trimers etc.) can be detected. The only detectable states of peptide are monomer and high molecular weight oligomers.

The nucleation time is dependent on the concentration of monomer as shown in Equation 3.1 below:

Eq 3.1 $$\text{Nucleation time} = k[\text{monomer}]^n$$

where n is the number of monomers in the nucleus and k is a constant which is different for each protein assembly. Slight differences in monomer concentration can have a dramatic effect on the nucleation time. For example, if n=8, a 10% increase in the concentration of the monomer would have a $(1.1)^8$ or over two fold effect on the nucleation time. If n=20 the same 10% increase would have over a seven fold effect on the nucleation time. This increase, considered within the context of *in vivo* mechanisms for protein degradation, could easily be sufficient to cause protein deposits to form in certain instances. Other well-studied nucleation-dependent

polymerization processes, such as sickle-cell hemoglobin fibril formation, have this concentration dependence.[3, 4, 5] The measurement of this effect can be difficult due to the narrow range over which it can be measured experimentally, a concentration dependence of nucleus size., and the effect of agitation and surface interactions on the rate of polymerization.[6] Agitation can also have a significant effect in small molecule crystallizations.[7]

The nucleation time may be thermodynamically- or kinetically-limited.[8] In the thermodynamically-limited mechanism, there is a rapid (before the first measurement) pre-equilibrium of all species smaller than the nucleus. The production of aggregates is slow due to the low equilibrium concentration of nuclei as is the case for actin and tubulin polymerization.[9, 10, 11, 12] In this mechanism, some growth can be detected immediately.

The other extreme is a kinetically-limited mechanism. In this mechanism, the formation of small oligomers is still thermodynamically unfavorable, but the slow formation of aggregate is due to the slow rate of these initial steps. The nucleation time of hemoglobin S polymerization *in vitro* can be modeled using this mechanism.[3, 13] In this mechanism, the plots of the aggregation kinetics are flatter in the initial stages than in the thermodynamically-limited nucleation. Secondary nucleation effects also play a role in hemoglobin polymerization.[13] Prenuclei are stabilized by contacts with preexisting fibrils (seeding occurring off the side of the fibril) resulting in auto catalysis and a faster approach to equilibrium after nucleation than seen in the tubulin case. The differences between these two mechanisms has been discussed in detail elsewhere.[8]

The nucleation phase can be eliminated by the addition of an ordered oligomer or seed to which the monomer can add. This seed is sometimes referred to as a nucleus although the nucleus is the highest energy species and

is unlikely to be trapped in a test tube. In this way the unfavorable initial equilibrium are bypassed and growth begins immediately. The rate of growth will depend on the number of surfaces available in the added seed. In protein crystallization a similar effect is observed. Formation of crystals is frequently inconsistent and can be facilitated by the addition of a seed crystal. This "seeding" effect has also been seen in other protein polymerizations.[14]

Fibril Formation in Unstirred Solutions

Supersaturated solutions were formed from HFIP films of PrP 118-133 Met 129 and Scr 3. As with many peptides, it is possible to dissolve these peptides temporarily at a concentration higher than their solubility, forming metastable or "kinetically" soluble solutions. This effect can have significant experimental consequences. In many of the studies of the effect of β1-40 on neurons in cell culture, the peptide was dissolved at concentrations above its thermodynamic solubility. The period of time between dissolution and use then becomes critical to the exact nature of the peptide used. "Aged", aggregate containing preparations of β1-40 are neurotoxic in cell culture whereas freshly dissolved solutions exhibit neurotrophic effects.[15] This difference may in part explain the controversial and conflicting results of earlier studies. These studies also suggest that the formation of aggregates could have important *in vivo* consequences. We studied the kinetics of fibril formation from these metastable solutions.

Supersaturated solutions of PrP 118-133 Met and Scr 3 were prepared at 300 μM peptide in buffer. The fibril formation was measured by the turbidity, or light scattering, at 400 nm. These solutions were left undisturbed and were agitated briefly by vortexing before measuring the turbidity. Agitation was important to disperse aggregate uniformly in the light path, and because

solutions left completely undisturbed could remain homogeneous for weeks. Solutions agitated continuously by stirring formed fibrils within a few hours, whereas the solutions measured here, with occasional agitation, formed fibrils over several days. These experiments can also be affected by many factors, such as trace impurities, different agitation, and surface nucleation effects, which may be difficult to control. Because of the importance of agitation and other factors, the best comparison is of fibril formation experiments that were done at the same time.

In addition to the similarity in solubility, morphology by EM, and secondary structure by FTIR, PrP 118-133 Met 129 and Scr 3 showed no consistent difference in the kinetics of fibril formation (see Figure 3.3). The original hypothesis, which led to the synthesis of Scr 3, was that the spacing of glycine has a significant effect on the ability to form amyloid fibrils. It appears that this spacing is not a determinant of amyloid forming ability in this case. Scr 3 however, has been a useful tool to probe the specificity of the amyloid forming process. As shown by the diversity of proteins which form amyloid *in vivo*, many sequences are able to form ordered arrays. Although the sequence can have a large impact on solubility, the composition of a peptide or protein (the overall hydrophobicity) is an important determinant and may have an overriding effect on the solubility.

In the solutions of PrP 118-133 Met 129 and Scr 3, initially very little turbidity was measured although a small amount of early growth is seen. After a few days, the turbidity increased relatively rapidly, but still required several hours before aggregate formation was complete. This lag time where no apparent growth occurs is consistent with a nucleation-dependent mechanism for amyloid formation.

Figure 3.3 3 runs each of unstirred aggregations of PrP 118-133 Met 129 (o) and Scr 3 (•) at 300 μM peptide in buffer as measured by light scattering at 400 nm.

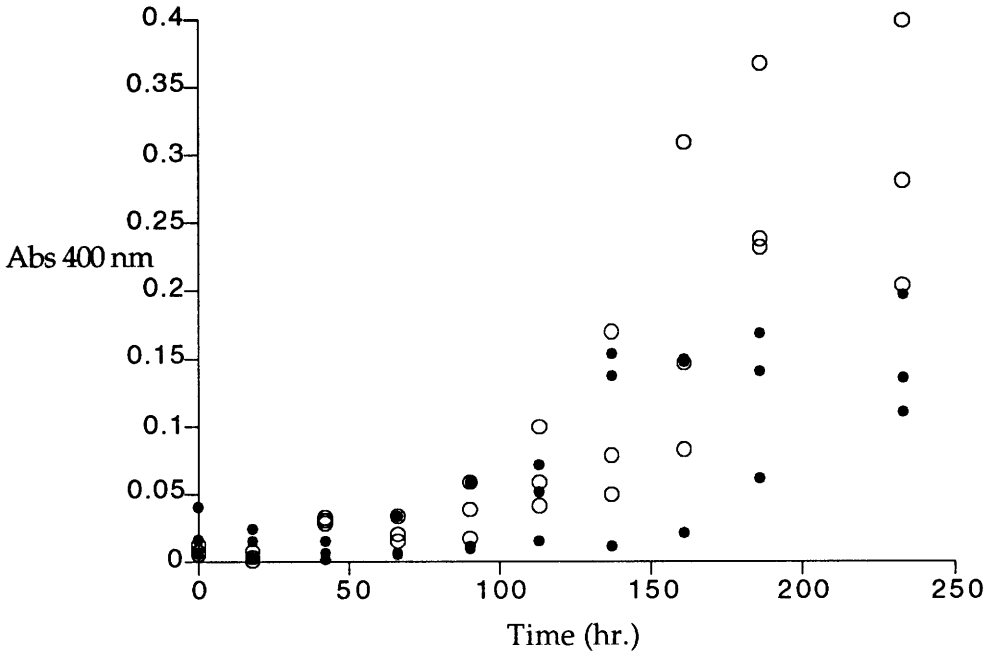

Seeded Fibril Formation

As discussed above, the nucleation phase of the polymerization can be bypassed in a nucleation-dependent polymerization if oligomers larger than the nuclei are added to the supersaturated solution at the beginning. This was done by the addition of preformed fibrils obtained from a previous run (5 molar %). The addition of these seed fibrils caused a significant increase in the rate of fibril formation. The seeding experiments were done with solutions of PrP 118-133 Met 129 and Scr3. Unseeded runs are shown along with runs where preformed fibrils were added (see Figures 3.4 and 3.5). In order to test the selectivity of the seeding effect, fibrils composed of the peptide in solution or fibrils composed of a different peptide were added to

Figure 3.4 Unstirred aggregation of PrP 118-133 Met 129 as measured by light scattering at 400 nm. Average of 3 runs are shown with standard deviations. •, unseeded solution. □, seeded with PrP 118-133 Met 129 (self-seeded). ◊, seeded with Scr3

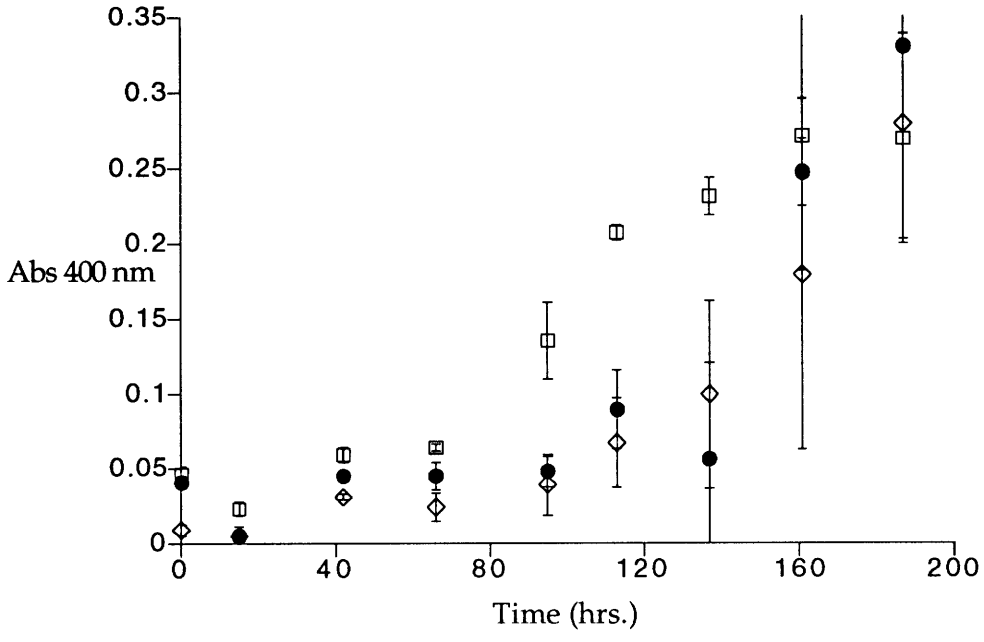

the supersaturated solution. That is, PrP 118-133 Met 129 was seeded with itself and fibrils composed of Scr3. The analogous experiment was done with supersaturated solutions of Scr3.

The data shown in Figure 3.4 is for the average of three runs each of PrP 118-133 Met 129 unseeded, self-seeded, and seeded with Scr3. Fibril formation occurs faster in the homogeneously seeded samples although some delay is observed. The growth phase in the self-seeded solution is less steep than the other two samples but begins much sooner. This could be the result of a small number of competent surfaces in the seed, which in turn could be a function of the length of the fibrils, or the degree in which they adhere together. The effectiveness of the seeding can be increased by sonicating the

fibrils before their addition, presumably by exposing more surfaces. Analogously, the infectivity of preparations of infectious agent can be increased by approximately 10-fold by sonication before injection into animals (B. Caughey, personal communication). The seeding may be less dramatic in this case because the fibrils settle to the bottom of the test tube in this unstirred experiment reducing the contact with the monomer.

This same effect was seen with supersaturated solutions of Scr 3 (see Figure 3.5). Only the matched seed has a significant effect on reducing the nucleation time. Three separate experiments are shown. In two of the experiments, fibrils from Met 129 had no effect on the fibril formation in solutions of Scr 3. In the other experiment (middle panel), seeds from Met 129 caused a decrease in the nucleation time compared to the unseeded solution. This decrease, however, was less than in the self-seeded case. A poorly matched but similarly hydrophobic seed may bring monomers into contact and increase the local concentration. This increase in local concentration may, in turn, increase the rate of fibril formation without the unmatched seed actually acting as a template.

The seeding was much more effective (or was only observed) if the fibrils were composed of the same peptide as the monomer in solution. The match required for seeding was seen with both PrP 118-133 Met 129 and Scr 3, eliminating the possibility that fibrils formed from one of these peptides was generally unsuitable for seeding. The two peptides studied (PrP 118-133 and Scr3) have the same composition and differ only by the interposition of three pairs of amino acids in a central region of seven amino acids (see Table 2.3). Apparently, this difference caused a sufficient change in the surface presented by the seed to hinder the unmatched monomer from effectively growing off of it.

Figure 3.5 Unstirred aggregation of Scr 3 at 0.3 mM. 3 sets of runs are shown. In each, o, unseeded Scr 3; □, seeded with Scr 3 (self-seeded); ◊, seeded with PrP 118-133 Met 129

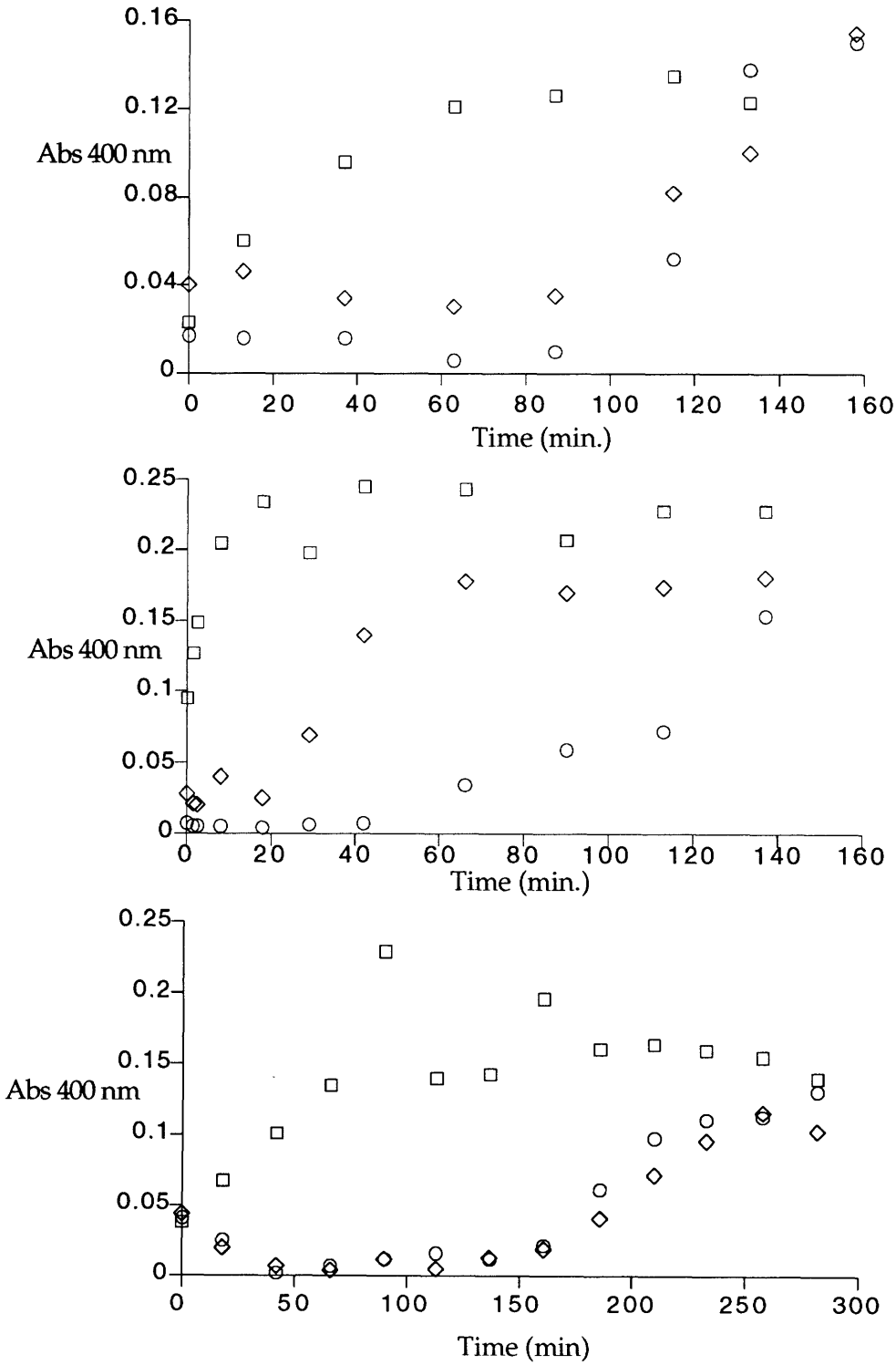

This specificity required for seeding demonstrates that the interactions are not described well by a model where the peptides aggregate in a hydrophobic collapse. If this were the case, any hydrophobic peptide could seed the formation of aggregate in another. Several examples from our lab argue against a non-specific hydrophobic collapse.[16, 17] The interactions are more analogous to what occurs in a crystallization. The specificity required was suggested by the ordered nature of the final fibril, as seen by fiber diffraction and implied by Congo red staining. In the seeding experiments between different peptides, the monomers may attach themselves to the unmatched seeds, but it appears that attachments made in this manner ultimately lose out to more favorable ones. With none of the proper monomer present in solution, presumably the unmatched seeds redissolve.

In an unseeded polymerization, many nuclei are being formed simultaneously, and as each one is formed, growth rapidly begins on it. This decreases the concentration of monomer and hinders the formation of additional nuclei. At some point, the concentration drops to a level where new nucleus formation does not occur at an appreciable rate. At about this time, the growth rate on a given nucleus is also dropping because of the decrease in monomer concentration, however the apparent growth rate is climbing as more nuclei are presented to grow on.

If the solution is seeded, growth will depend on the number of appropriate surfaces presented. Although the overall amount of peptide in the fibrils used as seeds is known, it is difficult to determine accurately the number of nucleation surfaces presented, on which the growth rate will depend. This immediate growth will lower the monomer concentration and further slow the process of nucleus formation. If the number of surfaces

presented in the seeded experiment is less than the number present after nucleation in the unseeded case, the growth will be slower but will occur immediately and may be complete sooner than in the unseeded case. Another factor which requires consideration is that there appears to be a limit to the size of a given fibril. Once this is reached more nuclei may be needed for further growth. These nuclei may form from monomer or be the result of fragmentation of other fibrils.

Formation of Fibrils from Mixtures of Scr 3 and PrP 118-133 Met 129.

The effect of mixing PrP 118-133 Met 129 with Scr 3 directly after preparation of the supersaturated solutions was also tested. Two experiments are shown in Figure 3.6. The homogeneous solutions are the average of two runs; the mixture is a single experiment in each. In these experiments Scr 3 has a shorter nucleation time than PrP 118-133 Met 129. The nucleation time of Met 129 is marginally less than the equimolar mixture of the two peptides at the same total peptide concentration. This is consistent with the inability of these two peptides to form fibrils with each other as shown in the seeding experiments.

Implications for In Vivo Infection in the Prion Diseases

The region of PrP modeled with these peptides is highly conserved across species and is present in all the truncated forms of PrP that have been shown to be competent for conversion to PrP^{Sc}, which is consistent with this region being important for protein-protein interactions involved in the polymerization process. This region of PrP, due to its hydrophobic nature is likely to be kept away from solvent in the properly folded protein, but if exposed it may likely be prone to fibril formation because of its hydrophobic

Figure 3.6 Fibril formation from mixtures of PrP 118-133 Met 129 and Scr 3. □, 0.3 mM PrP 118-133 Met 129; o, 0.3 mM Scr3; ◊, 0.15 mM PrP 118-133 Met 129 and 0.15 mM Scr3.

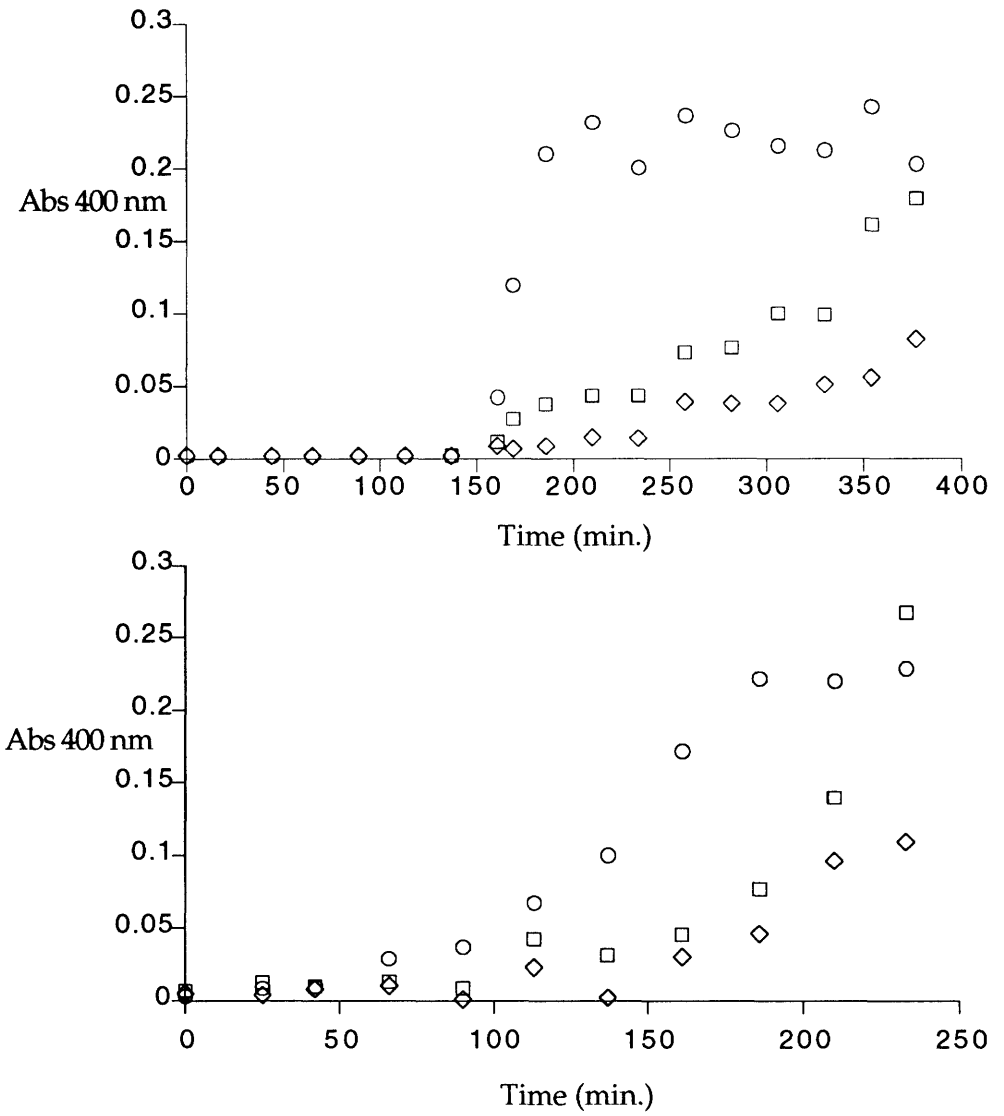

nature. These protein-protein contacts between PrP molecules would have to be sufficiently specific and enthalpically favorable to be selected over the interactions which can occur with components in the cell. We have shown here that the interactions in the fibril formation process in peptides derived

from PrP are very specific and that fibril assembly follows nucleation-dependent kinetics. If the kinetics of polymer assembly are similar in the whole protein, the local concentration of the form competent for polymerization will be critical because of the extreme dependence of nucleus formation on concentration. This mechanism could explain the disease characteristics. A detailed model of this mechanism applied to prion diseases is discussed in Chapter 5.

A similar effect to the one seen in this seeding experiment could account for the species barrier observed in the prion diseases. For example infection of rodents with human prion diseases is frequently unsuccessful, and there is a much longer incubation period. There is a similar effect observed between mice and hamsters, which have differences in PrP at 16 residues. If some of the positions are exposed during the polymerization process, the surface presented would not match exactly. A small change has been shown to be important in sickle-cell hemoglobin polymerization where a valine is substituted for a glutamate residue, exposing a hydrophobic patch to solvent in the deoxygenated form and causing aggregation. As shown with these models, even a subtle change in amino acid sequence could have a dramatic effect. The specificity of the hydrophobic interactions may be sufficient to govern which protein-protein interactions are favorable.

EXPERIMENTAL

Fibril formation experiments

Supersaturated solutions of peptide in H_2O were formed by adding a small volume (ca. 50 μL) of an HFIP solution to a test tube and concentrating to a clear film with a stream of nitrogen. To this film deionized water (Milli-

Q, Waters) was added and agitated briefly. This solution was filtered and the concentration was determined by BCA assay. The solution was then diluted to 333 μM and added to a 10X salt solution (1M NaCl, 100 mM phosphate, pH 7.4, 10% by volume) in a 10 mm x 75 mm test tube to yield the desired 300 μM solutions of peptides in standard buffer (100 mM NaCl, 10 mM phosphate, pH 7.4). These solutions were monitored for turbidity by placing the test tube in a disposable polyethylene cuvette, filling the remaining volume of the cuvette with water, and measuring the absorbance at 400 nm on a Hewlett-Packard model 8452A diode array spectrophotometer. Measurements were taken 1 or 2 times per day, with a brief (5 sec) agitation by vortexing before each measurement.

Seeding experiments

Solutions were prepared as above, followed directly by the addition of 5% by volume of fibrils formed from a previous experiment at the same concentration.

REFERENCES FOR CHAPTER 3

(1) De Young, L. R.; Fink, A. L.; Dill, K. A.; *Acc. Chem. Res.* **1993**, *26*, 614.
(2) Chothia, C.; Janin, J.; *Nature* **1975**, *256*, 705.
(3) Hofrichter, J.; Ross, P. D.; Eaton, W. A.; *Proc. Nat. Acad. Sci. U.S.A.* **1974**, *71*, 4864.
(4) Poillon, W. N.; Kim, B. C.; Rodgers, G. P.; Noguchi, C. T.; Schechter, A. N.; *Proc. Natl. Acad. Sci. USA* **1993**, *90*, 5039.
(5) Sunshine, H. R.; Hofrichter, J.; Eaton, W. A.; *J. Mol. Biol.* **1979**, *133*, 435.
(6) Sluzky, V.; Tamada, J. A.; Klibaov, A. M.; Langer, R.; *Proc. Natl. Acad. Sci. U.S.A* .**1991**, *88*, 9377.
(7) Kondepudi, D. K.; Bullock, K. L.; Digits, J. A.; Hall, J. K.; Miller, J., M.; *J. Am. Chem. Soc.* **1993**, *115*, 10211.
(8) Jarrett, J. T., Amyloid Fibril Formation in Alzheimer's Disease, *Ph.D. Thesis, Massachusetts Institute of Technology*, **1993.**
(9) Voter, W. A.; Erickson, H. P.; *J. Biol. Chem.* **1984**, *16*, 10430.
(10) Wegner, A.; Engel, J.; *Biophys. Chem.* **1975**, *3*, 215.
(11) Tobacman, L. S.; Korn, E. D.; *J. Biol. Chem.* **1983**, *258*, 32073214.
(12) Kirschner, M.; Mitchison, T.; *Cell* **1986**, *45*, 329.
(13) Eaton, W.; Hofrichter, J.; *Adv. Prot. Chem.* **1990**, *40*, 63.
(14) Beaven, G. H.; Gratzer, W. B.; Davies, H. G.; *Eur. J. Biochem.* **1969**, *11*, 37.
(15) Pike, C.; Walencewicz, A.; Glabe, C.; Cotman, C.; *Brain Res.* **1991**, *563*, 311.
(16) Ashburn, T. T.; Lansbury Jr., P. T.; *J. Am. Chem. Soc.* **1993**, *115*, 11012.
(17) Jarrett, J. T.; Lansbury, P. T.; *Biochem.* **1992**, *31*, 12345.

Chapter 4

Peptide models of the susceptibility for CJD of PrP codon 129 homozygotes

As discussed in Chapter 1, there is a nonpathogenic polymorphism in humans at codon 129 of PrP with variants having either methionine or valine found at this position. It appears neither methionine nor valine at this position segregates with cases of prion disease. However, people with sporadic CJD are more likely to be homozygous, for either methionine or valine, at codon 129.[1] The effect of this polymorphism on the assembly of ordered polymers, and by analogy PrP^{Sc}, was studied using our peptide models, PrP 118-133 Met/Val 129. The homozygotes were modeled using homogenous solutions of peptides, and the heterozygotes were modeled using heterogeneous mixtures (1:1) of the two peptides. The thermodynamic and kinetic aspects of fibril assembly will be discussed in this chapter.

Epidemiological Data on Homozygote Susceptibility

The allele frequency of the codon 129 polymorphism is 62% methionine and 38% valine in Caucasians; the frequency of the valine allele is lower in the Japanese population.[2] Collinge et al. determined that the homozygous valine genotype is more likely to be found in individuals afflicted with iatrogenic

(physician induced) CJD. They studied 7 individuals with CJD caused by administration of contaminated human growth hormone and gonadotropin and found 4 to be Val 129 homozygotes, 2 to be heterozygotes, and the remaining individual a Met 129 homozygote.[2] They also screened 106 healthy Caucasians and found 39 Met 129 homozygotes, 54 heterozygotes, and 13 Val 129 homozygotes. Although a significant excess of Val 129 homozygotes was found, the number of afflicted individuals studied was quite small (see Table 4.1).

Table 4.1. Distribution of position 129 genotype in Caucasians and CJD patients. Percentages are shown in parentheses.

	Met/Met	Met/Val	Val/Val
Population (normal)	39(37)	54(51)	13(12)
Iatrogenic CJD	1(14)	2(29)	4(57)
Confirmed sporadic CJD	16(73)	1(5)	5(22)
Suspected sporadic CJD	11(52)	4(19)	6(29)

In a similar but larger study, the same group looked at the genotype of sporadic CJD cases.[1] In this study, 21 of 22 confirmed cases of sporadic CJD, and an additional 19 of 23 suspected cases of sporadic CJD were homozygotes. Of the 22 confirmed CJD cases, 16 were Met 129 homozygotes, 5 were Val 129 homozygotes, and only one was heterozygous. For the 23 suspected cases, it was reported that 11 were Met 129 homozygotes, 6 were Val 129 homozygotes, and 4 were heterozygotes—leaving one to wonder where the other two people went. For the confirmed CJD cases, 95% were homozygous (compared with 49% in the normal population); the one heterozygous individual may have been a familial case, as it was later determined that the patient's father died with dementia. In the suspected cases, 82% were homozygotes. The excess for valine homozygotes

seen in the iatrogenic cases was not seen here. The sources of the inoculum may determine which genotype is more susceptible in the transmitted cases.

We hypothesized that homozygotes were more susceptibile to sporadic CJD than heterozygotes because PrP^{Sc} was more easily formed in the homozygotes. The experiments with the peptides described in this chapter are based on the assumption that PrP^{Sc} is the infectious agent and that the formation of aggregates of PrP is central to the pathogenesis of the disease. The difference between homozygotes and heterozygotes would be in the varying ability of the two variants to form ordered arrays with themselves versus arrays with the other variant. It was expected that the homogeneous fibrils would be more stable thermodynamically and form more rapidly, which would be consistent with PrP^{Sc} forming more readily in the homozygotes. The difference in the formation of homogeneous versus heterogeneous polymers was measured in 3 related ways: the thermodynamic preference for fibril formation, the rate of fibril formation, and the rate of dissolution of fibrils. In each case, fibril formation from homogeneous solutions of either variant was compared to fibril formation from mixtures of these two peptides. The region of the protein modeled here appears to be important since a change in this region alters the phenotype.[3] The peptides discussed herein serve as models for the interactions of this region of the protein.

Thermodynamic Preferences in Fibril Formation

The stability of fibrils formed from homogeneous solutions and those from heterogeneous solutions were studied. PrP with methionine at position 129 was modeled by PrP 118-133 Met 129 (abbreviated Met 129), and PrP with valine at position 129 was modeled by PrP 118-133 Val 129 (abbreviated Val 129). Initially we hoped to follow the composition of fibrils forming out of a

supersaturated equimolar mixture of Met 129 and Val 129 over time. We hypothesized that heterogeneous fibrils could form initially and then be converted into homogeneous fibrils. This measurement proved to be difficult, as no ready means of determining the composition of a given fibril is available. A sampling of the bulk mixture of fibrils at intervals found their composition to be equimolar in both peptides. This result was probably due to the sampling of populations of differently composed fibrils which on average contained equal proportions of both peptides.

In order to determine the stability of heterogeneous compared with homogeneous fibrils, supersaturated mixtures of the two peptides in unequal proportions were prepared. These mixtures were stirred and fibrils formed within hours. These fibrils were stirred for several more days to allow the fibrils to equilibrate to more stable arrays, after which the suspensions were filtered, and the ratio of the peptides in the soluble phase was determined. Three different outcomes were possible (see Figure 4.1):

1) If heterogeneous and homogeneous fibrils are equally stable, that is, if no selection occurs in fibril formation, no difference will be found in the composition of the soluble phase before and after fibril formation. Therefore, the two variants will be randomly distributed in the fibrils. The ratio of the variants will be the same in the fibril and in solution because no selection process has occurred.

2) If heterogeneous fibrils are more stable than homogeneous fibrils, the soluble phase after precipitation will be enhanced in the major component. Conversely, the fibrils will be enhanced in the minor component because it will be tied up in the more stable heterogeneous fibrils. If the interaction of the twovariants leads to a more stable fibril, these heterogeneous fibrils will form preferentially until the solubilty of the heterogeneous fibril (determined by the

Figure 4.1 Schematic of the 3 possibilities for fibril formation from mixtures of two peptides in unequal proportions (the same would apply to the opposite ratios). The numbers over the arrows correspond to the possibilities discussed in the text. The pool of initial soluble monomers is shown in the upper left. The ratios of monomers shown are hypothetical.

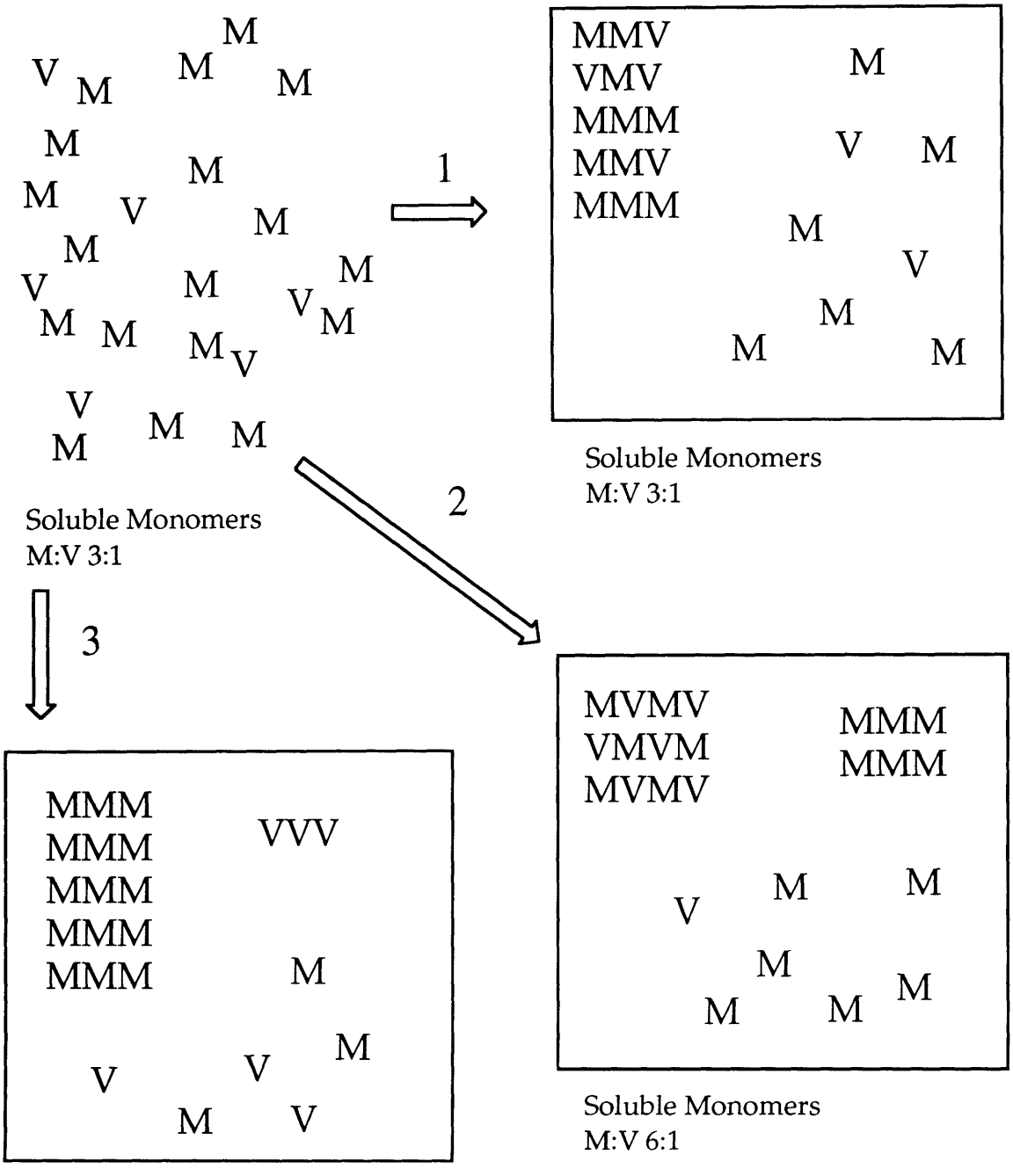

limiting minor component) is reached. After this point, fibrils composed of the remaining variant will also form until the solubility of these homogeneous fibrils (determined by the major component) is reached.

3) If the homogeneous fibrils are more stable than the heterogeneous fibrils, the soluble phase will be enhanced in the minor component after fibril formation because the fibrils will be mostly homogeneous. Both peptides will form separate fibrils until their solubility is reached. The observed ratio of peptides in the soluble phase will be the addition of the equilibria between the the two separate fibrils and their associated monomers. Because the minor component started at a lower concentration, the change in concentration of the minor component will be less than for the major component.

Fibrils were prepared from mixtures of Met 129 and Val 129. Supersaturated solutions of peptide in approximately 1:9 and 9:1 ratios were prepared at 300 μM total peptide concentration in buffer. These solutions were stirred for several days and then filtered. Because these two peptides are very similar and inseparable by RPHPLC, the relative amounts of the two peptides in solutions was determined by plasma desorption mass spectrometry (PDMS). The similarity of these two peptides suggests they would have similar ionization characteristics, which was confirmed by comparing the ratios determined by standard protein assays and PDMS. Also, uneven ratios were tested in both directions. Shown in Figure 4.2 are the ratios of soluble peptide before and after aggregation. The total amount of peptide in solution is approximately 10 fold higher before aggregation (percentages are plotted) so the bars before and after aggregation cannot be compared with each other.

The ratios of peptides in solution after fibril formation approached equimolar ratios starting from either direction. Therefore, to balance the mass the fibrils must be enriched in the major component (see possibility 3 above).

Figure 4.2 Thermodynamic preference for fibril formation. On the left are initial solutions predominately Met 129. On the right are initial solutions predominately Val 129.

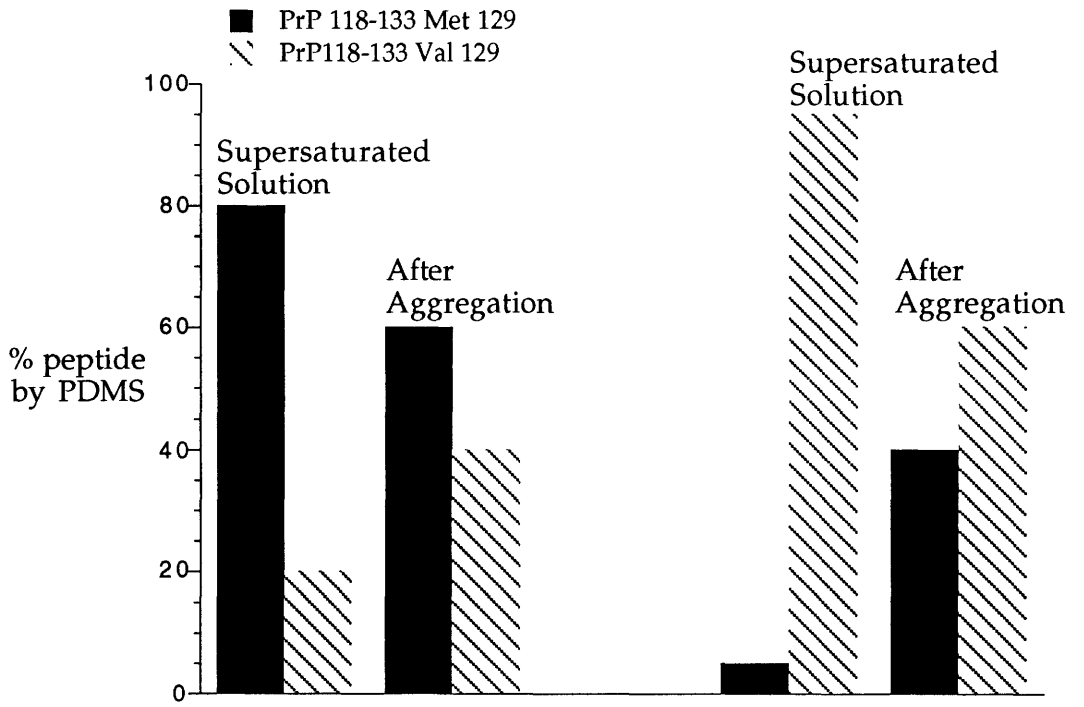

The homogeneous fibrils are favored thermodynamically over heterogeneous fibrils, and heterogeneous fibrils, if formed, are ultimately converted into homogeneous fibrils. In other words, the two peptides form fibrils as if the other peptide were not present and continue to precipitate until their solubility is reached. Similar effects are seen when crystals are formed from mixtures of components. The crystals are composed of one kind of molecule and other kinds of molecules are not incorporated into the crystal. After crystallization the remaining supernatant is enriched in the minor components (usually thought of as less pure).

In these experiments, the ratios in the soluble phase approach, but do not reach, unity, suggesting that some heterogeneous fibrils (or fibrils containing impurities) are formed. The fibrils are in equilibrium with the soluble monomer,

and the amount of mixed fibrils will be determined by ratio of the two equilibria between homogeneous and heterogeneous interactions. The larger the difference between these two equilibria, the greater the selection which will occur.

The solubility of heterogeneous mixtures of Met 129 and Val 129 is about twice that of homogeneous peptide solutions in terms of total peptide. If this is also true for the whole protein, the heterozygotes can solubilize more protein, and may therefore prevent polymerization. The total cellular concentration of PrP is likely to be below its solubility, however PrP may be concentrated in certain parts of the cell, such as endosomal compartments. The homozygotes will have twice the concentration of protein which may push it pass the solubility in some instances and lead to aggregate formation.

Kinetics of Fibril Formation in Homogeneous and Heterogeneous Solutions

The kinetics of fibril formation in Met 129 and Scr 3 were discussed in the previous chapter. Fibril formation follows nucleation-dependent kinetics. The studies described in Chapter 3 were done without agitation except directly before the measurement of turbidity was taken. Unagitated solutions exhibited much longer nucleation times than stirred or otherwise agitated solutions. No differences were determined between homogeneous solutions of Met 129 or Val 129 and mixtures using the unstirred assay. A stirred assay allows for more consistent agitation and a more convenient time period for running the assay. One complication of a stirred assay is that shorter nucleation times are seen implying that a different mechanism might be involved. Attempts to couple a stirred system to turbidity measurements led to difficulties because of inconsistent distribution of the fibrils in the light path, generally caused by the aggregate floating to the top of the container. This problem, along with the difficulty correlating turbidity to the molar amount of fibrils, led us to use an

assay based on measuring the amount of soluble peptide in a stirred supersaturated solution over time. This was done by using tritium-labeled peptide and scintillation counting.

Supersaturated mixtures were made in buffer of 100% Met 129, 100% Val 129, and 50% Met 129 : 50% Val 129 (all at 300 μM total peptide concentration) to mimic the MM, VV, and MV genotypes respectively. These solutions were stirred, aliquots were taken at intervals, filtered through 0.22 μm filters, and scintillation counted to determine the amount of soluble peptide. The specific activity was calculated from the initial solution, and the counts at later time points were converted to concentrations. The results are shown in Figure 4.3. The Met 129 solution had a shorter nucleation time than the Val 129 solution which had a shorter nucleation time than the Met/Val 129 solution. Met 129 is significantly different from the Met/Val 129. The data for Val 129 overlaps slightly with the data on either side of it. The average nucleation times are shown in Table 4.2.

Table 4.2 Nucleation times for fibril formation from homogeneous and heterogeneous solutions calculated as 20 % of the maximal turbidity. Errors are standard deviations.

Solution of peptide	Met 129	Val 129	Met/Val 129
Nucleation time (min.)	48±11	76±18	107±14

As shown above, nucleus formation is slower in the heterogeneous solution, implying that mixed nuclei are formed more slowly than homogeneous nuclei possibly because they are less stable. Mixed nuclei may form transiently, but they will be more likely to revert to monomers. The difference in stability between homogeneous and heterogeneous nuclei is the difference of the sum of

Figure 4.3. Fibril formation from supersaturated solutions. **A**. 4 runs of 0.3 mM PrP 118-133 Met 129. **B**. 7 runs of 0.3 mM PrP 118-133 Val 129. **C** 4 runs of 0.3 mM total peptide, 1:1 Met 129:Val 129.

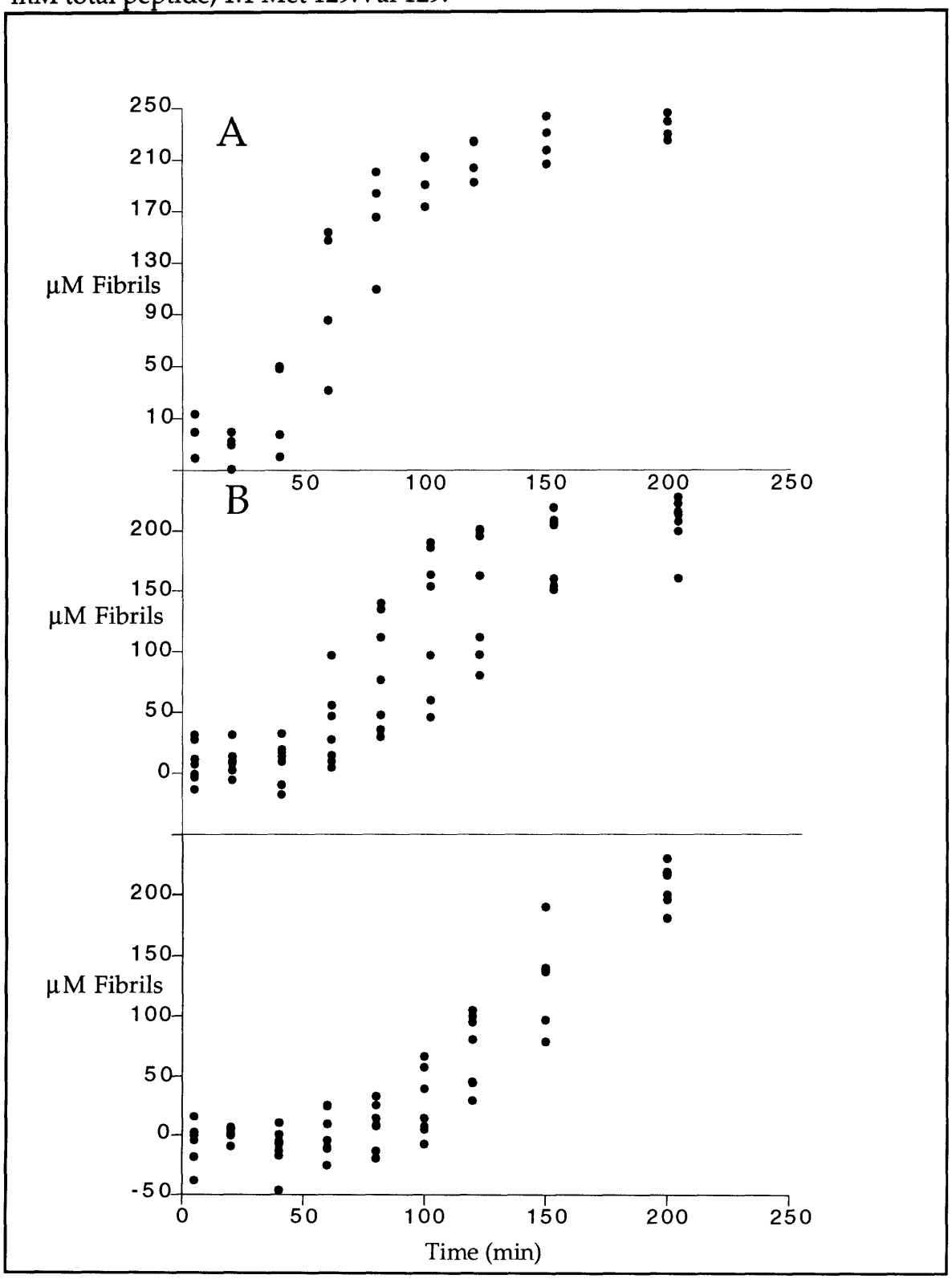

Figure 4.4 Scheme for the formation of amyloid from peptide mixtures.

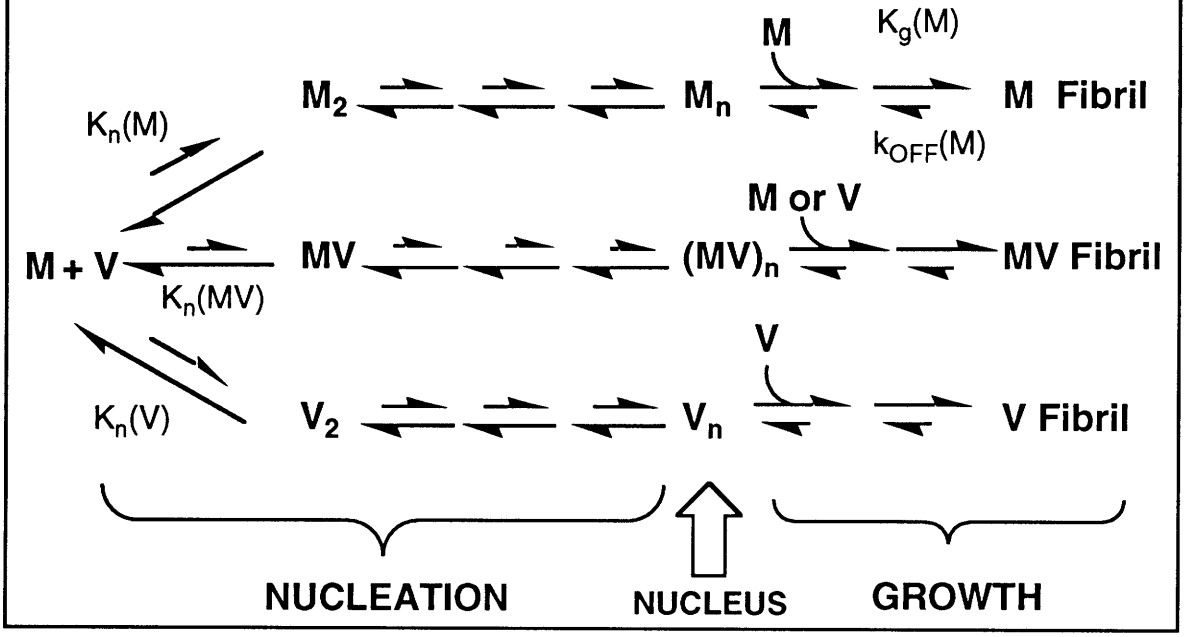

all the interactions between the monomers. Therefore any suboptimal interactions between the two different peptides will be magnified because oligomers are not stable until they reach the nucleus size. A diagram of the possibilties for a peptide mixture is shown in Figure 4.4. The formation of homogeneous nuclei in the heterogeneous solution would likely occur instead of the formation of mixed nuclei because of their greater stability. (The central pathway of Figure 4.4 is disfavored.) The homogeneous nuclei would form more slowly out of the heterogeneous solution than out of the homogeneous solution because the concentration of monomer is halved. The decrease in concentration decreases the rate of nucleus formation potentially by much more than half. Therefore even added together the formation of fibrils by the two variants at half the concentration does not begin as early as in the homogeneous case. The effect of concentration would be expected to be much less for the growth after nucleation because it only depends on the concentration of nuclei and the concentration of monomer to the first power.

The growth rate for Met 129 was faster than for either Val 129 or Met/Val 129. The growth rates in Val 129 and Met/Val 129 solutions were not significantly different. A difference in the growth rate might have been expected between the heterogeneous and homogeneous solutions, although the effect on growth rate would probably not be as dramatic as the effect on nucleation because the concentration dependence of the growth phase is of a lower magnitude. However, the molecular level interactions involved in both nucleation and growth are likely to be similar. As discussed in Chapter 3, the growth rate will also depend on the number of viable nuclei on which monomer can grow. Because of the difference in nucleation time, it is conceivable that the number of nuclei is different in the heterogeneous solution compared with the homogeneous solution. The following expression describes the growth rate in the homogeneous solution:

growth rate = k [monomer] [nuclei]

and the rate from a mixture of monomers M and V would be described by the following:

growth rate = k [monomer M] [nuclei M] + k [monomer V] [nuclei V]

The effect of concentration on the number of nuclei formed is unknown and not easily determined experimentally. Because of this uncertainty, it is difficult to draw conclusions regarding inhibition of fibril growth by the unmatched variant.

One aspect of the heterogeneous polymerization that cannot easily be measured is the formation of mixed fibrils that are ultimately converted to homogeneous fibrils. As in the case of the thermodynamic measurement, this

assay only measures the peptide that can pass through the filter; the composition of individual fibrils is not determined. Therefore it is not known if the aggregate is a mixture of homogeneous fibrils or fibrils composed of both peptides. Less stable heterogeneous aggregates are probably formed early in the process and converted to more stable homogeneous fibrils. Reorganization of fibrils appears to occur since the fibrils continue to equilibrate and become more stable well after the maximal turbidity is reached. This effect will be discussed in the next section.

The fibril formation of the homogeneous solutions was also done at 150 μM for each peptide as shown in Figure 4.5. The lag time was slightly longer compared with the 300 μM runs. This difference is not as dramatic as might be expected for a nucleation-dependent process. Stirring greatly enhances the rate of fibril formation possibly through the formation of secondary nuclei, which may be formed by breaking up small fibrils as they are formed. Shearing or breaking up fibrils has a similar effect on the infectious agent. Treating the infectious agent with sonication or by dispersing it in detergent frequently increases the titer by up to an order of magnitude (B. Caughey personal communication). Sonication also seems to increase the effectiveness of seeding in peptide polymerizations. The nature of the surface presented and the ability to increase the number of surfaces by shortening the fibril can have a significant effect on the rate of fibril growth.

The separate 150 μM runs are added together and compared to the solution containing 150 μM of each peptide in Figure 4.6. The averages of 4 runs are shown. The math addition is about the same or slightly faster than theheterogeneous mixture. The higher concentration of peptide in the heterogeneous case does not increase the rate suggesting that the two variants do not form productive aggregates with each other. One variant may even interfere

Figure 4.5. Fibril formation from supersaturated solutions. A. 3 runs of 0.15 mM PrP 118-133 Met 129. B. 3 runs of 0.15 mM PrP 118-133 Val 129.

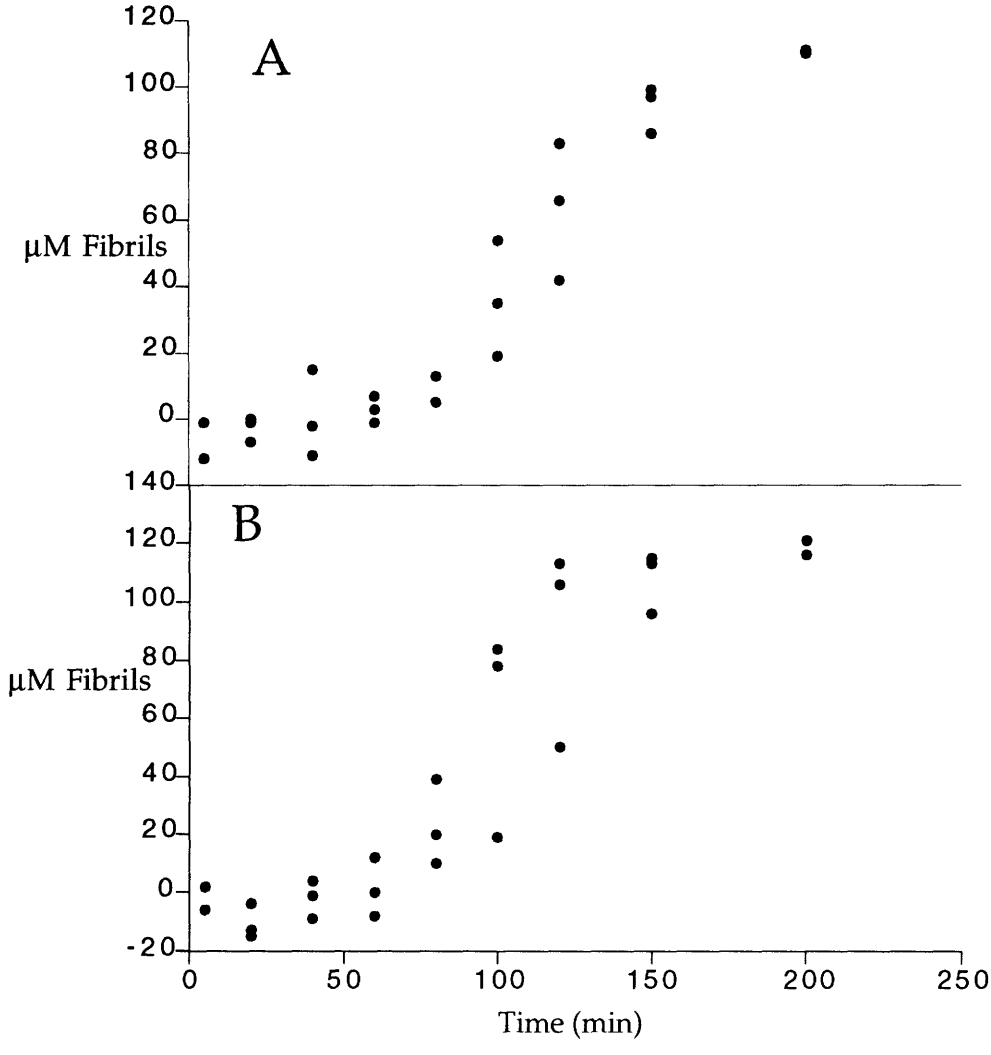

with the formation of homogeneous polymers of the other variant (and vice versa) by forming weaker heterogeneous interactions transiently (see Figure 4.4). The existence of this effect however, cannot be stated conclusively from the data.

The aggregation of these peptides could be seeded by the addition of preformed fibrils as discussed in the previous chapter. Somewhat suprisingly, no difference was seen between homogeneous and heterogeneous seeding. Preformed fibrils of Met 129 could seed solutions of Met 129 and Val 129 equally

Figure 4.6. Fibril formation from supersaturated solution. o, a mixture of 0.15 mM PrP 118-133 Met 129 and 0.15 mM PrP 118-133 Val 129. □, math addition of 0.15 mM PrP 118-133 Met 129 and 0.15 mM PrP 118-133 Val 129.

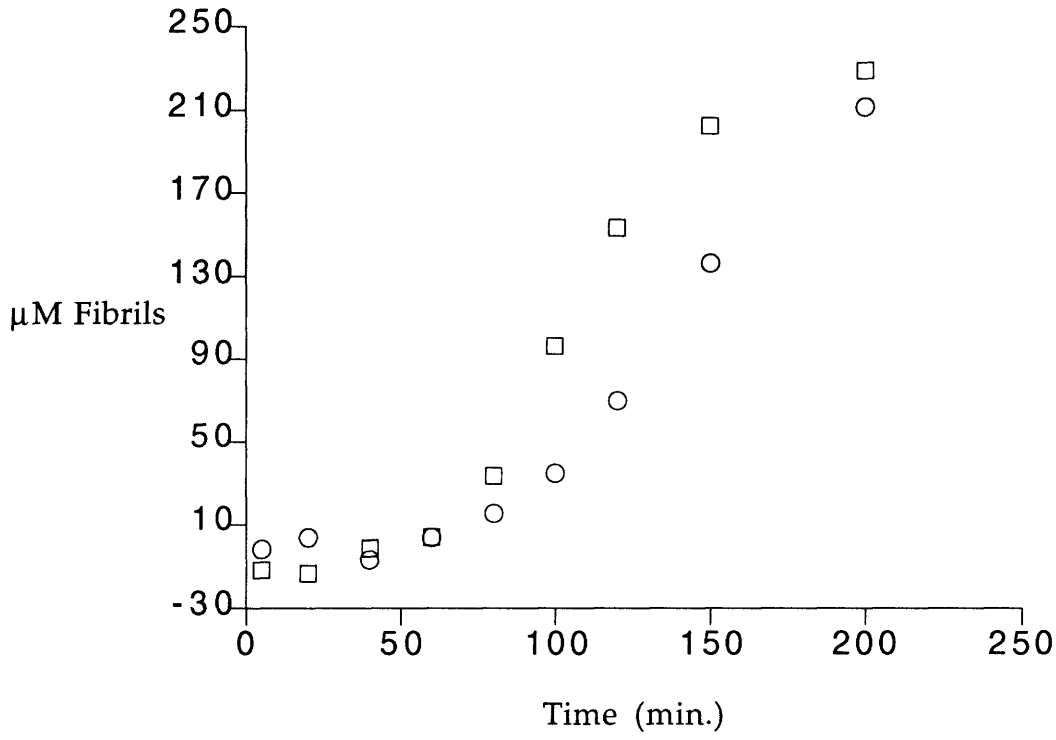

well. The seeding of Val 129 with fibrils composed of Met 129 is shown in Figure 4.7 and compared to the average unseeded polymerization. Possibly, when one peptide is seeded with the other, a new surface composed of the peptide in solution is formed quickly; growth then continues on that surface as in the matched seeded case. It is also possible that the initial fibrils are less stable, butjust as filterable, in the heterogeneous case. The effect of seeding would be expected to be similar to the effect on growth rate. The absense of selectivity in seeding suggests that the difference between homogeneous and heterogeneous interactions is small and not detectable unless they are magnified as in the case of the nucleation time.

Figure 4.7. Seeding fibril formation in supersaturated solutions. A. 4 runs of PrP 118-133 Val 129 seeded with PrP 118-133 Met 129. B. Averages of unseeded and seeded runs. □, PrP 118-133 Val 129 unseeded. o, PrP 118-133 Val 129 seeded with PrP 118-133 Met 129.

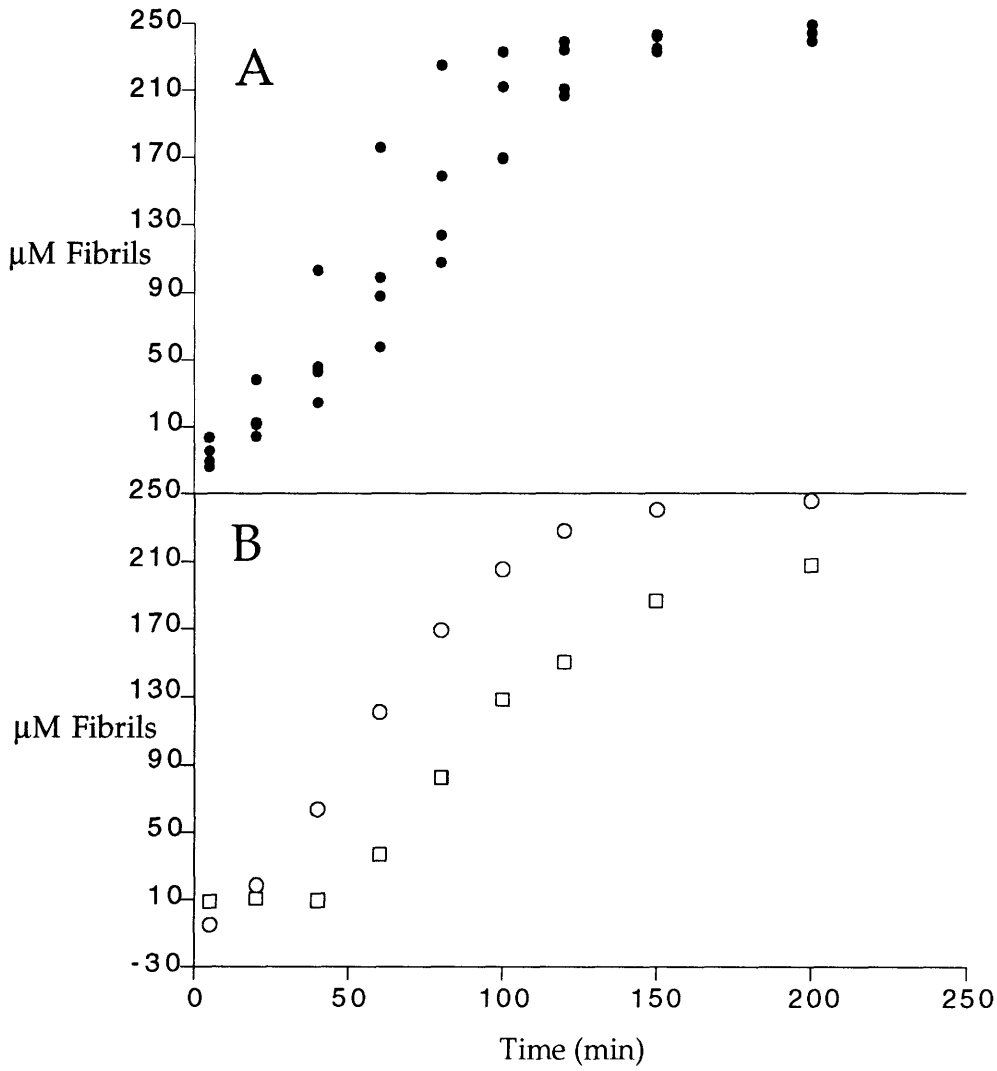

The longer nucleation time for fibril formation in the heterogeneous mixtures of peptides could have significant consequences for the *in vivo* case. If mixed nuclei are sufficiently less stable, they will not be formed; homogeneous nuclei will be formed instead. The concentration of each variant in the heterozygotes will be half the concentration in homozygotes. Because the

concentration dependence of nucleus formation is nth order, where n is the nucleus size, a decrease of 50% in protein concentration could have a dramatic effect on the polymerization process. The concentration in heterozygotes may be insufficient for nucleus formation or may be at a rate slow enough that other events (such as protease digestion) can occur first. The nucleation-dependent character of this polymerization can magnify a small difference in association energy (as is likely with the conservative change of Met to Val) that might not be significant in other mechanisms.

Dissolution of Fibrils

The dissolution of fibrils formed out of homogeneous or heterogeneous solutions was also studied. Radiolabeled fibrils were prepared from either homogeneous solutions of Met 129 or Val 129, or from a 50:50 mixture of Met 129/ Val 129, all at 300 μM total peptide. These fibrils were collected by centrifugation and the supernatant was decanted. Fresh buffer was added, and aliquots were filtered at intervals and counted. Fibrils formed from heterogeneous solutions gave about twice the amount of soluble peptide compared with fibrils from either of the homogeneous solutions (see Figure 4.8).

Why did the fibrils from the heterogeneous solution yield more soluble peptide? If heterogeneous fibrils are less stable than homogeneous fibrils, two populations of homogeneous fibrils (one for each variant) will form out of the heterogeneous solution. The greater amount of soluble peptide observed will be due to the presense of two different types of fibrils in the mixture. Therefore, the larger amount of soluble peptide measured in the heterogeneous case is the sum of the two individual equilibria between the homogeneous fibrils and their associated monomers. The dissolution of homogeneous fibrils is the

Figure 4.8. Dissolution of previously formed fibrils. ●, Fibrils formed from 0.3 mM PrP 118-133 Met 129. □, fibrils formed from 0.3 mM PrP 118-133 Val 129. ◇, fibrils formed from a mixture of 0.15 mM PrP 118-133 Met 129 and 0.15 mM PrP 118-133 Val 129. Standard deviations are shown with error bars.

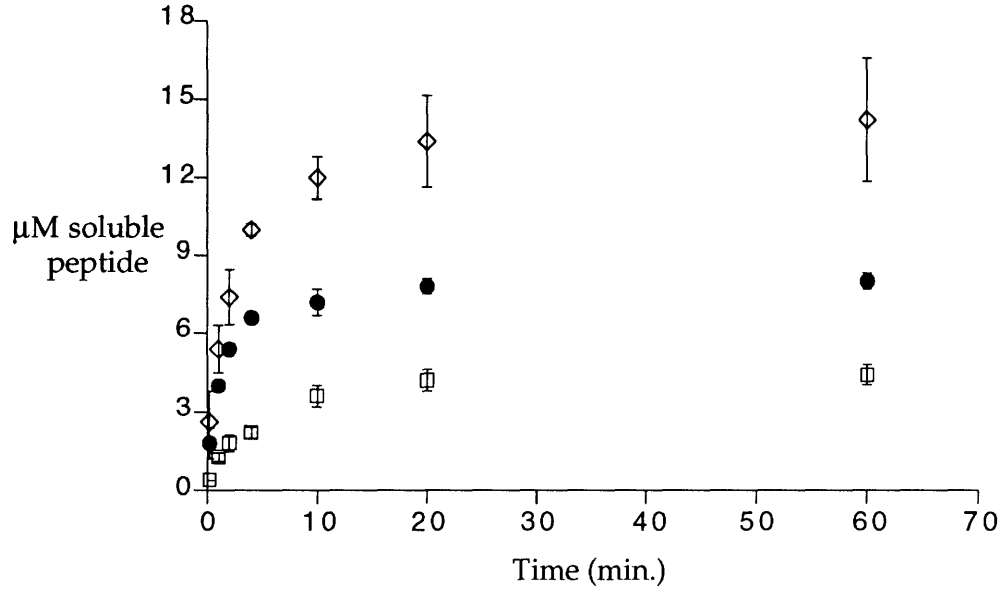

measurement of one of these equilibria. Indeed, using this method, the sum of the two individual measurements of solubility in the homogeneous cases is equal or possibly slightly less than the solubility of the fibrils formed from the heterogeneous solution. Although this difference is within a standard deviation, once again there is the suggestion that the two variants interfere with the polymerization of each other.

The amount of peptide that can be solublized from the fibrils decreased with increasing time for fibril formatiom. The dissolution of fibrils formed for different lengths of time is shown in Figure 4.9. This "aging" effect continued well after the concentration of soluble peptide was virtually constant or decreasing only gradually. This implies that early fibrils, which are not the most stable, can form and subsequently be converted to more stable arrays. This may occur by adjustments made while still in the solid state or by dissolution and

reattachment in the proper orientation. Conceivably, nuclei of different morphology form and grow in the early stages of fibril assembly, but ultimately all the peptide becomes incorporated into the more stable arrays.

The dissolution measurement is consistent with the observations made using the other two methods described in this chapter. The heterogeneous fibrilis not as stable a structure as the homogeneous fibril. This difference in stability is reflected in the composition of the fibrils after equilibrium and in the rate which the fibrils form.

A similar situation has been seen in other proteins as has the converse. The upregulation of fetal hemoglobin production increases the overall

Figure 4.9. Stability of fibrils over time. Fibrils were formed from supersaturated solutions of PrP 118-133 Val 129 and spun down after 1, 2, and 7 days. These fibrils were resuspended in fresh buffer and the amount of soluble peptide was measured at intervals. □, 1 day old fibrils. •, 2 day old fibrils. ◊ , 7 day old fibrils.

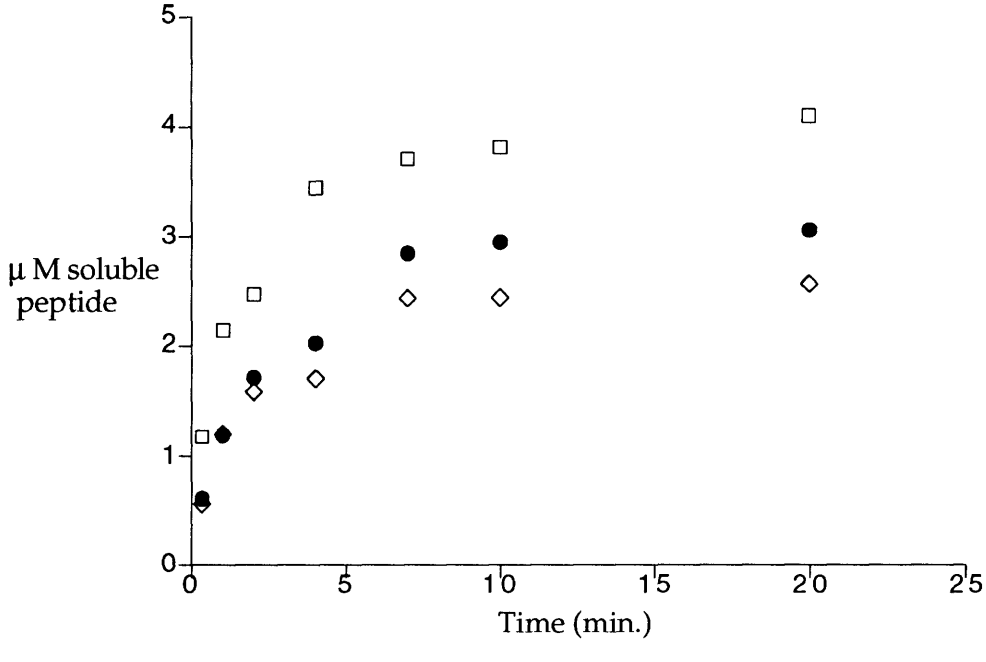

hemoglobin solubility. In the sickle-cell form of hemoglobin, a hydrophobic residue (valine) is substituted for a polar residue (glutamic acid) resulting in a less soluble protein.[4, 5] In mixtures of sickle-cell hemoglobin with other hemoglobins, only the sickle-cell form polymerizes; mixed polymers are not seen.[6] In contrast, in tropomyosin assembly the heterodimer is preferred over the homodimer.[7, 8] Tropomyosin consists of two subunits which differ slightly in amino acid sequence. Tropomyosin preferentially formed heterogeneous dimers over homogeneous dimers when refolded under equilibrating conditions. Fos and Jun heterodimer formation is similarly favored.[9]

In the case of PrP, heterozygotes at position 129 may be less susceptible to sporadic or spontaneous prion disease because polymer assembly is not favored between the two variants. The phenotype observed implies that position 129 of the PrP is important in the disease process, probably because of monomer-monomer or monomer-aggregate interactions which occur during the assembly of PrP^{Sc}. The models described herein suggest that the interactions between the two variants are not as favorable as the homogeneous interactions. This small difference is magnified if protein assembly occurs by a nucleation-dependent mechanism. The increased susceptibilty of homozygotes may then be due to slighty more favorable protein-protein interactions which greatly shortens the nucleation time. Polymer assembly then becomes more competitve with other paths the protein may take, such as proteolysis. An effect similar to what is seen with the peptides discussed in this chapter may play a role in the species barrier observed. The infecting protein generally differs at several positions with the host protein. These differences may lead to the loss of several contacts between the monomer and the aggregate (PrP^{Sc}) resulting in a less efficient nucleation of polymerization.

As discussed in Chapter 2, this region of the protein is unlikely to be exposed in the properly folded PrP^C form of the protein because of its hydrophobic nature. Therefore, the assembly of abnormal polymers may require conditions where the protein is partially unfolded (see Chapter 5). There is evidence that the conversion of PrP^C to PrP^{Sc} in infected cell lines occurs in the endosomal pathway.[10] This site may also be a likely location for the unseeded formation of PrP^{Sc}.

Experimental

Synthesis of ^3H Peptides

Tritium-labeled peptides were synthesized as described in Chapter 2.

Thermodynamic Measurement of Fibril Composition

Supersaturated solutions of peptide in H_2O were formed by adding a small volume (ca. 50 µL) of an HFIP solution to a test tube and concentrating to a clear film with a stream of nitrogen. To this film MilliQ water (ca. 1-2 mL) was added and agitated briefly. This solution was filtered, and the concentration was determined by BCA assay. The solution was then diluted to 111% of the final desired concentration (usually 333 or 162 mM) and added to 10% the volume of a (10X) salt solution to yield the desired ratio of peptides in standard buffer (100 mM NaCl, 10 mM phosphate, pH 7.4). PDMS was taken of these solutions as described in Chapter 2. These solutions were then capped and stirred at room temperature for 2-6 days. At this point an aliquot was filtered, and a PDMS was taken.

Kinetic Assay for Fibril Formation

Supersaturated solutions of peptide were made as described above. The concentration of these solutions was determined by absorbance at 276 nm

(tyrosine). The extinction coefficient (ε=1700) was calculated from a sample whose concentration was determined by amino acid analysis and was the same for both peptides. This supersaturated solution was then added to an HFIP/H_2O derived film of radiolabeled peptide, agitated briefly, and filtered through 0.22 μM filters. The concentration was determined by absorbance at 276 nm. These solutions were then added to concentrated salt solutions to give the final solutions, which were either 150 μM or 300 μM in peptide in standard buffer. The specific activity of the solution was determined by measuring an aliquot by scintillation counting. These solutions were stirred continuously on a magnetic stir plate, and aliquots were taken over a period of about 4 hours. These aliquots were filtered, and known amounts of these solutions were measured by scintillation counting. This measurement of counts per minute was then converted to the concentration of soluble peptide left in solution, and by subtraction from the starting concentration, the amount of peptide contained in the fibrils was determined.

Dissolution of Fibrils

Fibrils were formed by the addition of a concentrated DMSO solution of cold peptide, along with a small amount (10% of the cold peptide solution volume) of a solution of ^3H labeled peptide in HFIP/H2O, to standard buffer to give solutions 300 μM in peptide with 5% DMSO. This was stirred for 1-14 days, at which time a 0.3 mL aliquot was taken and centrifuged for 15 min in a clinical centrifuge. The supernatant was decanted, and 3 mL fresh buffer was added (peptide concentration ca. 30 μM). Aliquots were taken at intervals and filtered; measured amounts of these solutions were measured by scintillation counting.

REFERENCES FOR CHAPTER 4

(1) Palmer, M. S.; Dryden, A. J.; Hughes, J. T.; Collinge, J.; *Nature* **1991**, *352*, 340.
(2) Collinge, J.; Palmer, M. S.; Dryden, A. J.; Lancet **1991**, *337*, 1441.
(3) Goldfarb, L. G.; Peterson, R. B.; Tabaton, M.; Brown, P.; LeBlanc, A. C.; Montagna, P.; Cortelli, P.; Julien, J.; Vital, C.; Pendelbury, W. W.; Halta, M.; Willis, P. R.; Hauw, J. J.; McKeever, P. E.; Monari, L.; Schrank, B.; Swergold, G. D.; Autillo-Gambetti, L.; Gajdusek, D. C.; Lugaresi, E.; Gambetti, P.; *Science* **1992**, *258*, 806.
(4) Eaton, W.; Hofrichter, J.; *Adv. Prot. Chem.* **1990**, *40*, 63.
(5) Hofrichter, J.; Ross, P. D.; Eaton, W. A.; *Proc. Nat. Acad. Sci. U.S.A.* **1974**, *71*, 4864.
(6) Sunshine, H. R.; Hofrichter, J.; Eaton, W. A.; *J. Mol. Biol.* **1979**, *133*, 435.
(7) Lehrer, S. S.; Qian, Y.; *J. Biol. Chem.* **1990**, *265*, 1134.
(8) Lehrer, S. S.; Stafford, W. F.; *Biochem.* **1991**, *30*, 5682.
(9) O'Shea, E. K.; Rutkowski, R.; Stafford, W.; Kim, P. S.; *Science* **1989**, *245*, 646.
(10) Caughey, B.; Raymond, G. J.; *J. Biol. Chem.* **1991**, *266*, 18217.

Chapter 5

A Cell-Free Conversion of PrP^C to a Protease-Resistant Form

Can knowledge of the mechanism of polymerization in peptides be applied to the study of full-length PrP? The nature of the infectious agent is still a subject of great debate. The purification of the agent has identified an abnormal form of a host protein, PrP^{Sc}, however to many people, the unique properties of the agent cannot be described by protein alone. The formation of PrP^{Sc} that is infectious, from purified components, outside the cell, would greatly help in settling this controversy. Since the formation of PrP^{Sc} from PrP^C is key to the protein-only model for scrapie, the obvious experiment is the direct conversion of PrP^C to PrP^{Sc}. Unfortunately, PrP^C (PrP from uninfected sources) cannot yet be obtained in large quantities, so it is difficult to test a large number of conditions with PrP purified directly from cell culture.

A more feasible system is to use PrP^{Sc} (from infected animals) as the source of PrP since it is easier to obtain than PrP^C (from uninfected sources). PrP^{Sc} has to first be rendered uninfectious to use as a source of PrP for the conversion experiment. This task can be accomplished by treatment with denaturants such as guanidine or urea. In this preparation of PrP, everything necessary to compose the infectious agent is present since the material was

infectious before denaturation, although other substances may facilitate their assembly. Once conditions for the renaturation of PrP^{Sc} are determined, the conversion with PrP^{C} (from uninfected sources), possibly through the interaction with PrP^{Sc}, can be attempted. In this chapter, experiments to convert PrP^{C} to a protease-resistant form are described. The implications of these experiments and possible mechanisms for scrapie infectivity will be discussed.

Previous Experiments to Form PrP^{Sc} from noninfectious components

Experiments of this kind have been tried before.[1, 2] Prusiner and coworkers treated the scrapie agent (PrP27-30, proteinase K treated form with MW of 27-30 kDa) with chaotropic salts and measured the resulting titers of infectivity. Exposure to 6M guanidine thiocyanate (GdnSCN) rapidly inactivated the agent, whereas inactivation with 3M GdnSCN required a longer exposure but was complete after 24 hours. Similar results were obtained with urea, although higher concentrations were required for inactivation. Prusiner states that guanidine hydrochloride (GdnHCl) had an effect similar to the other chaotropes, but the data is not given. Attempts were made to regain infectivity from denatured samples either by diluting the denaturant or removing it slowly by dialysis This experiment was done at several denaturant concentrations for urea and for 6M GdnSCN. No return of infectivity was found in any of these cases. In some cases dilution of the denaturant also caused PrP to be diluted considerably. If a PrP^{Sc} is a multimeric species, dilution will dramatically slow the rate of assembly. Dilution of the solution to low protein concentrations may be more appropriate for a unimolecular reaction like protein refolding.

The effect of denaturants on PrP^{Sc} has been studied by other workers. Safar et al. treated PrP27-30 with GdnHCl and monitored the CD spectra and measured its properties by size exclusion (SE) HPLC.[3] As determined by SE HPLC, PrP^{Sc} appeared to monomerize at about 1.5 M GdnHCl. The CD spectra changed significantly at approximately 3.5 M GdnHCl, which suggests partial unfolding at this concentration of denaturant; higher guanidine concentrations led to complete unfolding.

Attempts at Seeded Renaturation of PrP^{Sc}

Can the reassembly of PrP^{Sc} into the protease resistant and infectious form be initiated by the addition of a small amount of PrP^{Sc} to the denatured material? This kind of seeding effect dramatically increases the rate of fibril formation in peptides derived from the PrP sequence. Analogously, we wanted to denature PrP^{Sc}, dilute the denaturant, and then seed the reassembly of unfolded PrP into PrP^{Sc} with a small amount of untreated PrP^{Sc}. The formation of PrP^{Sc} can be assayed for by protease-resistance; PK resistance is the simplest way to distinguish PrP^{Sc} from PrP^{C}. The plan was to first produce completely protease-sensitive material, with the minimum amount of denaturant, in order to keep the protein as concentrated as possible during the subsequent dilution of the denaturant. A minimum denaturant concentration also might allow some protein structure to remain intact, which, although not sufficient for protease resistance, may facilitate its recovery. Then a small amount (about 1%) of untreated PrP^{Sc} would be added as a seed to nucleate the reformation of PrP^{Sc} from the rest of the unfolded PrP.

The PrP^{Sc} was purified from hamster brain homogenates as described previously. The homogenates are first centrifuged at low speed to remove

the structural proteins such as myelin. The supernatant is then pelleted at high speed. This pellet is taken up and repelleted from different buffers (the third one containing nucleases) three more times. The pellet after nuclease treatment is denoted as P4 (also PrP33-35) and is substantially purified. This material can be treated with proteinase K, which removes other proteins and truncates PrP^{Sc}. The preparation after PK treatment is denoted as P5 (also PrP27-30).

Because we thought the formation of PrP^{Sc} involves intermolecular contacts similar to crystal growth, the highest possible concentrations of PrP were used to favor the formation of a fibrillar assembly. Higher protein concentrations favor the formation of multimolecular assemblies. In contrast, if protein refolding was desired (e.g. after purification of bacterial-derived protein by inclusion body formation), dilute conditions would be used to favor the unimolecular refolding reaction over the multimolecular aggregation process. In order to maintain the concentration of PrP during the removal of denaturant, the removal was attempted using a filter which allows all molecules below a certain molecular weight (3 or 10 kDa) to pass through it (centricon®). In this way the denaturant could be removed and the protein exposed to various conditions. Unfortunately, attempts to concentrate PrP with the centricon filters led to a loss of protein, apparently because of non-specific binding of the small amount of protein used to the filter. Another important experimental consideration was noted during the initial attempts at denaturing/renaturing PrP^{Sc}. The first preparation of PrP^{Sc} used was P5 (PrP27-30), which had been treated with Proteinase K to remove other proteins. When P5 was treated with GdnHCl, PrP was degraded, presumably because of residual proteinase K in the preparation. We initially chose to use P5 rather than full-length PrP because P5 is more homogeneous

Figure 5.1 Schematic of the experiments described in this chapter. **A**) Seeded renaturation of PrP^{Sc}. **B**) Reversible partial denaturation of PrP^{Sc}. Some remaining PrP^{Sc} is required to act as a seed. **C**) Conversion of PrP^{C} into a protease-resistant form seeded by PrP^{Sc}.

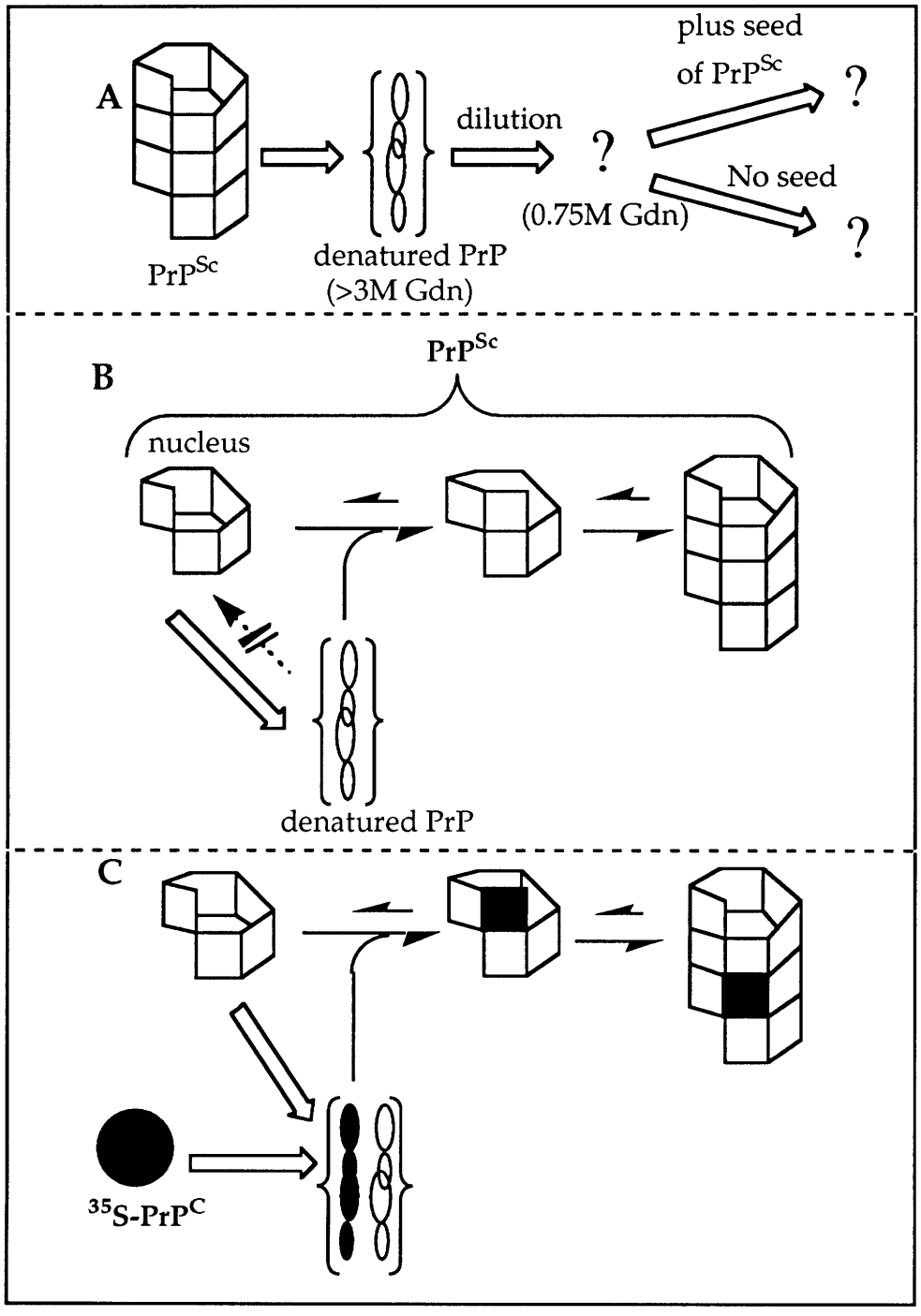

than full-length PrP since most of the other proteins remaining after the first four centrifugations are destroyed by PK. However, since P5 did not tolerate treatment with GdnHCl, further experiments were done using P4, (PrP33-35), which is the same as P5 except for the elimination of the proteinase K treatment. This material was not degraded upon denaturation with GdnHCl and additionally, because it is not truncated, has a greater similarity to the PrP that is converted *in vivo*.

The experiments discussed are outlined in Figure 5.1. The original plan is described in panel A. The PrP^{Sc} is denatured to a protease-sensitive form, the denaturant is diluted, and the sample is split in half and a seed of PrP^{Sc} is added to one portion. The P4 preparation was treated with 3M GdnHCl for 16 hours at 37°C, and the denaturant was then diluted to 0.37-0.75 M GdnHCl. The sample was then divided into two parts. To one part, a small amount (0.5-1%) of untreated P4 was added as a seed. The formation of protease-resistant material was assayed for at intervals by treating aliquots with PK. A return of protease-resistance over time was seen in some samples, however it was inconsistent and independent of the presence of seed.

David Kocisko determined that this renaturation effect could be seen consistently under certain conditions. Renaturation was observed more consistently at 37°C than room temperature. Using a more stable and water soluble protease inhibitor to inactivate the PK and increasing the minimum volume of the transfers involved also improved the reproducibility. The renaturation effect was not dependent on the addition of untreated PrP^{Sc} to act as a seed. It does appear however, that some residual PrP^{Sc} in the sample is required to see renaturation. Conditions which denature all of the PrP^{Sc} (treatment with higher concentrations of GdnHCl (>3.5M) or treatment with

> 1M GdnSCN) irreversible eliminate protease-resistance. This reversible renaturation is depicted schematically in panel B of Figure 5.1 and the experiment is shown in Figure 5.2 (courtesy of D. Kocisko). PrP^{Sc} that is not denatured can seed the reassembly of unfolded PrP. Why does the partial denaturation show refolding and the seeded experiments do not? The amount of seed may be greater in the experiments where PrP^{Sc} is only partially denatured. Additionally, exposure to GdnHCl may free up fresh surfaces and enhance the seeding effect. Under the proper conditions experiments of the type depicted in panel A may be feasible.

The protease-resistance of the renaturing samples increases over time, going from about 2-10% protease-resistant material at time 0 to almost 100% protease-resistant protein after 2 days; Figure 5.2 shows the time course of the renaturation. In the control lanes, the truncation of PrP^{Sc} with PK treatment is seen. The return of PK-resistance material is shown in the next three lanes. The PrP in those three lanes shows the characteristic truncation on PK treatment. A more precise picture of this process comes from probing with antibodies specific for different epitopes of PrP. Three different antibodies have been used to examine the denaturation/renaturation process with epitopes corresponding to regions 89-103, 141-154, and 218-232. The immunoblots using the antibody to the N-terminus of P5 (89-103) showed the greatest change over time. The immunoblots using the antibody to the C-terminal region (218-232) showed the least change with time and detected smaller molecular weight bands. This result suggests that the N-terminus is unfolded to a larger extent upon treatment with denaturants. This region is also more protease-sensitive in the P4 preparation and cleaved by treatment of P4 with proteinase K.

Purification of PrP^C and PrP^{Sc}

Next, the conversion of PrP^C to PrP^{Sc} was attempted. The first requirement for this experiment is purified PrP^C.

PrP^C was derived from cell culture. Two different constructs which had been prepared previously at Rocky Mountain Labs (RML) were used. One construct was full-length hamster PrP expressed in mouse neuroblastoma cells (MNB hamster). The protein from this construct when analyzed by SDS-PAGE shows a series of bands between 30-40 kDa, corresponding to differently glycosylated monomeric species (similar to the PrP from hamster brain), and a band at about 60 kDa, corresponding to a dimeric species (S. Priola, personal communication). The other construct was a mutated hamster PrP secreted by mouse fibroblasts. Normally PrP is cleaved between amino acids 231 and 232 and a GPI anchor is attached. The 23 C-terminal amino acids (including Ser 231 to which the GPI anchor is attached) are not encoded on the gene in this construct, which causes the generation of a truncated form of PrP. The net difference between the full-length and secreted form after biosynthesis is that the secreted form lacks Ser 231 and the attached GPI anchor, which is the reason it is secreted into the medium. The secreted construct of PrP also appears to be less heavily glycosylated than the MNB hamster PrP.

Two different preparations of P4 were used in these experiments. Both were purified by the same protocol but one preparation (denoted as P4.5) was partially degraded during purification. The truncation is similar to what occurs with treatment with PK but not as extensive (see Figure 5.3 for comparison of P4 and P5. The cause of the degradation is unknown but may have been the result of protease contamination in some of the reagents used.

Conversion of PrP^C to a Protease-Resistant Form

Having observed the refolding of partially denatured PrP^{Sc}, the next step was to see if PrP^C could be converted to PrP^{Sc}, which would be characterized by protease-resistance. Unlike in the renaturing of PrP^{Sc}, PrP^C derived from uninfected cells has never been in a protease-resistant form so there is no question of residual PrP^{Sc}-like structure. We hypothesized the conversion of PrP^C to PrP^{Sc} could be caused by a direct interaction of PrP^C with PrP^{Sc} outside the machinery of the cell. Conditions had already been determined for refolding PrP^{Sc} that had been partially denatured (as defined by protease-resistance). We thought the conversion of PrP^C to PrP^{Sc} might occur by incorporating PrP^C into the renaturing PrP^{Sc}. If PrP^C were added to this mixture, in a similarly unfolded state, it might be converted along with PrP^{Sc} that was refolded (see Figure 5.1, Panel C).

The experiment was done by adding [^{35}S]-PrP^C to unlabeled PrP^{Sc}, which had been treated under various conditions (suspended in buffer, 3M GdnHCl, or 6M GdnHCl). The conversion was tested by the development of protease-resistant material derived from PrP^C. The mixture was treated with Proteinase K directly after mixing and after a 2 day incubation; any labeled protein observed (as judged by fluorography after SDS-PAGE) must have been derived from the PrP^C.

First, radiolabeled PrP^C was needed. PrP^C (and all the other proteins in the cell) were metabolically labeled with [^{35}S] methionine. PrP^C was purified by immunoprecipitation from detergent cell lysates in the case of MNB hamster PrP, and from detergent cell lysates and the supernatant for the secreted PrP.[4] Ideally for the secreted form, PrP could be purified from the medium, however it appears that proteases act upon PrP in the medium. The cell lysate derived material was consistently more homogeneous. The

immunoprecipitation was done with an antibody (3F4) that binds hamster PrP but not mouse PrP based on differences between mouse and hamster PrP at residues 109 and 112 (hamster PrP numbering)[5]. The antibody was then attached to protein A sepharose beads and after washing the beads to remove unbound material, PrP was eluted from the beads with 3M GdnHCl. These conditions are likely to denature PrP^C, however since there is no assay for the activity of PrP^C, it cannot be determined if it is properly folded. We felt that unfolding PrP^C might facilitate its incorporation into protease-resistant assemblies.

The conversion of PrP^C to a protease-resistant form was tried by adding [^{35}S]-PrP^C (in 3M GdnHCl) to the PrP^{Sc} in 3M GdnHCl, and then diluting the denaturant as in the renaturation experiments, in the hope that PrP^C would be incorporated in the same way denatured PrP^{Sc} may be refolding. Also, [^{35}S]-PrP^C was mixed with PrP^{Sc} that was suspended in buffer, or PrP^{Sc} that was treated with 6M GdnHCl (conditions known to destroy PrP^{Sc} infectivity and protease-resistance[2]). As a control, [^{35}S]-PrP^C alone was also assayed for protease-resistance. Aliquots were treated with PK directly after mixing (time=0) and after 2 days. Three different experiments are shown in Figures 5.3-5.5.

In all three experiments, labeled protease-resistant bands were seen in the PK treated samples after incubation of PrP^C with PrP^{Sc} (pretreated with buffer or 3M GdnHCl) for 2 days. No protease-resistant bands were seen in the samples of [^{35}S]-PrP^C alone or [^{35}S]-PrP^C mixed with PrP^{Sc} pretreated with 6M GdnHCl. Also no labeled protease-resistant bands were seen in any samples directly after mixing. Apparently, PrP^C was converted to a protease-resistant form like PrP^{Sc}, by incubation with PrP^{Sc}. The protease-resistant material formed had similar elution profiles as PrP^{Sc} treated with PK

(truncated by approximately 8 kDa). That is, it was partially protease-resistant to the same extent as PrP^{Sc} and was cleaved at about the same site. An exact match in apparent molecular weight was not expected because the PrP^{C} and PrP^{Sc} used in this experiment are derived from different sources (cell culture vs. hamster brains), and have different elution properties, probably because of differences in glycosylation which alter the apparent molecular weight. Similar results were obtained with PrP^{C} derived from two sources. The details of the three experiments are discussed below.

The conversion experiment with the secreted PrP construct and the P4 preparation is shown in Figure 5.3. The PrP^{C} used in this experiment has been partly degraded resulting in the ladder of bands observed. As expected, labeled protein was seen in all the samples without PK treatment, although some degradation occurs over time, particularly in the sample of PrP^{C} alone (lane 9 vs. 11). Of the samples treated with 50 μg/mL PK, only the 2 day incubations of PrP^{C} with P4 (pretreated with 3M GdnHCl) showed any labeled protein bands. The samples of PrP^{C} alone, and PrP^{C} mixed with P4 that was treated with 6M GdnHCl, did not contain any protease-resistant labeled protein. Apparently in those samples the PrP^{C} was completely degraded to small peptides.

Another experiment is shown in Figure 5.4. In this experiment, the PrP^{C} was from cells producing full-length hamster PrP and from the cell lysates of the secreted PrP. These two preparations were mixed with P4.5 instead of P4. In this experiment most of the PrP^{C} is converted to protease-resistant material (7 times more protein was loaded into the PK-treated lanes) after 2 days incubation with P4 in buffer (final GdnHCl conc. = 0.37 M) or P4 which had been treated with 3M GdnHCl. The two forms of PrP^{C} show differences in the protease-resistant product formed. In the case of MNB

Figure 5.2 Immunoblots of SDS-PAGE analysis using an antibody raised to a peptide corresponding to residues 90-103 (courtesy of David Kocisko).

Figure 5.3 SDS-PAGE-fluorography analysis of [^{35}S]-PrP (secreted into the medium) mixed with PrP^{Sc} (P4 preparation) that had been treated with varying conditions. Lanes 1,3,6,7,9,11 sample not treated with PK. Lanes 2,4,5,8,10,12 samples treated with 50 μg/mL PK final concentration. Lane 1-4 plus P4 in buffer; lanes 1&2, t=0, lanes 3&4, t=2 days. Lanes 5-8 plus P4 treated with 3M GdnHCl; lanes 5&6 t=0, lanes 7&8 t=2 days. Lanes 9-12 plus P4 treated with 6M GdnHCl; lanes 9&10 t=0, lanes 11&12 t=2 days.

Figure 5.4 SDS-PAGE-fluorography analysis of [^{35}S]-PrP mixed with PrP^{Sc} (P4.5). A. Hamster PrP^{C} from MNB. B. Hamster PrP^{C} from lysates of secreting construct. For both A&B: Samples in even number lanes treated with 10 μg/mL PK. Samples in odd number lanes not PK treated. Lanes 1-4 plus P4.5 in buffer. Lanes 5-8 plus P4.5 treated with 3M GdnHCl. Lanes 9-12 PrP^{C} alone. Lanes 1,2,5,6,9,10 are samples at t=0. Lanes 3,4,7,8,11,12 are samples at t= 2 days.

Figure 5.5 SDS-PAGE-fluorography analysis of [^{35}S]-PrP (secreted into the medium) mixed with PrP^{Sc} (P4.5 preparation) that had been treated with varying conditions. A. Samples not treated with PK. B. Samples treated with 10 μg/mL PK. For both A&B: lanes 1&2 plus P4 in buffer, lanes 3&4 plus P4 treated with 3M GdnHCl, lanes 5&6 plus P4 treated with 6M GdnHCl. Odd lanes t=0, even lanes t=2 days.

Figure 5.2

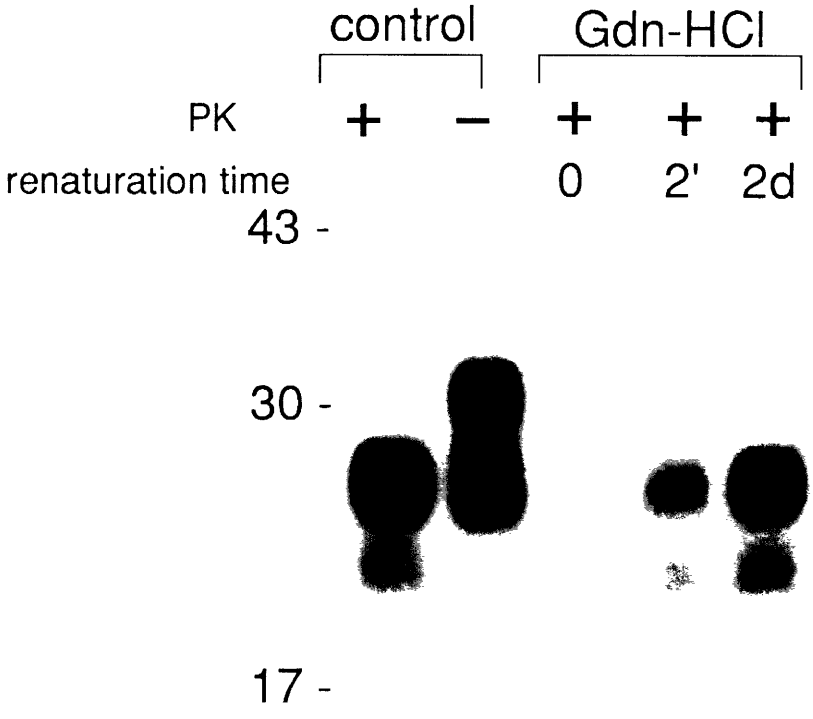

Figure 5.3

Lanes 1 2 3 4 5 6 7 8 9 10 11 12

Figure 5.4

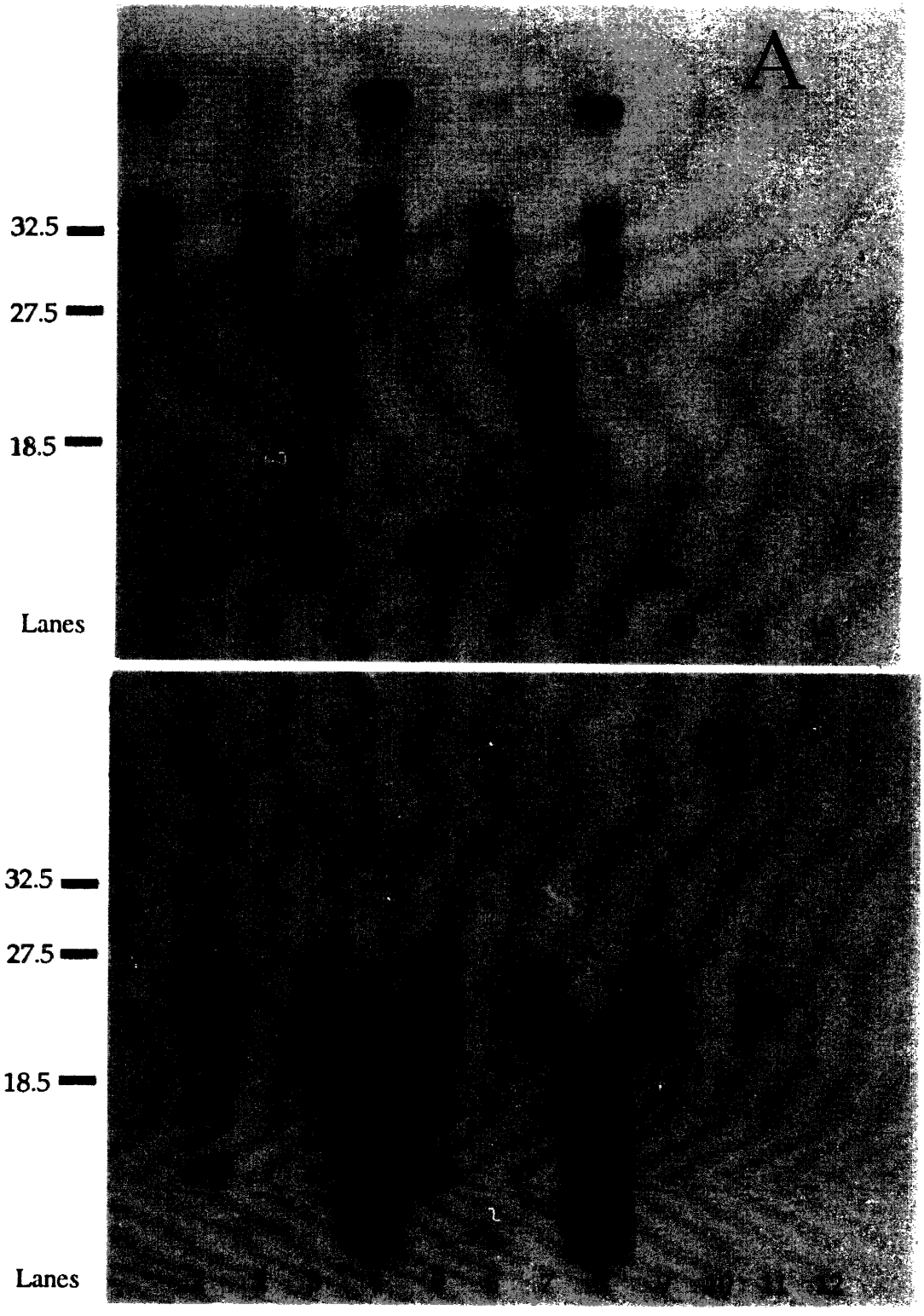

Figure 5.5

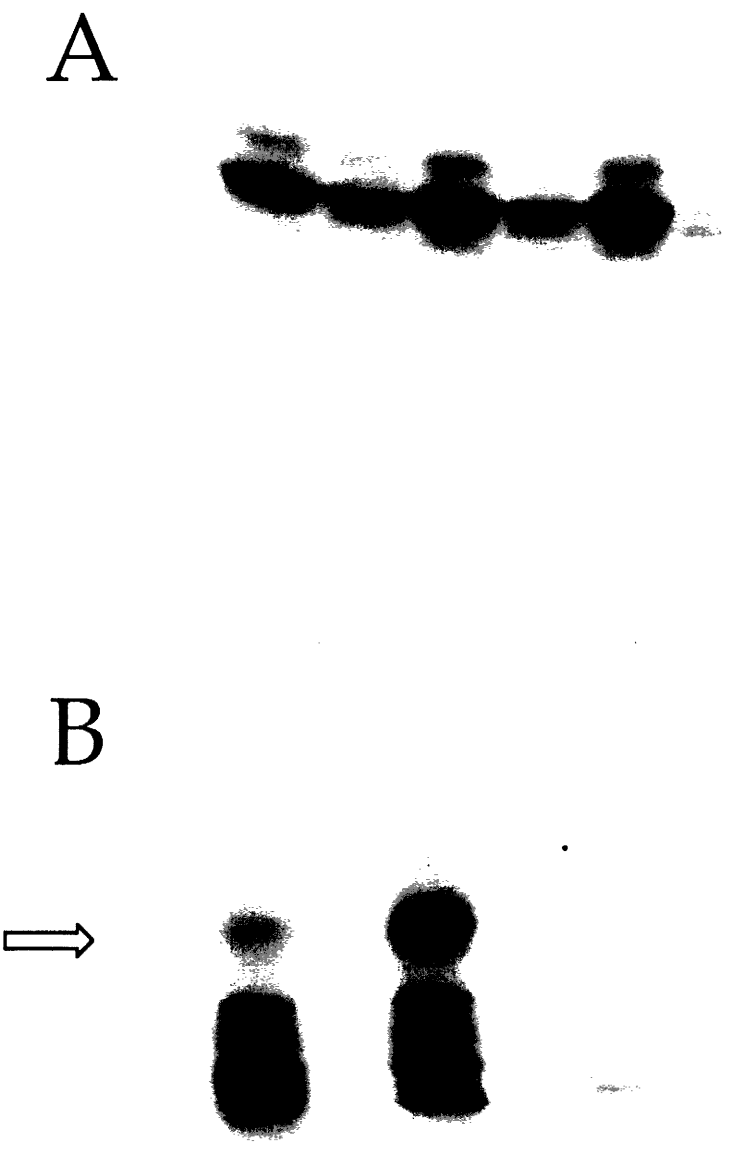

hamster PrP, the dimeric band is converted to a shorter, apparently monomeric band at about 24 kDa. Below this prominent band is a smear of bands which may correspond to the conversion of the monomeric species. The secreted form is converted to a prominent band at about 16 kDa with a ladder of smaller bands below it. The lower molecular weight of the bands in the secreted form may at least partly be due to differences in glycosylation. In this experiment a lower concentration of PK was used (10 μg/mL). In other experiments using a higher concentration of proteinase K to assay for protease-resistance, the conversion is approximately 10-20%. These differences may reflect the fact that although protease-resistant, PrP^{Sc} is eventually degraded by proteases.

A third experiment is shown in Figure 5.5. PrP^{C} is derived from the detergent cell lysate of the secreting construct and is mixed with P4.5 in this experiment. The P4.5 was first suspended in buffer, treated with 3M GdnHCl for 16 hr., or treated with 6M GdnHCl for 16 hr. PK treatment (final PK concentration 10 μg/mL) was done at 0 and 2 days. As seen in the other experiments, after 2 days protease-resistant protein was observed in the samples of PrP^{C} mixed with P4.5 suspended in buffer or treated with 3M GdnHCl, but not in the sample mixed with P4.5 treated with 6M GdnHCl. With the P4 preparation, the conversion is enhanced by treatment with 3M GdnHCl. This enhancement was also seen in one experiment with the P4.5 preparation. Possibly the exposure of "fresh" surfaces enhances the effectiveness of seeding.

In all three experiments, the formation of protease-resistant material derived from PrP^{C} was observed. Protease-resistance is one of the properties that distinguishes PrP^{C} from PrP^{Sc}. The formation of this material suggests that PrP^{C} is converted to PrP^{Sc}. Further evidence that the material formed is

PrP^{Sc} is that the protease-resistant protein bands observed correspond to protein that has been shortened by exposure to PK in the same manner PrP^{Sc} is truncated. Apparently, the protein was accessible to PK, but only specific regions were sensitive to protease digestion, as is the case for PrP^{Sc} purified from the brains of infected animals. The shortening of PrP to protein seen as discrete bands by SDS-PAGE is evidence for a specific conversion of PrP^{C} into a form similar to PrP^{Sc}.

Radiolabeled protease resistant bands were not observed in any of the samples directly after mixing, or in samples of PrP^{C} alone, or in samples where PrP^{C} was mixed with PrP^{Sc} that was first treated with 6M GdnHCl (conditions known to irreversibly destroy protease-resistance and infectivity[2]). This data suggests that some residual structure is required in the PrP^{Sc} to cause the conversion to occur. It does not appear that the protease resistance arises from non-specific trapping of PrP^{C} in aggregates of PrP^{Sc} because that would be expected to lead to nonspecific proteolysis products. Also the PrP^{C} mixed with the 6M GdnHCl-treated PrP^{Sc} is diluted to the same conditions as the other samples but does not exhibit any protease-resistance. Apparently having all the components of PrP^{Sc} present is not sufficient to produce protease-resistance material. The PrP^{Sc} has to be in a particular structure to bring about the conversion. The results are consistent with PrP^{C} folding into a structure, or being incorporated into an assembly, like PrP^{Sc}.

In this system, a large amount of "seed" is present compared to the added PrP^{C} being converted. The stoichiometry allows the conversion to be detected even though the seeding may not be very efficient. The amount of seed required may be substantially less under different conditions; more experiments are required to determine the necessary stoichiometry.

In these experiments, the requirements for the conversion of PrP^C to a protease resistant form are mixing it with PrP^{Sc} and diluting the denaturant. The PrP^{Sc} can be treated with GdnHCl (up to 3M) to partially denature it or just suspended in buffer before mixing. It is not known if the PrP^C has to be unfolded to undergo the conversion. It may be that the exposure of hydrophobic or other regions of the protein, which are not exposed in folded forms of the protein, is required for PrP^C to become protease-resistant. Further experiments using PrP^C purified under different conditions (nondenaturing conditions) are needed to elucidate the requirements of the structure of PrP^C.

These experiments are the first example of PrP^C being converted to a protease-resistant form outside the machinery of the cell. No new protein synthesis or virus replication is needed for this conversion to occur. Because of the excess of PrP^{Sc} used in this experiment, the small amount of additional infectivity from the converted PrP^C cannot be detected in this experiment. The next step is to cause the conversion without the use of PrP^{Sc}. Improvements in the purification of PrP^C will greatly help experiments of this type. Also, additional structural information about the components will help elucidate the mechanism of conversion.

Mechanisms for conversion of PrP^C to PrP^{Sc}

Protected Nucleic Acid

Many proposals have been put forth to explain the unusual properties of scrapie. Some investigators believe that the agent is viral in nature.[6] This proposal does not seem likely because no virus-like particles have been found despite extensive searching. Also, the agent is not destroyed by conditions

which would destroy all other known viruses. However, the putative virus may have properties different from other viruses that cause it to elude detection.

Because of the unusual nature of the agent, its important to keep an open mind to different hypotheses, particularly testable ones. Although the agent appears not to be a virus like any seen previously, it possibly contains a well protected agent-specific nucleic acid in small amounts that is responsible for replication or plays a role in infection. However, there is no evidence to support this proposal. No agent-specific nucleic acid has been found.

Some investigators still believe other nonprotein components are required to explain the characteristics of the infectious agent based upon three lines of evidence: radiation target sizes, the number of molecules in an infectious unit, and the existence of strains.[7, 8]

Radiation target sizes have been cited to support the small size (relative to a virus) of the scrapie agent.[9] Deactivation by ionizing radiation is based on the premise that when struck by high energy radiation, the macromolecule of interest will be completely destroyed (by some unknown mechanism).[10] The likelihood of the macromolecule being hit will be proportional to its size. This method has been useful for determining enzyme volume. This method has been used to try to measure the size of the scrapie agent. However, it is unclear whether this type of determination would be accurate for an aggregate that seeds the polymerization of more protein. The "activity" of the aggregate would depend on the number of surfaces exposed. Destruction of protein inside the aggregate may have no effect on the aggregate or possibly break it up into smaller oligomers which have more surfaces for polymer growth to occur. Without knowledge of the nature of the agent, it is difficult to interpret the data from these experiments.

Another piece of data cited as evidence for various theories is the number of molecules of PrP in an infectious unit. This number has been calculated to be 10^5 PrP molecules for preparations of PrP as rod-like particles.[11, 12] That is, dilution of the infectious agent below 10^5 PrP molecules will eliminate infectivity. These rods could be dispersed into liposomes which were calculated to have 2-4 PrP molecules each.[13] These investigators stated that this data was consistent with an infectious unit containing 2-4 PrP molecules. That is, they believed a liposome of 2-4 PrP molecules was infectious. However, the infectivity was only increased by 10-fold (going from rods to liposomes). This result means that 10^4 of these liposomes were required for an infectious unit. The main problem with using the size of, or number of molecules in, an infectious unit as evidence for the nature of the agent is that the effectiveness of infection is unknown. If the majority of the inoculum is disabled by the host, the number of particles, or size of the particles in the infectious unit will appear much larger, not because large particles are required, and not because only a small percentage of the particles have the potential for infectivity, but because only a small percentage of the potentially infectious particles reach their site of action. Without knowledge of the mechanism of infection, this data is also difficult to interpret.

The different strains of scrapie observed are difficult to explain without invoking the involvement of nucleic acid.[14] Genetic material in the infectious agent would help explain the different strains seen. Although there are nucleic acids associated with preparations of the scrapie agent, they are generally only 50-100 bases in length; this size is insufficient to encode even a small protein. Conceivably, this nucleic acid interacts with the host in some way to cause phenotypic differences in the disease. It is already

established that differences in the PrP sequence cause phenotypic differences in the disease.[12, 15] The search for such a nucleic acid is fraught with problems. Amplification of DNA or RNA by polymerase chain reaction (PCR) can lead to artifactual amplification of contaminants. Also, without information on the nucleic acid you are looking for, it is difficult to choose the appropriate primers. Further purification of the infectious agent will probably be necessary to determine if such a molecule is involved.

Weissmann's Proposal

Weissmann has proposed what he calls a "unified theory" of prion propagation.[16] In his proposal, Weissmann suggests that the infectious agent consists of two components: PrP^{Sc} (the apoprion) and a nucleic acid component (coprion). He states that PrP^{Sc} itself is pathogenic but the phenotypic properties are caused by a nucleic acid which can be exchanged with host nucleic acid. He states that a testable hypothesis from this proposal is that the strain variation should depend on preparations of agent containing nucleic acid. If nucleic acid can be removed from preparations of agent, strain variations should be removed.

In the majority of studies of strain variation, crude brain homogenates are used in the passage experiments. The greater the number of manipulations the greater the risk of contamination with agent from other preparations. However, semipurified preparations (nuclease or protease treated) can be used and maintain the characteristics of the strain (Richard Bessen, personal communication). However, it is difficult to completely remove all the nucleic acid because high resolution conditions (e.g. SDS-PAGE, HPLC) which might be able to purify the protein to homogeneity

eliminate infectivity. This problem makes it difficult to test Weissmann's theory.

In addition, it is unclear how this small, interchangeable nucleic acid could causes the strain differences, and why this nongenomic nucleic acid is associated with the agent.

Griffith's Proposal

If the infectious agent is devoid of genetic material, how might it work? As discussed briefly in Chapter 1, Griffith proposed three mechanisms for how this might be possible, one of which still may be applicable.[17] Given protein subunits α which can undergo the following reactions:

$$\alpha_2 + \alpha \longrightarrow \alpha_3$$

$$\alpha_3 + \alpha \longrightarrow \alpha_4$$

$$\alpha_4 \longrightarrow 2\alpha_2$$

and if

$$\alpha + \alpha \longrightarrow \alpha_2$$

cannot occur directly, then the dimerization of α can only occur if α_2 is already present. Griffith postulated that this reaction scheme might be reasonable if α is generally found in a different conformation, α', which does not undergo the conversion. This conformational change could be facilitated by higher oligomers of α. Therefore, the spontaneous conversion would be very rare but the presence of higher oligomers could catalyze its conversion. This mechanism is not specific, and of course, it does not account for all the details elucidated in the intervening years, but in general terms, it

encompasses many of the protein-only explanations that have appeared in the literature.

Prusiner's Proposal

Prusiner has put forth a mechanism for this conversion on several occasions.[12, 18, 19] In his proposal, the conversion of PrP^{C} to PrP^{Sc} is caused by the formation of a heterodimeric complex between the two forms, which catalyzes the conversion of PrP^{C} to PrP^{Sc} (see Figure 5.6). According toPrusiner, this conversion is a conformational change where regions of α-helices are converted to β-strands or β-sheets.[19] The new homodimeric complex of PrP^{Sc} then dissociates, producing two molecules of PrP^{Sc} to continue the process. The spontaneous conversion of PrP^{C} would presumably be too slow to occur but favorable thermodynamically. Complexation of PrP^{Sc} with PrP^{C} would lower the activation barrier.

One problem with this mechanism is that the "enzyme" (PrP^{Sc}) would be severely inhibited by the product because the dissociation rate is very unfavorable as determined by the low solubility. Most of the PrP^{Sc} would be in an aggregate rather than monomeric. Also, there are no examples of two stable, kinetically trapped protein conformers. It is unclear how the conversion would take place and whether folded PrP^{C} interacting with PrP^{Sc} would be sufficient for the conversion.

Even Prusiner may no longer favor this mechanism, as a recent publication from his group does not discuss formation of a heterodimer, although interactions between PrP^{C} and PrP^{Sc} are invoked.[20] Prusiner also does not, as he has in the past, specifically rule out the role of oligomerization.[12, 19, 21] Oligomerzation is crucial in other mechanisms

Figure 5.6. Prusiner's model for the transmission of the prion diseases.

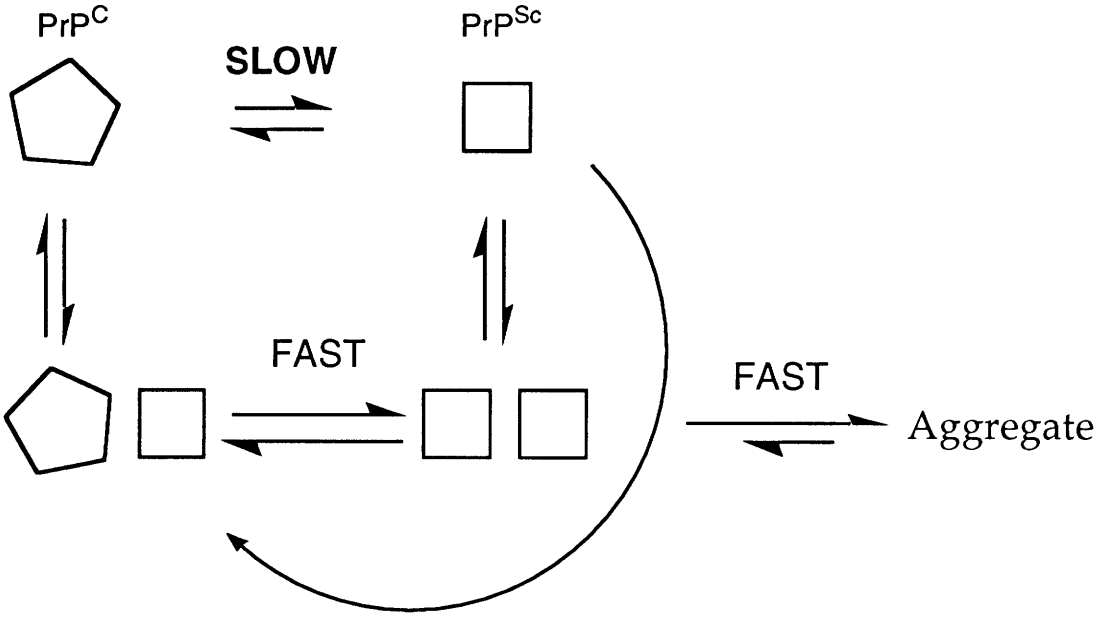

which have been presented previously (see seeded polymerization below).[22, 23, 24] In this recent article Prusiner also discusses for the first time the possible importance of the unfolding of PrP^C in the transformation. The possible requirement of unfolding PrP^C has been proposed previously but was not referenced.[23]

The Seeded Polymerization Model

A seeded polymerization mechanism (Figure 5.7), which is consistent with the peptide studies described herein, may be more likely. In this mechanism, PrP^{Sc} acts as a nucleus for the polymerization of PrP^C.[22, 23, 24] The conformation of PrP in PrP^{Sc} is stabilized through intermolecular interactions. Normally, PrP does not form aggregates but is degraded by the cell, possibly because the formation of polymers follows a nucleation-dependent mechanism. In this mechanism, small oligomers are unstable and revert back to monomers until the nucleus is reached; after this point, the

Figure 5.7. Seeded polymerization model for the prion diseases.

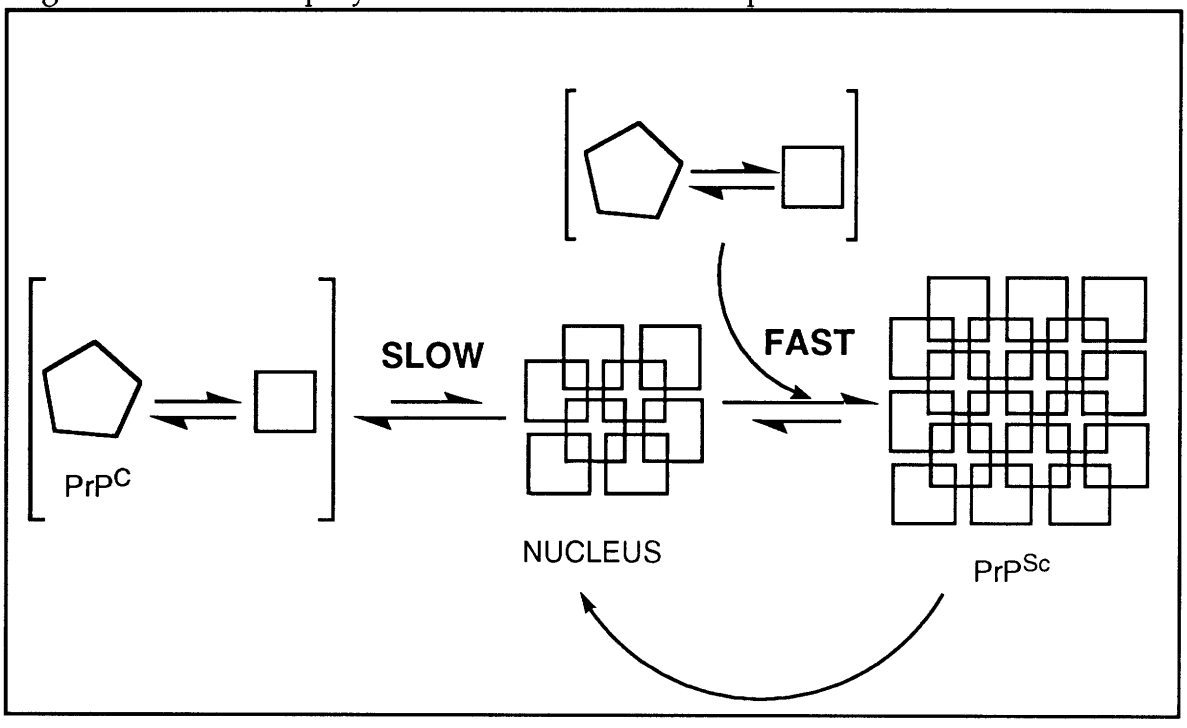

addition of more PrP becomes energetically favorable. If the polymerization process is too slow, the protein will be drawn off by other pathways, such as proteolysis. In this mechanism, PrP^{C} can access the conformation of PrP^{Sc} under certain conditions to which it is exposed, but the conversion of PrP^{C} to PrP^{Sc} does not take place because the concentration of PrP is insufficient for nucleus formation to occur at a significant rate. The concentration of PrP may be sufficient to support growth on nuclei already present, however.

Infection could occur by the introduction of oligomers onto which PrP can grow. The direct contact of PrP^{Sc} and folded PrP^{C} may not be sufficient for this to occur. As in many cases of inclusion body formation, polymerization may require the partial unfolding of the aggregating protein. Partial denaturation increased the aggregation tendency of apomyoglobin[25] and transthyretin.[26] Unfolding can expose hydrophobic residues which provide crucial intermolecular contacts. In this scenario, the unfolded protein (PrP^{U}) is sampling many different conformations, including conformations similar

to PrP^{Sc}, but none of these are stable without the formation of intermolecular interactions. The introduction of a nucleus of PrP^{Sc} would allow PrP^{U} to grow on the surface, bypassing nucleation.

Possibly, some combination of Prusiner's mechanism and the seeded polymerization mechanism is at work. For instance, the PrP^{U} may form a complex with the nucleus of PrP^{Sc} and then undergo a realignment to the most tightly binding conformation. The formation of less specific hydrophobic interactions may bring two molecules in contact, increasing the likelihood of the proper interactions forming. In a sense then, PrP^{Sc} is catalyzing the conformational change by stabilizing the aggregating conformer.

Additional molecules may also be required for the conversion of PrP^{C} to PrP^{Sc}. Proteoglycans, such as heparin, are found bound to PrP in preparations of the infectious agent and also bind to PrP^{C} *in vitro*.[4] This interaction may be largely electrostatic between the negatively charged proteoglycan and the positively charged PrP. The proteoglycan may serve to bind PrP molecules together. Other molecules could also act as cofactors in the assembly of PrP^{Sc}.

How can the existence of strains be explained? Strains are difficult to explain in a protein-only model. Strains may be caused by PrP^{Sc} being targeted to different regions of the brain. If accumulation was more likely in one part of the brain or another, differences in symptoms might be expected. But how could PrP be targeted to specific regions of the brain? There might be information in the tertiary structure that makes certain cell types more susceptible. The differently glycosylated forms of PrP may also play a role in targeting PrP to certain cell types. Possibly, different cell types have differences in glycosylation which make the fit between PrP^{Sc} and PrP^{C} better

in certain regions of the brain. This selectivity may then be passed on because the PrP^{Sc} would develop in the region of the brain with the best match. Rectifying the characteristics of the scrapie agent (particularly the existence of strains) with the data on the physical nature of the scrapie agent remains one of the great puzzles in biology.

EXPERIMENTAL

General Procedures

PrP^{Sc} was purified from scrapie infected hamster as described previously.[27] PrP was analyzed by SDS-PAGE using a NOVEX gel apparatus and prepoured 14%, 1 or 1.5 mm denaturing polyacrylamide gels (NOVEX) or on a PhastGel system (Pharmacia) using 20 % denaturing polyacrylamide gels. Proteins were visualized by immunoblotting, or in the case of radiolabeled protein, by fluorographic detection.[4] Protein concentrations were determined by BCA assay using BSA as standard. Cells were metabolically labeled with [^{35}S] methionine and PrP immunoprecipitated from detergent lysates as described previously.[4] The PrP^{C} was eluted with 3M GdnHCl. The P4 preparation was approximately 7 μg/μL in protein. The P4.5 preparation was approximately 4 μg/μL in protein. Tris buffer refers to 10 mM Tris, 100 mM NaCl, at pH 7.4. SDS-PAGE sample buffer: was 1mmol EDTA, 5% SDS (w/v), 6% urea (w/v), 4% β-mercaptoethanol (v/v), .05 % bromophenol blue (w/v) in 10 mmol Tris, pH 8.3. Pefabloc® was used at 0.1 mmol (5X = 0.5 mmol).

Experiment shown in Figure 5.1.

PrP purified from the medium containing the cells with the secreted construct was mixed with P4 treated in 2 ways: A) To P4 (3 μL) was added 6 μL

of 9M GdnHCl and B) to P4 (3 μL) was added 3 μL H_2O followed by 3 μL 9M GdnHCl. After 16 hrs to A was added 9 μL Tris bufffer, to B was added 9 μL 3M GdnHCl. Both samples are now X μg/μL in protein in 3M GdnHCl. Three samples of PrP^C were made (final volme 32 μL).

Sample 1: 4 μL A plus 4 μL [^{35}S] PrP^C

Sample 2: 4 μL B plus 4 μL [^{35}S] PrP^C

Sample 3: 4 μL 3M Gdn HCl plus 4 μL [^{35}S] PrP^C

To all samples 24 μL Tris buffer was added. After about 5 min and after 2 days the samples were treated as follows: 15 μL (~1/2) was diluted with 65 μL Tris buffer, 70 μL of this sample was added to 3.5 μL of a 1 mg/mL solution of PK and incubated at 37°C for 1 hr. Then 15 μL of a 5X (0.5 mmol) of Pefabloc® was added and incubated for 10 min. The remaining 10 μL was diluted with 40 μL Tris buffer and treated as the PK-treated samples. To all samples, 20 μg of thyroglobulin (in 4 μL) was added as a carrier followed by 350 μL of cold MeOH. The samples were kept at -20°C for 2 h. and then spun down at 14,000g for 10 min. The MeOH was removed and the pellet taken up in 24 μL of SDS-PAGE sample buffer, boiled, and loaded onto Novex 1.5 mm 14% denauring polyacrylamide gels.

Experiment shown in Figure 5.2

PrP purified from detergent cell lysates from both cells with the secreted construct and from the MNB cells and mixed with P4 treated in 2 ways: A) To P4 (4 μL) was added 24 μL of Tris buffer, and B) to P4 (3 μL) was added 3 μL H_2O followed by 3 μL 9M GdnHCl. After 6 hrs., three sample of PrP^C for each construct were made (final volume 16 μL).

Sample 1: 14 μL A plus 2 μL [^{35}S] PrP^C

Sample 2: 2 µL B plus 2 µL [^{35}S] PrP^{C}

Sample 3: 2 µL 3M Gdn HCl plus 2 µL [^{35}S] PrP^{C}

To samples 2&3, 12µL of Tris buffer was added. After about 5 min and after 2 days the samples were treated as follows: To 7 µL (~1/2) 33 µL Tris buffer was added. 35 µL of this sample was added to 3.5 µL of a 0.1 mg/mL solution of PK and incubated at 37°C for 1 h. Then 7 µL of a 5X (0.5 mmol) of Pefabloc® was added and incubated for 10 min. The remaining 5 µL was diluted with 20 µL Tris buffer and treated as the PK-treated samples. To all samples, 20 µg of thyroglobulin (in 4 µL) was added as a carrier followed by 200 µL of cold MeOH. The samples were kept at -20°C for 2 h. and then spun down at 14,000g for 10 min. The MeOH was removed and the pellet taken up in 20 µL of SDS-PAGE sample buffer, boiled, and loaded onto Novex 1.5 mm 14% denaturing polyacrylamide gels.

Experiment shown in Figure 5.3

PrP purified from the detergent cell lysates derived from the cells with the secreting construct was mixed with P4.5 treated in 3 ways: A) To P4.5 (3 µL) was added 6 µL of Tris buffer, and B) to P4.5 (3 µL) was added 3 µL H_2O followed by 3 µL 9M GdnHCl, and C) to P4.5 (3 µL) was added 6 µL of 9M GdnHCl. After 16 hrs, three samples of PrP^{C} were made (final volume 16, 24, and 24 µL).

Sample 1: 2 µL A plus 12 µL Tris buffer plus 2 µL [^{35}S] PrP^{C}

Sample 2: 2 µL B plus 2 µL 3M GdnHCl plus 2 µL [^{35}S] PrP^{C} plus 18 µL Tris buffer

Sample 3: 2 µL C plus 2 µL [^{35}S] PrP^{C} plus 20 µL Tris buffer

After about 5 min and after 2 days the samples were treated as follows: For sample 1: 8 μL (~1/2) was diluted with 60 μL Tris buffer plus 4 μL 3M GdnHCl. For samples 2&3, 12 μL was diluted with 64 μL Tris. Then for all samples, 63 μL of this sample was added to 6.5 μL of a 0.1 mg/ml solution of PK and incubated at 37°C for 1 h. Then 13 μL of a 5X (0.5 mmol) of Pefabloc® was added and incubated for 10 min. The remaining 7 μL was diluted with 20 μL Tris buffer and treated as the PK-treated samples. To all samples, 20 μg of thyroglobulin (in 4 μL) was added as a carrier followed by 330 μL of cold MeOH. The samples were kept at -20°C for 2 h. and then spun down at 14,000g for 10 min. The MeOH was removed and the pellet taken up in 24 μL of SDS-PAGE sample buffer, boiled, and loaded onto Novex 1.5 mm 14% denauring polyacrylamide gels.

REFERENCES FOR CHAPTER 5

(1) Raeber, A. J.; Borchelt, D. R.; Scott, M.; Prusiner, S. B.; *J. Virol.* **1992**, *66*, 6155.
(2) Prusiner, S. B.; Groth, D.; Serban, A.; Stahl, N.; Gabizon, R.; *Proc. Natl. Acad. Sci. USA* **1993**, *90*, 2793.
(3) Safar, J.; Roller, P. P.; Gajdusek, D. C.; Gibbs, C. J.; *J. Biol. Chem.* **1993**, *268*, 20276.
(4) Caughey, B.; Raymond, G. J.; *J. Virol.* **1993**, *67*, 643.
(5) Kascsak, R. J.; Rubenstein, R.; Merz, P. A.; Tonna-DeMasi, M.; Fersko, R.; Carp, R. I.; Wisniewski, H. M.; Diringer, H.; *J. Virol.* **1987**, *61*, 3688.
(6) Manuelidis, E. E.; Manuelidis, L.; *Proc. Natl. Acad. Sci. USA* **1993**, *90*, 7724.
(7) Carp, R. I.; Kascak, R. J.; Wisniewski, H. M.; Merz, P. A.; Rubenstein, R.; Bendheim, P.; Bolton, D.; *Alzheimer Dise. Assoc. Disorders* **1989**, *3*, 79.
(8) Carp, R. I.; Kascsak, R. J.; Rubenstein, R.; Merz, P. A.; *Trends Neurosci.*. **1994**, *4*, 148.
(9) Bellinger-Kawahara, C. G.; Kempner, E.; Grath, D.; Gabizon, R.; Prusiner, S. B.; *Virology* **1988**, *164*, 537.
(10) Kempner, E. S.; Schlegel, W.; *Anal. Biochem.* **1979**, *92*, 2.
(11) Prusiner, S. B.; Bolton, D. C.; Groth, D. F.; Bowman, K. A.; Cochran, S. P.; McKinley, M. P.; *Biochem.* **1982**, *21*, 6942.
(12) Prusiner, S. B.; *Science* **1991**, *252*, 1515.
(13) Gabizon, R.; Mckinley, M. P.; Prusiner, S. B.; *Proc. Natl. Acad. Sci. USA* **1987**, *84*, 4017.
(14) Bruce, M. E.; Fraser, H. in *Transmissible Spongiform Encephalopathies: Scrapie, BSE and Related Disorders*; Chesebro, B. W.; Springer-Verlag, Berlin-Heidelberg, **1991**; pp 125.
(15) Goldfarb, L. G.; Peterson, R. B.; Tabaton, M.; Brown, P.; LeBlanc, A. C.; Montagna, P.; Cortelli, P.; Julien, J.; Vital, C.; Pendelbury, W. W.; Halta, M.; Willis, P. R.; Hauw, J. J.; McKeever, P. E.; Monari, L.; Schrank, B.; Swergold, G. D.; Autillo-Gambetti, L.; Gajdusek, D. C.; Lugaresi, E.; Gambetti, P.; *Science* **1992**, *258*, 806.
(16) Weissmann, C.; *Nature* **1991**, *352*, 679.
(17) Griffith, J. S.; *Nature* **1967**, *215*, 1043.
(18) Prusiner, S. B.; *Annu. Rev. Microbiol.* **1989**, *43*, 345.
(19) Pan, K.-M.; Baldwin, M.; Nguyen, J.; Gasset, M.; Serban, A.; Groth, D.; Mehlhorn, I.; Huang, Z.; Fletterick, R. J.; Cohen, F. E.; Prusiner, S. B.; *Proc. Natl. Acad. Sci. USA* **1993**, *90*, 10962.
(20) Cohen, F. E.; Pan, K.-H.; Huang, Z.; Baldwin, M.; Fletterick, R. J.; Prusiner, S. B.; *Science* **1994**, *264*, 530.
(21) Prusiner, S. B.; *Biochem* **1992**, *31*, 12277.
(22) Brown, P.; Goldfarb, L. G.; Gajdusek, D. C.; *The Lancet* **1991**, *337*, 1019.
(23) Come, J. H.; Fraser, P. E.; Lansbury, J. P. T.; *Proc. Natl. Acad. Sci. U.S.A.* **1993**, *90*, 5959.
(24) Ridley, R. M.; Baker, H. F.; *Trends Neurosci.* **1993**, *16*, 425.

(25) De Young, L. R.; Dill, K. A.; Fink, A. L.; *Biochem.* **1993**, *32*, 3877.
(26) Colon, W.; Kelly, J. W.; *Biochemistry* **1992**, *31*, 8654.
(27) Caughey, B. W.; Dong, A.; Bhat, K. S.; Ernst, D.; Hayes, S. F.; Caughey, W. S.; *Biochemistry* **1991**, *30*, 7672.(

Appendix A

Methods to improve the synthesis of hydrophobic peptides

Hydrophobic peptides can be difficult to synthesize and purify in substantial quantities. Aggregation can occur during both synthesis on a solid support and in the subsequent purification. Peptides of more than about 15-20 residues with a large percentage of hydrophobic, and in particular, β-branched residues, are usually only slightly soluble in aqueous or organic solvents. When peptides of this type are synthesized in a stepwise manner, small quantities of a large number of different deletion impurities will likely form. These impurities will be difficult to separate from the desired product at the end of the synthesis. One way to circumvent this problem is to produce smaller fragments, which are more easily purified to homogeneity, and then couple these fragment together to produce the final product. In this manner, the final purification involves only the separation of peptides which differ significantly in molecular weight.

In addition to fragment coupling, other methodology is needed to improve the synthesis of difficult sequences. Temporary modifications of the peptide chain to increase its solubility may help in both synthesis and purification. Also a method to purify peptides without HPLC would may increase the yields of hydrophobic peptides. These two methods will be discussed in the appendix.

Amide Protection by Alkylation

Alkylation of the amide nitrogen in hydrophobic peptides greatly increases their solubility in organic solvents. Optimally this alkylation

should be compatible with the other protecting groups used in solid-phase peptide synthesis. We set out to place substituted benzyl groups on selected amide nitrogens to improve the solubility of these peptides. The 4-methoxybenzyl group is easily placed onto an amino acid according to a literature procedure.[1] The amino group can then be protected at a t-butylcarbamate (t-boc). Attempts to use such an amino acid in a stepwise synthesis led to a low level of incorporation. In order to avoid the problems associated with placing such a low yielding step in the middle of a multi-step solid-phase synthesis, the coupling at the benzyl amine was done in solution, and the resulting dipeptide purified by silica gel chromatography and used to synthesize larger peptides. The synthesis of these peptides was done according to the scheme shown below.

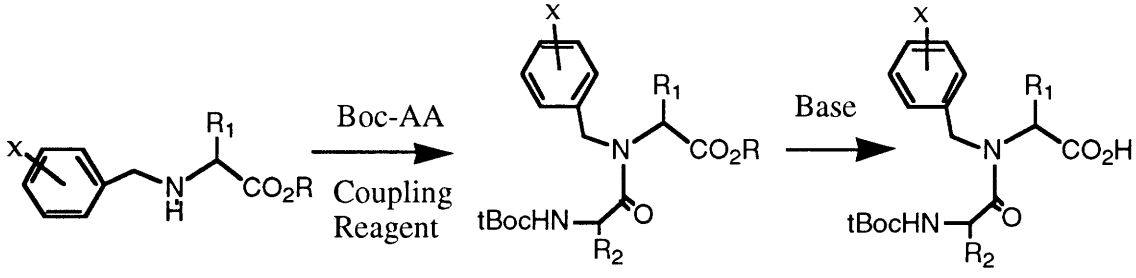

This protecting group (4-methoxybenzyl) was incorporated into β34-42 at two positions, Gly 37 and Val 39. This modification greatly increased the solubility in organic solvents. For instance, this protected peptide was freely soluble in MeOH. It was uncertain, before the synthesis, whether this protecting group could be removed by HF. Attempts to deprotect this peptide by treatment with anhydrous HF were unsuccessful. The placement of an additional methoxy group on the benzene ring would make this moiety labile in acid. Since this work was started a similar protecting group 2-hydroxy-4-methoxybenzyl has been shown to be an effective protecting group in the synthesis of β 1-43[2].

Affinity Purification

A method for extracting the peptide of interest directly out of the cleavage mixture would be of great help in the production of peptides, particularly longer hydrophobic peptides which are not as easily purified by methods employing aqueous solvents systems, such as HPLC. A method has been developed by Irving Sucholeiki in the Lansbury lab where the last amino acid contains a protected thiol group. This thiol can be deprotected and attached to a solid support to separate all the components with this group (ideally only the full length peptide) from other impurities (particularly truncated, acetylated peptides). The protecting group is shown below.

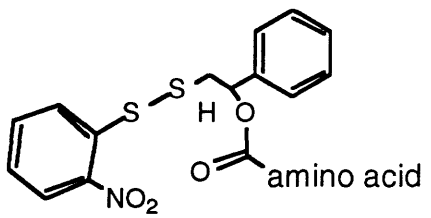

This group (nitro-Irvoc) can be removed by 100% TFA. In order to make it more acid stable, a nitro version was synthesized by the same basic procedure. This protecting group was incorporated into a 10 amino acid peptide (PrP110-119). The thiol moiety can be freed by treatment with dithiothreitol and DIEA in DMF. The thiol containing peptide can then be attached to an iodoacetamide resin, nonbinding material washed away, and the peptide cleaved from the resin with 10% TFMSA in TFA to give pure peptide in moderate yield. The synthesis was done following the scheme outlined below.

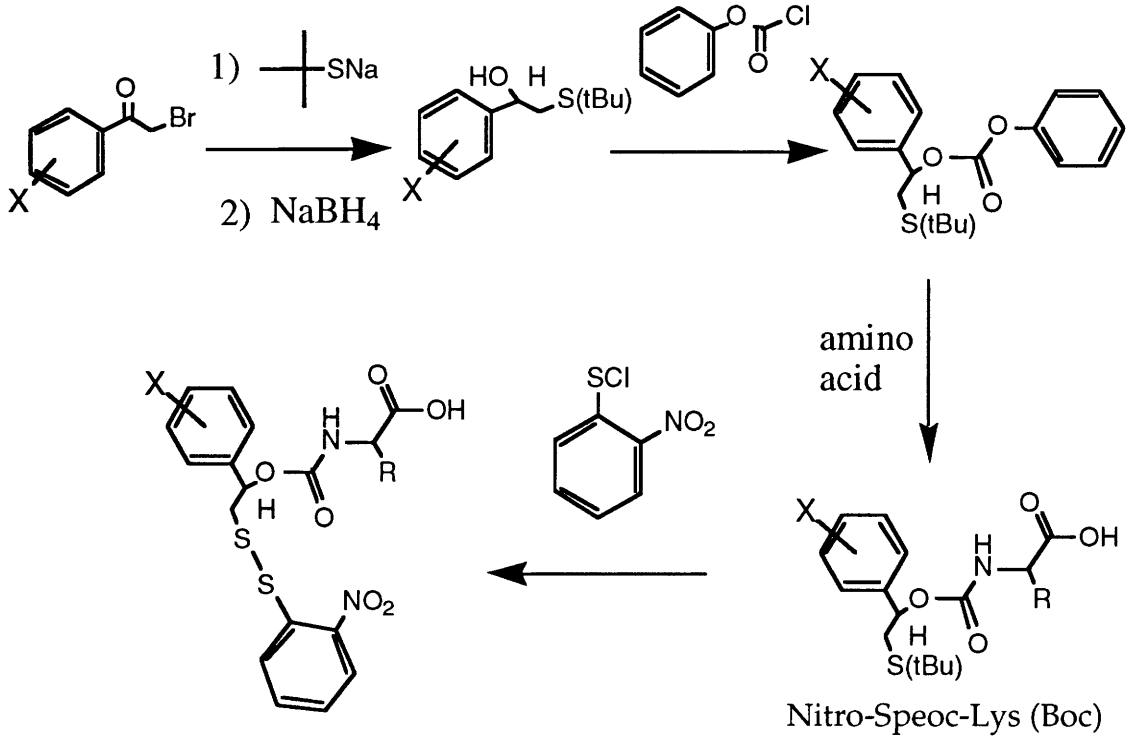

EXPERIMENTAL

Preparation of N-(4-methoxybenzyl) valine methyl ester (JHC2-123)

Valine methyl ester HCl (5.0g, 30 mmol) and p-anisaldehyde (4.0mL, 33 mmol) were dissolved in 70 mL methanol and 5 mL acetic acid. To this solution sodium cyanoborohydride (1.5g, 25 mmol) was added as a solid. After 16 hours the solvent was removed and the residue taken up in CH_2Cl_2 (100mL) and 1N HCl (100mL). The organic layer was concentrated to a white solid which was triturated with 1:1 diethyl ether/hexane, filtered, and dried to 6.2g (21.6 mmol, 72%) of a white solid. Rf 0.29 (1:1 EA/Hex) as the free amine. NMR(HCl salt) (300MHz, $CDCl_3$) δ 7.51 (d, 2H, J= 7.1Hz) 6.80 (d, 2H, J=7.1 Hz) 4.21 (d, 1H, J=13.3 Hz) 4.13 (d, 1H, 13.3 Hz) 3.75 (s, 3H) 3.40 (d, 1H, J=4.5 Hz) 2.61 (m, 1H)

Preparation of t-Boc-Gly-Val(N-4-methoxybenzyl)-OMe (JHC2-139)

N-(4-Methoxybenzyl) valine methyl ester HCl (2.43g, 8.5 mmol and t-Boc-Gly-OH (2.2g, 12.8 mmol) were dissolved in 25 mL DMF. To this solution 6.0g (12.8 mmol) PyBrop was added along with 4.5 mL (26.4 mmol) DIEA. After 18 hours an additional 2.0g (4.3 mmol) PyBrop and 1.5 mL (8.8 mmol) DIEA were added and the reaction stirred at room temperature. After 48 hours the solvent was removed under reduced pressure, and 0.5N NaOH(aq) and CH_2Cl_2 were added. The layers were separated and the organic layer was washed with 1N HCl, dried over $MgSO_4$, and concentrated to a brown oil.

This was purified by flash silica chromatography (1:3 EA/Hex) to give 1.85g, 4.5mmol (53%) of a yelllow oil. Rf 0.27 (1:1 EA/Hex).

Preparation of t-Boc-Gly-Val(N-4-methoxybenzyl)-OH (JHC2-147)

Boc-Gly-Val(N-4-methoxybenzyl)-OH (1.7g,4.16 mmol) was dissolved/suspended in 50 mL methanol and 30 mL 1N NaOH(aq) at room temperature. After 18 hours, the methanol was removed. The solution was acidified to pH4 with 80 mL 10% citric acid and extracted with CH_2Cl_2. The organic layer was dried over $MgSO_4$, filtered, and concentrated to 1.4g, 3.55 mmol (85%) a white foam. Rf 0.18 (1:1 EA/Hex)

Preparation of N-(4-methoxybenzyl)-glycine methyl ester (JHC2-149)

Glycine methyl ester (12.5g, 0.1 mol) and p-anisaldehyde were dissolved in 150 mL methanol and 12 mL acetic acid. To this solution 5.2g (83 mmol) sodium cyanoborohydride was added as a solid. After 48 hours, the solvent was removed and H_2O and CH_2Cl_2 were added. The solution was then taken to pH8 with NaOH. The layers were separated, and the organic layer was dried over $MgSO_4$, concentrated to an oil, and purified by flash silica chromatography (25%EA/Hex,50%EA/Hex, 50%EA/Hex with 1%NEt_3) to give 8.0g, 0.038 mol (38%) of a brown oil. Rf 0.2 (60%EA/Hex). NMR (300 MHz, CDCl3) δ7.5 (d, 2H, J=9Hz) 6.9 (d, 2H, J=9Hz) 3.85 (s, 3H) 3.78 (s, 3H) 3.42 (s, 3H)

Preparation of t-Boc-Val-Gly(N-4-methoxybenzyl)-OMe (JHC2-155)

N-(4-Methoxybenzyl)glycine methyl ester (2.08g 10 mmol) and Boc-Val-OH (2.6g, 12 mmol) were dissolved in 30 mL DMF. To this solution PyBrop (7.0g, 15 mmol) and 5.1 mL (30 mmol) DIEA were added. After 24 hours 3.0g (6.4 mmol) more PyBrop was added. After 6 hours more, the solvent was removed; CH_2Cl_2 and 0.5 N NaOH(aq) were added. The layers separated, and. the organic phase was washed with 10% citric acid, dried over $MgSO_4$, concentrated to a brown oil, and purified by flash silica chromatography (10-20-25%EA/Hex) to give 1.72g ,4.2 mmol (42%) of a colorless oil. Rf 0.51 (60% EA/Hex).

Preparation of t-Boc-Val-Gly(N-4-methoxybenzyl)-OH (JHC2-157)

Boc-Val-Gly(N-4-methoxybenzyl)-OH 1.7g (4.2 mmol) was dissolved/suspended in 100 mL 2:1 methanol/ 0.8 N NaOH. After 4 hours the methanol was removed and 10 mL 6N HCl was added to bring the pH to 0. The suspension was extracted with CH_2Cl_2, dried over $MgSO_4$, and concentrated to 1.44g (3.6 mmol, 87%) of a white foam. Rf 0.26 (1:1 EA/Hex)

Synthesis of Boc-LMVG(N-Mbz)GV(N-Mbz)VIA-oxime resin

The synthesis was started with 2.0g (0.6 mmol/g) of Boc-Ala-oxime (JHC2-161). The resin was acetylated with Ac_2O and DIEA for 4 hours. The deprotections were 30 min. long with 25% TFA/CH_2Cl_2,and the couplings were in DMF with 3 eq amino acid, 3 eq BOP, and 5.3 eq DIEA for the single

amino acids. The alkyl dipeptides were coupled 3.5 eq BOP, 5.3 eq DIEA, and 1.5 eq of the dipeptide. The dipeptide coupling reactions gave faint blue Kaiser tests and were followed by exhaustive acetylation. The only problematic single amino acid coupling was the final one which was double coupled. This problem exhibited itself in the crude cleaved material. The resin was taken directly on to be cleaved with 120 mg HOPip in CH_2Cl_2 for 16 hours. This was filtered, the solvent was removed, and the residue dissolved in acetic acid to which Zn was added. After 4 1/2 hours, the reaction was filtered, washed with acetic acid, concentrated to about 5 mL, and precipitated with H_2O, to give 0.46g of a white powder. Two major products were purified by HPLC. 169-1 FABMS 1086, 980 169-2 FABMS 1199 MH^+ 1221 MNa^+, 1151, 1099, 898, 756 Purification of 200 mg crude material gave 50 mg 169-2 (85-90% pure)

*Treatment of 9*mer (JHC2-169-2) with HF*

The protected peptide (10 mg) was treated with 0.2 mL thioanisole, 0.2 mL m-cresol, 4.5 mL HF at 0°C for 1 hour. The HF was removed under vacuo and the residue dissolve in DMSO. HPLC analysis revealed no products which coelutes with H_2N-34-42-OH.

Preparation of Nitro-Irvoc-K(Boc)H(Bom)MAGAAAG-OH

Preparation of 4'-Nitro-2-(t-butylsulfhdryl)acetophenone

To a suspension of sodium hydride (0.84g, 20.5 mmol) in dry THF, t-butyl mercaptan (2.3 mL, 20.5 mmol) was added in THF. To this suspension, 4'-Nitro-2-bromoacetophenone (5.0g, 20.5 mmol) was added at 0°C in THF over 5 minutes. After 1 hour the solvent was removed, and the residue was dissolved in chloroform and washed with water. The organic was dried and concentrated to 5.0g, 19.7 mmol (96%) of an orange oil. Rf 0.41 ($CHCl_3$). NMR(300MHz, $CDCl_3$) d8.3 (d, 2H, J=9Hz) 8.1 (d, 2H, J=9Hz) 3.9 (s, 2H) 1.3 (s, 9H)

Preparation of 2-(4'-Nitrophenyl)-2-hydroxyethyl t-butylthioether (JHC2-137)

4'-Nitro-2-(t-butylsulfhdryl)acetophenone (5.0g, 19.7 mmol) was dissolved in 100 mL methanol, and to this solution 0.38g (10mmol) sodium borohydride was added at 0°C as a solid. The reaction went from red to deep purple. After 30 minutes the solvent was removed. Water and CH_2Cl_2 were added, and the organic layer was dried, concentrated to an orange oil, and purified by flash silica chromatography (Hex, 1:1 Hex/$CHCl_3$, $CHCl_3$, 1% MeOH/$CHCl_3$) to give 3.36g,13.2 mmol (67%) of an orange oil. Rf 0.16 ($CHCl_3$) 0.57 (1%MeOH/$CHCl_3$). NMR(300MHz, $CDCl_3$) d8.20 (d, 2H, J=9Hz) 7.55 (d, 2H, J=9Hz) 4.8 (m, 1H) 3.12 (d, 1H, J=3Hz) 2.95 (dd, 1H, J=13Hz, 4.5Hz) 2.72 (dd, 1H, J=13Hz, 9Hz) 1.3 (s, 9H)

Preparation of 2-(4'-Nitrophenyl)-2-hydroxyethyl t-butylthioether phenyl carbamate(JHC2-141)

2-(4'-Nitrophenyl)-2-hydroxyethyl t-butylthioether (3.35g, 13.1 mmol) was dissolved in dry CH_2Cl_2 with 1.34 mL pyridine. To this solution 1.6 mL, 13.1 mmol phenyl chloroformate was added as a neat liquid. After 2 hours the reaction was poured into H_2O, and the layers separated. The organic was dried, concentrated, and purified by flash silica chromatography (25-50-100% CH_2Cl_2/Hex) to give 4.37g, 11.6 mmol (89%) of a yellow oil. Rf .71 (0.5% MeOH/CH_2Cl_2) NMR (300MHz, $CDCl_3$) d8.2 (d, 2H, J=9Hz) 7.6 (d, 2H, J=9HZ) 7.3 (d, 2H, J=9Hz) 7.21 (m,1H) 7.12 (d, 2H, J=9Hz) 5.80 (t, 1H, J=7Hz) 3.15 (dd, 1H, J=13.2 Hz, 7.0Hz) 2.95 (dd, 1H, J=13Hz, 7Hz) 1.31 (s, 9H).

Preparation of NO_2-Speoc-Lys (JHC2-145)

Triton B (2.0 mL, 40% in MeOH, 3.6 mmol) was added to 1.1g, 4.5 mmol of t-Boc-Lys-OH. This was heated to 60°C until homogeneous and the solvent was then removed under vacuum. Twice DMF was added and the solvent removed and then the phenyl carbamate was added in10 mL DMF. The solution was heated to 65°C for 4 hours, then let stand at RT overnight. The DMF was removed, H_2O and CH_2Cl_2 were added, and the aqueous layer was acidified to pH2 with 6N HCL. The aqueous was extracted with CH2Cl2, and the organic layer was dried and concentrated to an orange oil. This was purified by flash silica chromatograpy (10, 50%EA/Hex then 1/1 EA/Hex w/ 1% HOAc) to give 0.5g of a brown oil (0.95 mmol, 26%) Rf 0.5 (3/1 EA/Hex w/2% HOAc).

Preparation of NO_2-Irvoc-Lys (JHC2-153)

NO_2-Speoc-Lys(e-Boc) (0.48g, 0.91 mmol) was dissolved in 7 mL HOAc, 3 mL DMF, 0.7 mL H_2O. To this 1.1 eq of 2-Nitrophenylsulfenyl chloride was added in 1 mL DMF. After 4 hours the solvent was removed, H_2O and CH_2Cl_2 were added and the layers separated. The organic was dried, concentrated to an oil and purified by flash silica chromatography (Hex, 1/1 EA/Hex, 3/1 EA/Hex) to give 0.301g, 0.48 mmol (53%) of a yellow foam.

Synthesis of Nitro-Irvoc-K(Boc)H(Bom)MAGAAAG-Rink acid resin

Fmoc-Gly-OH was attached to the Rink acid resin to a substitution level of 0.18 mmol/g as determined by quantitative ninhydrin. The deprotection were 10-15 min. with 1/1 DMF/piperidine. The reagents were added in the following order: 3 eq DIEA, 0.5 eq HOBt, 3 eq Fmoc-aa, 1.5 eq BOP and coupled for 30-40 minutes followed by acetylation. The first coupling (Ala) was double coupled. The final coupling used 2.5 eq of NO_2-Irvoc-Lys(Boc)-OH and gave a positive (though qualitatively less blue) Kaiser test.

Cleavage and purification of Nitro-Irvoc-K(Boc)H(Bom)MAGAAAG-OH

The resin (1.1g) was shaken with 10 mL 1%TFA/CH_2Cl_2 and filtered into 2 mL MeOH/0.2 mL pyridine. This was repeated a total of 4 times, and the solvent was removed to give 0.94g of a yellow solid (contains salt). The amount of Nitro Irvoc containing protecting was assayed for by treatment of portions of the crude mixture with DIEA and β-mercaptoethanol (BME) in

DMF to release the 2-nitrothiophenol. (Extinction coefficient 1680cm $^{-1}$ M^{-1}).[3] 3.41 mg crude was dissolved in 1 mL DMF. To 0.7 mL of this solution .04 mL DIEA and .04 mL BME was added; the absorbance at 490 nm was 0.71. This assay was repeated with 2.62 mg of crude material dissolved in 2 mL DMF, 0.4 mL DIEA, and 0.4 mL BME to give a solution with an absorbance at 490 nm of 0.37. The peptide was calculated to be approximately 25 % of the crude product from this assay. This percentage was used to calibrate the amount of resin used in the affinity purification.

Affinity Purification

Crude reaction mixture (50 mg) from the cleavage of Nitro-Irvoc-K(Boc)H(Bom)MAGAAAG-OH was diisolved in 4 mL DMF. To this solution 1.6 mg dithiothreitol (DTT) in 0.1 mL DMF and 0.05 mL DIEA was added. The solution turned red. After 15 min. 100 mg iodoacetamide resin (provide by I. Sucholeiki as described in ref X) was added with stirring. Within 1 min. the solution became colorless. After 3 hrs. the resin was filtered, washed with DMF, MeOH, and CH_2Cl_2, and dried to 102 mg. A portion (82 mg) was treated with 5% TFMSA/TFA at 0°C for 30 min and then warmed to room temperature and stirred for an additional 80 min. The reaction was then filtered and the filtrate concentrated by passing a stream of nitrogen over it. The residue was treated with Et_2O, centrifuged, and dried to 3.4 mg, 2.8 μmol, 43% yield.

References

(1) Ohfune, Y.; Kurokawa, N.; Higuchi, N.; Saito, M.; Hashimoto, M.; Tanaka, T.; *Chem Lett.* **1984**, 441.

(2) Quibell, M.; Turnell, W. G.; Johnson, T.; *J. Org. Chem.* **1994**, *59*, 1745.

(3) Sucholeiki, I.; Lansbury Jr., P. T.; *J. Org. Chem* **1993**, *58*, 1318.

PAGES (S) MISSING FROM ORIGINAL

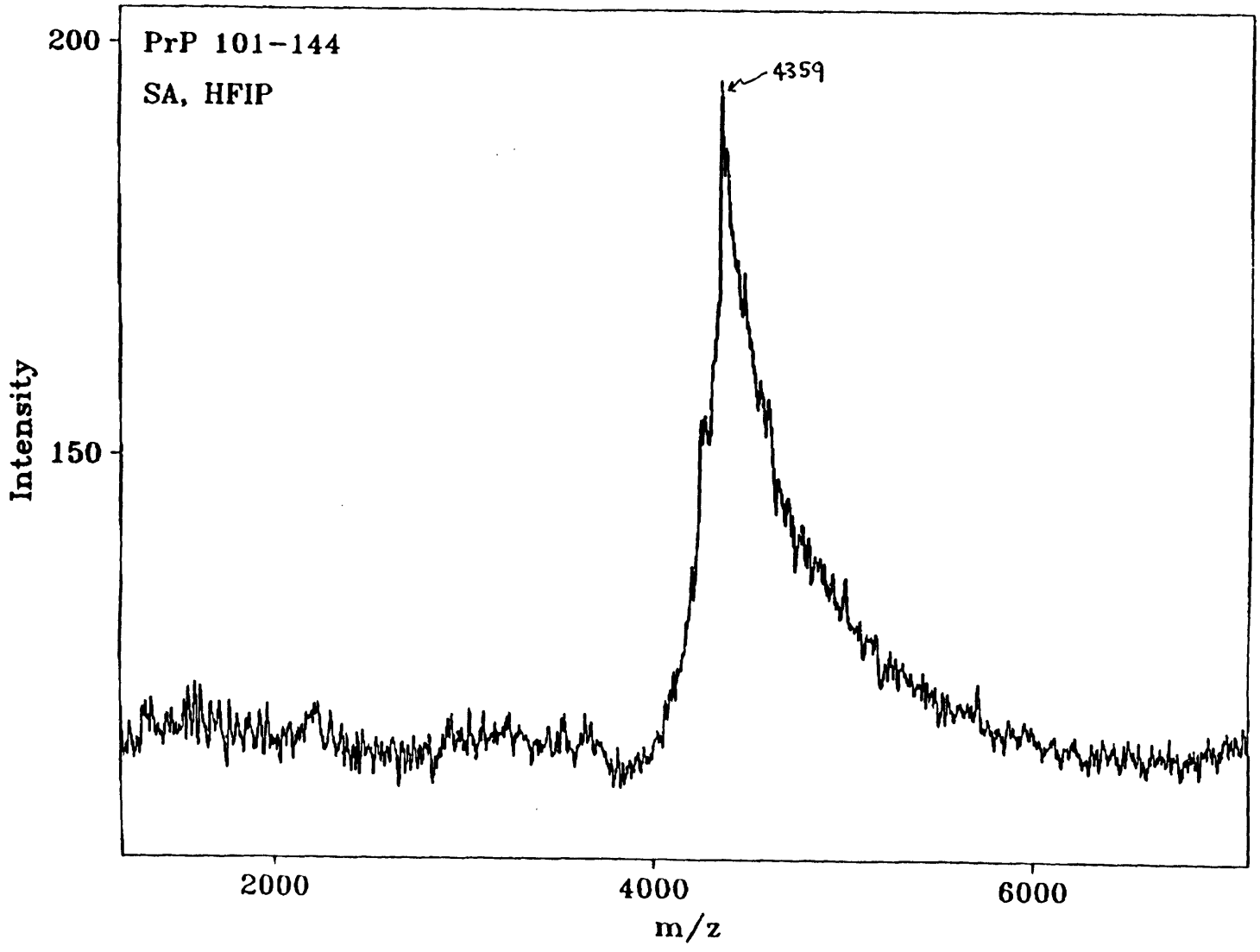
PrP 101-144
SA, HFIP
4359
200
150
Intensity
2000
4000
6000
m/z
L2843C
X
09/21/93 15:32

31-AUG-1992 21:36 File: JHC1.DAT

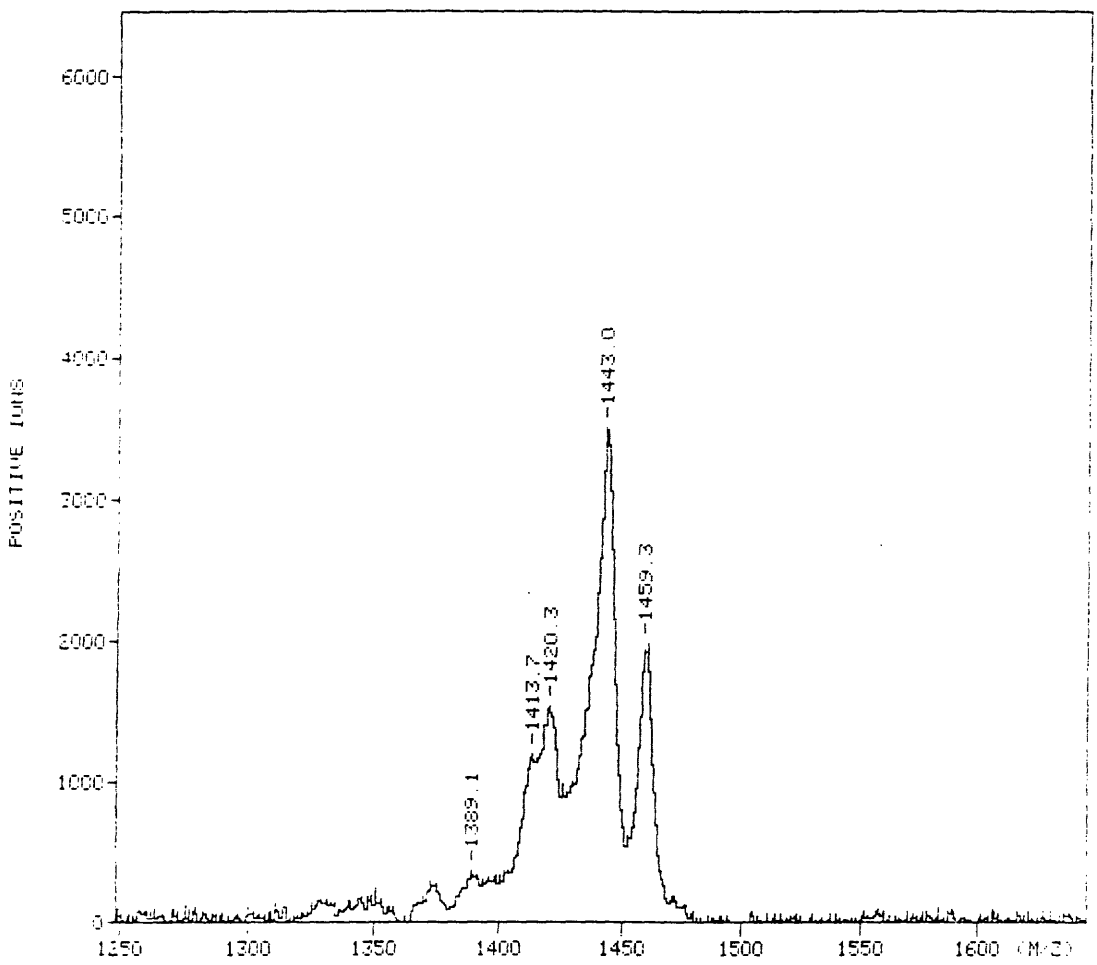

SCR4/SCRV MIXTURES
90/10 INITIAL

31-AUG-1992 23:18 File: JHC2.DAT

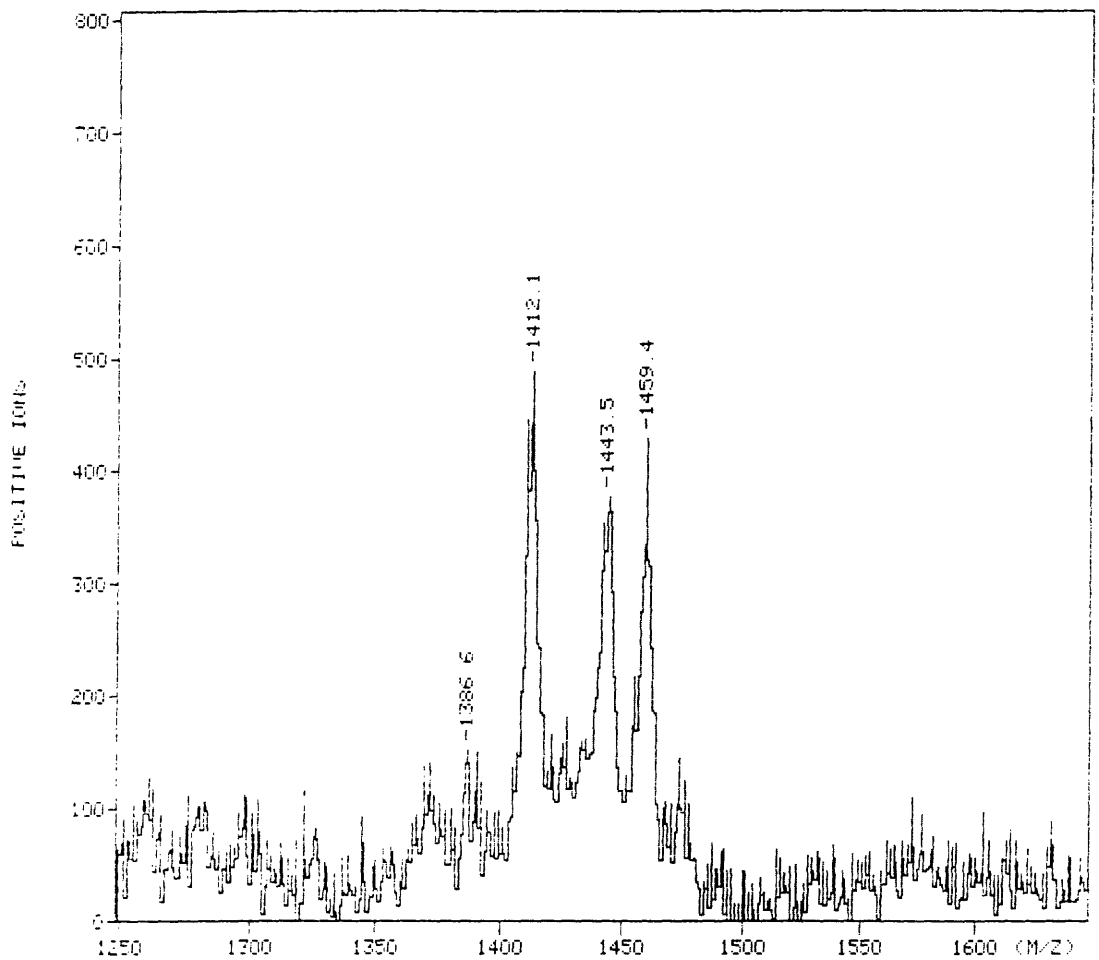

SCR4/SCRV MIXTURES
90/10 AGGREGATED

01-SEP-1992 08:14

File: JHC5.DAT

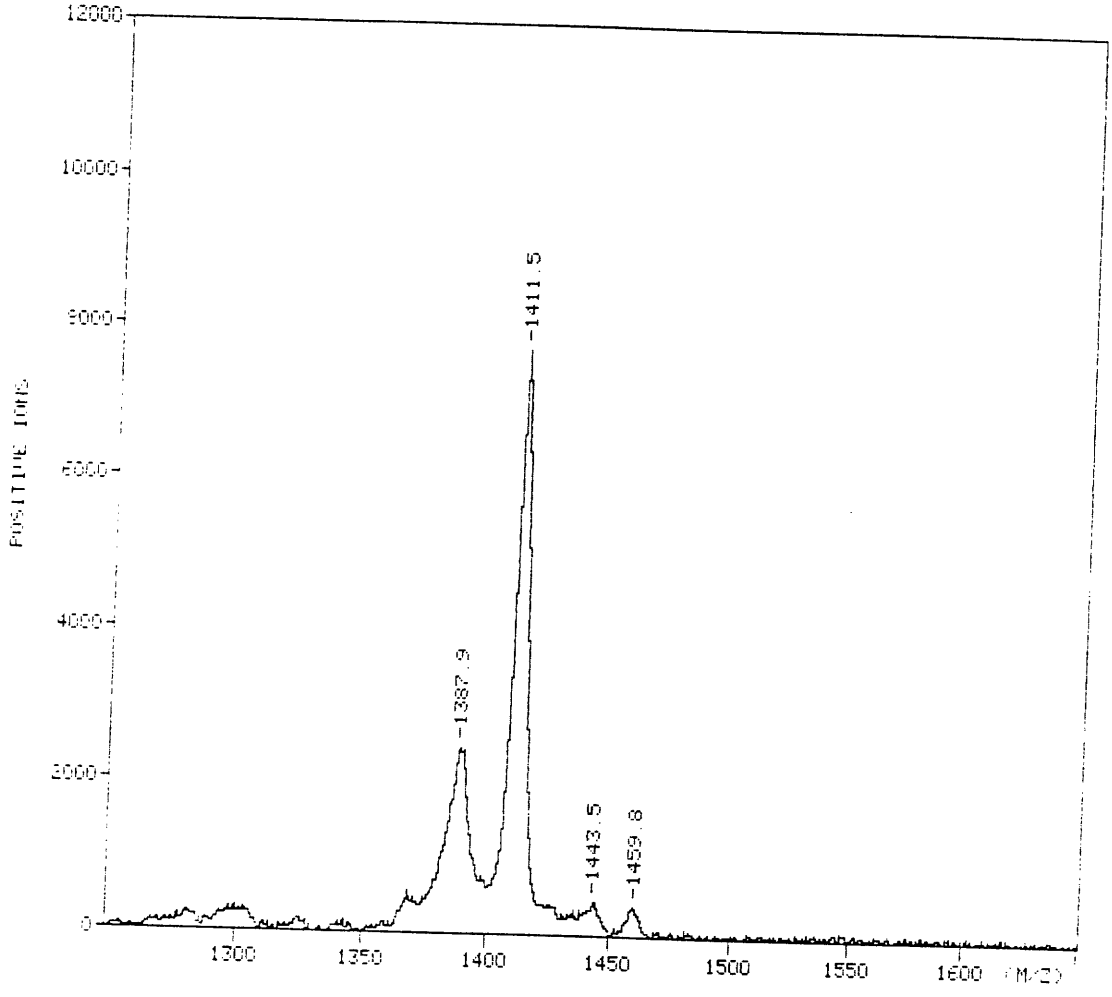

SCR4/SCRV MIXTURES
10/90 INITIAL

01-SEP-1992 08:16 File: JHC6.DAT

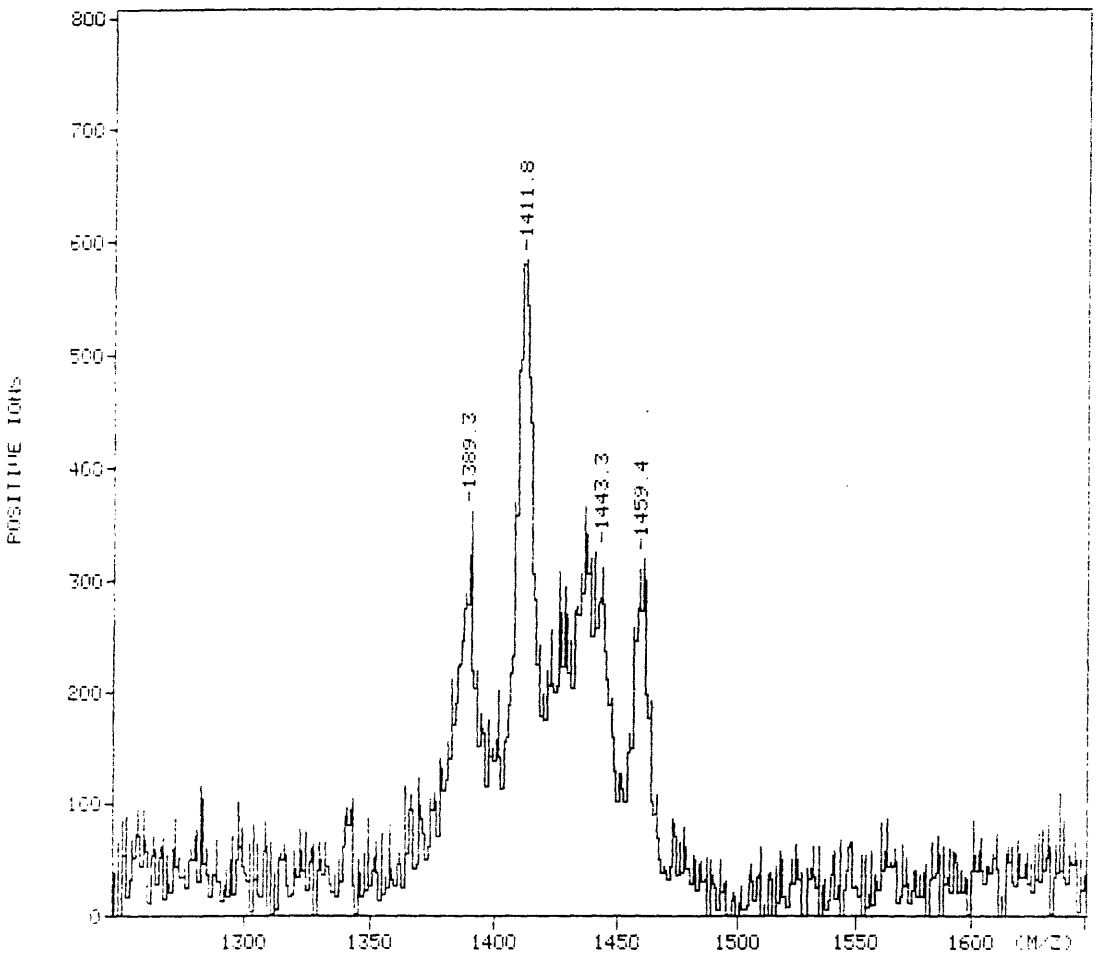

SCR4/SCRV MIXTURES
10/90 AGGREGATED

23-AUG-1992 15:27 File: SCR1.DAT

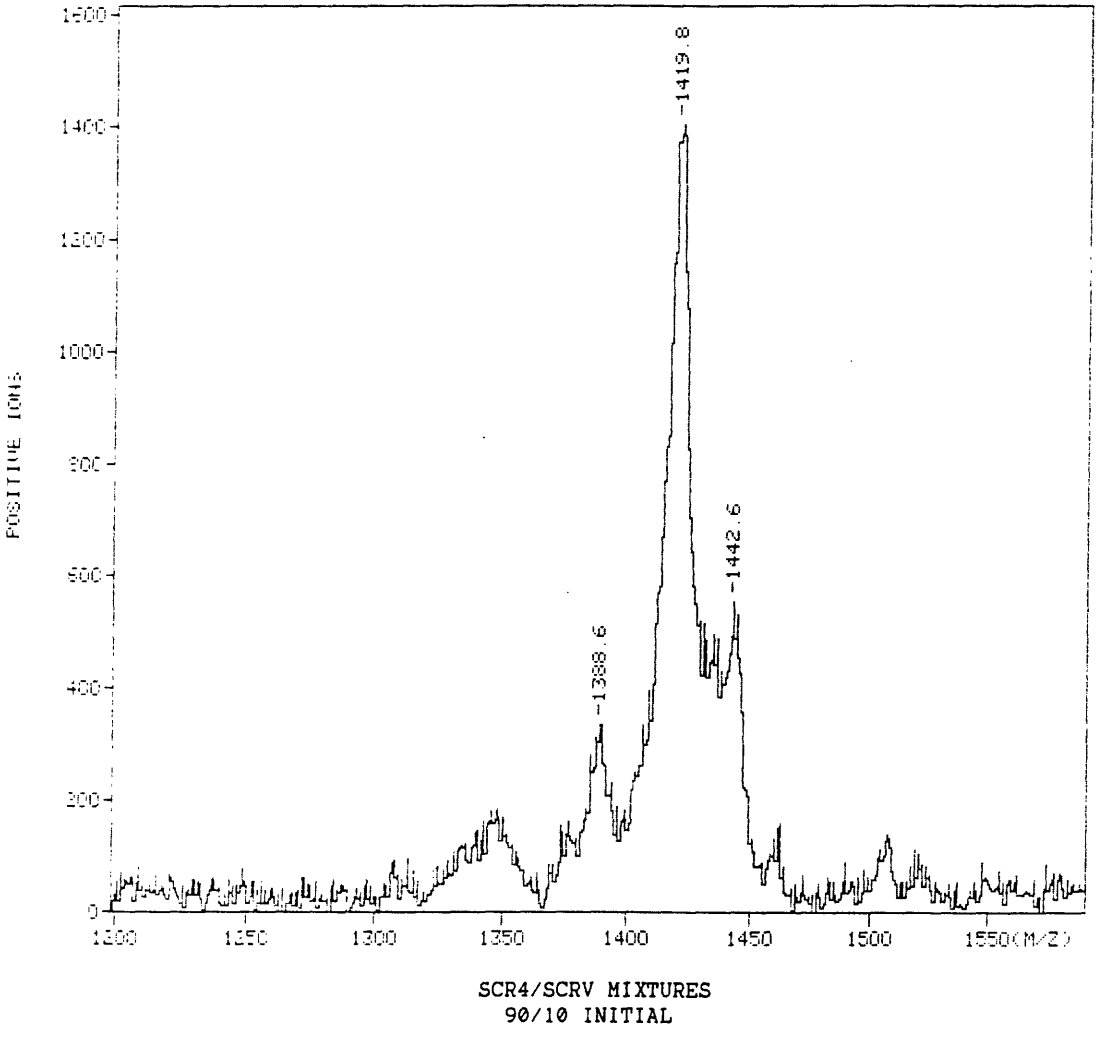

SCR4/SCRV MIXTURES
90/10 INITIAL

23-AUG-1992 15:36 File: SCR2.DAT

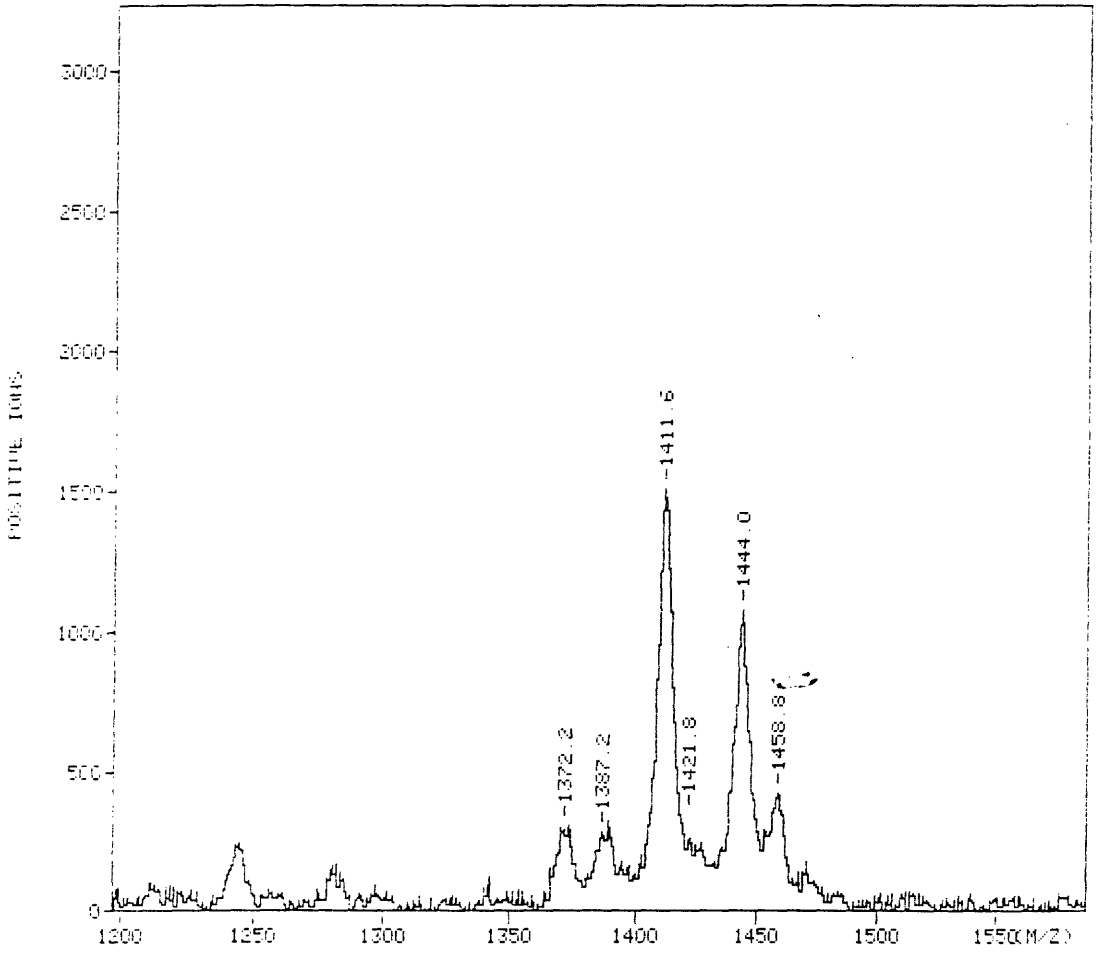

SCR4/SCRV MIXTURES
90/10 AFTER AGGREGATION

23-AUG-1992 18:30 File: SCR5.DAT

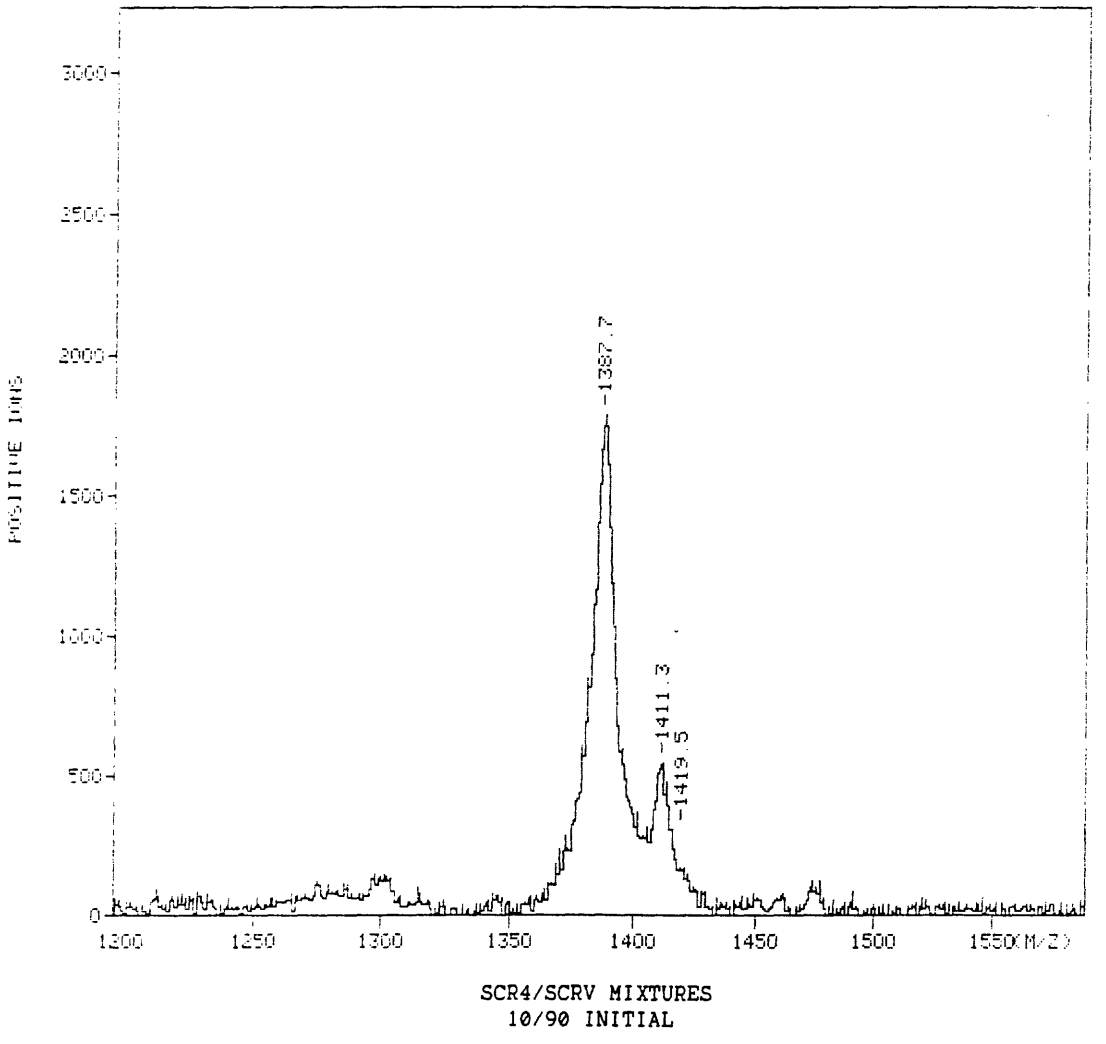

SCR4/SCRV MIXTURES
10/90 INITIAL

23-AUG-1992 18:33 File: SCR6.DAT

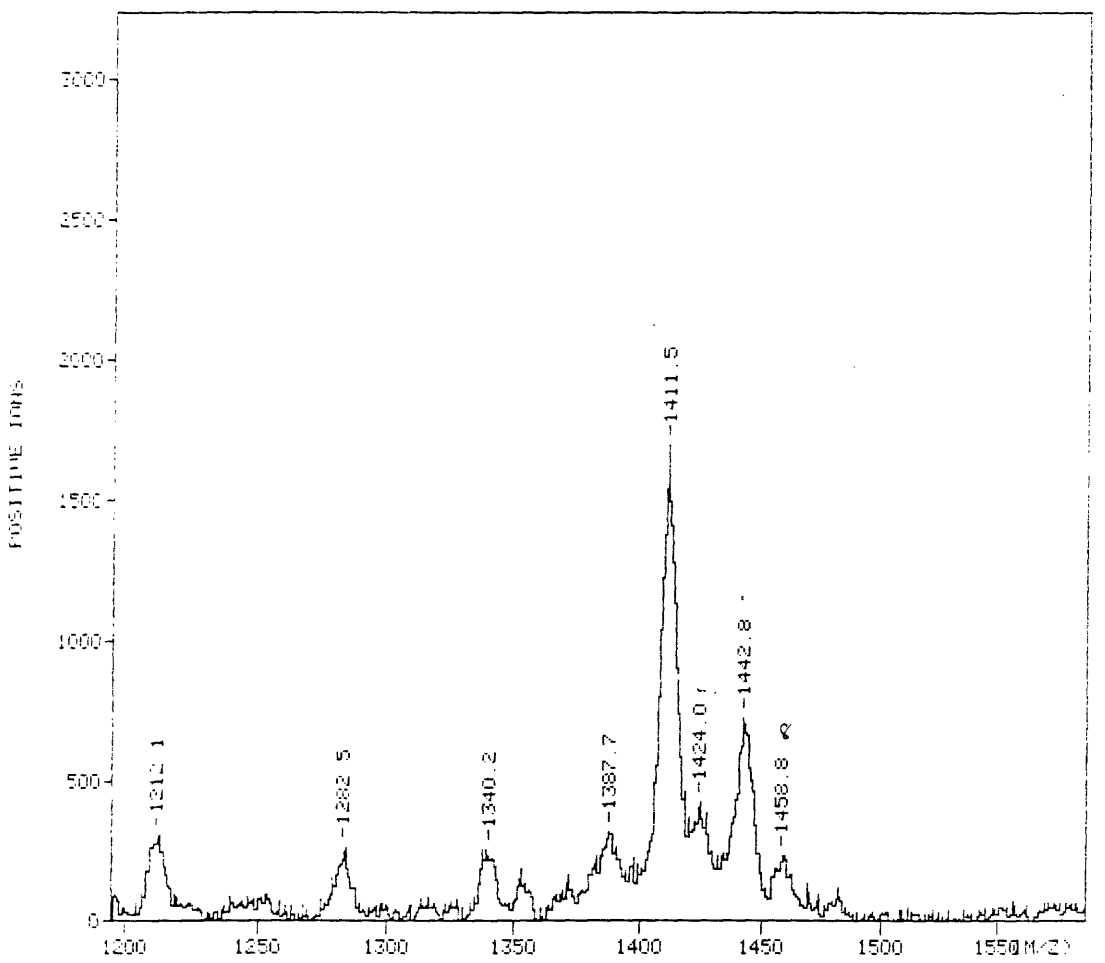

SCR4/SCRV MIXTURES
10/90 AFTER AGGREGATION

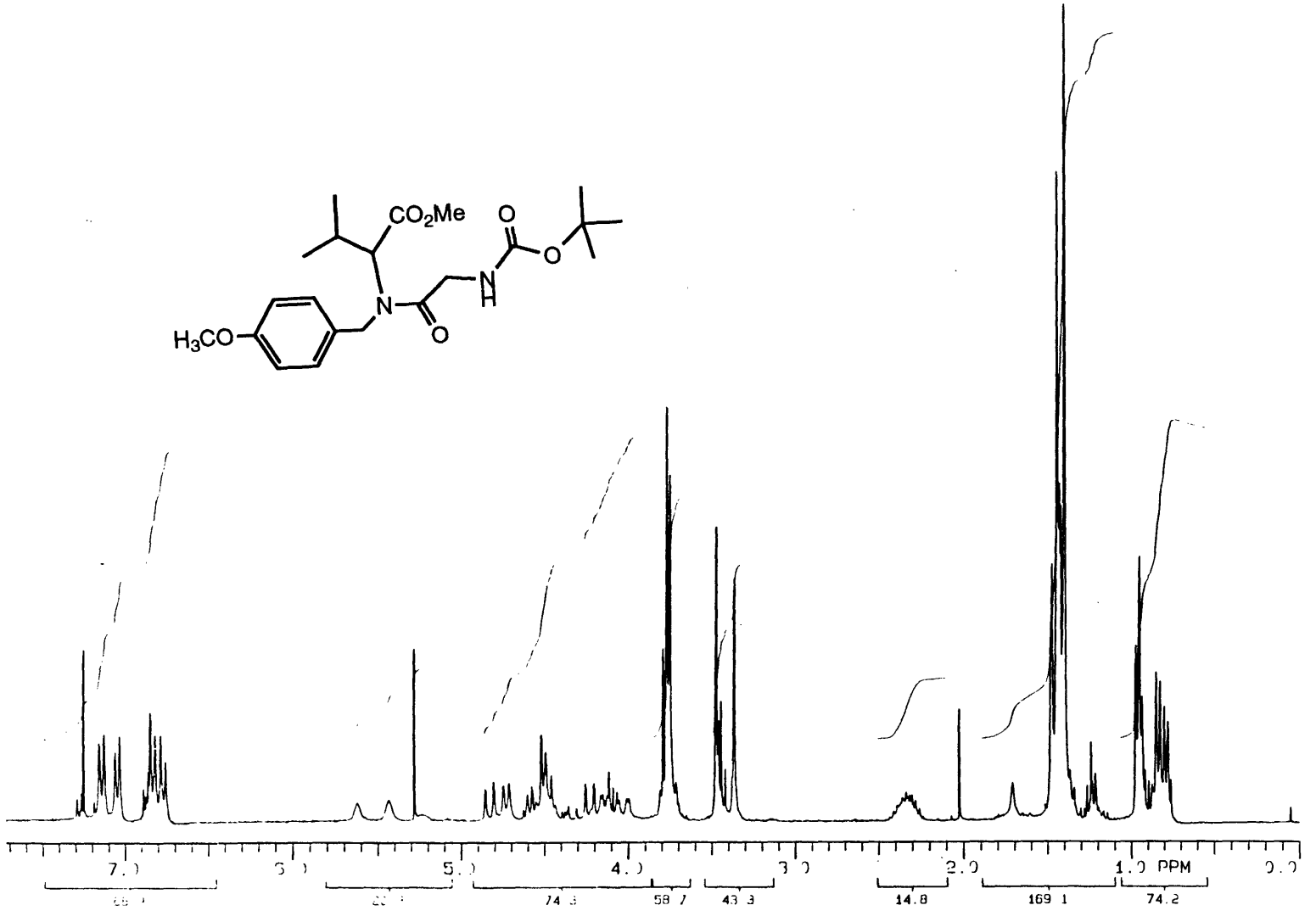
CO2Me
O
O
N
H
N
O
H3CO
7.0
5.0
4.0
2.0
1.0 PPM
0.0
74.3
58.7
43.3
14.8
169.1
74.2

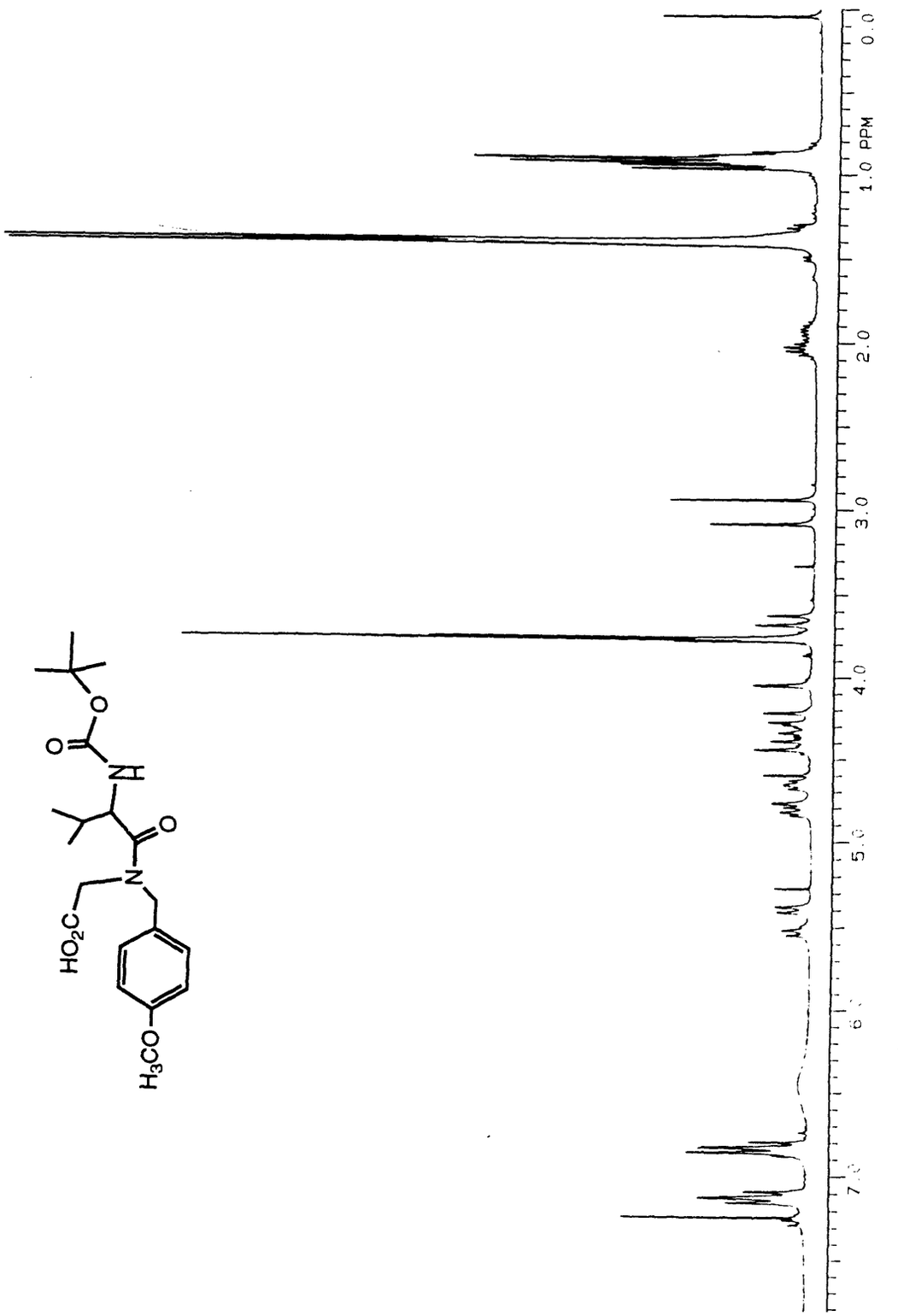
HO2C
H3CO
O
N
H
7.0
5.0
4.0
3.0
2.0
1.0 PPM
0.0

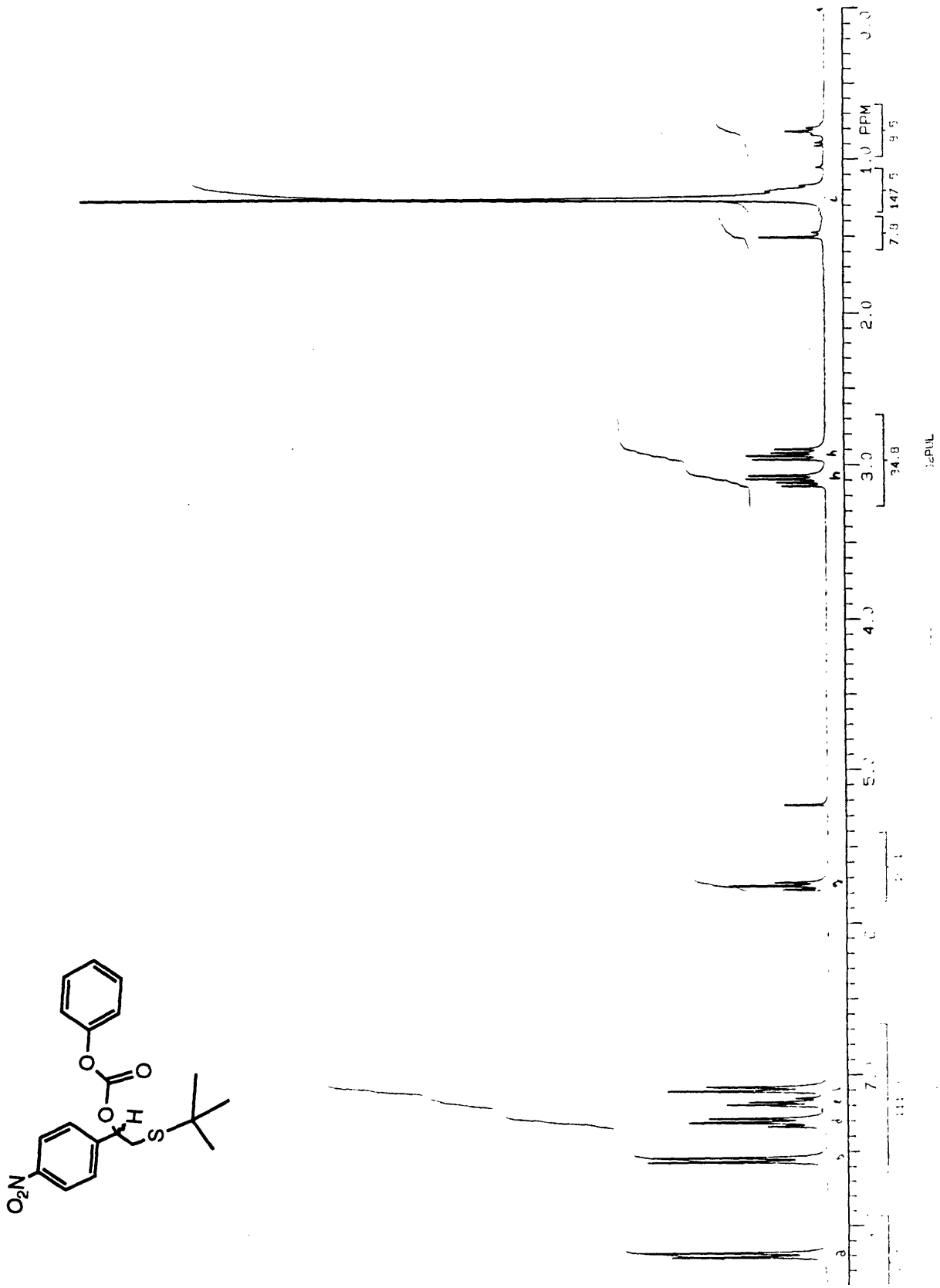
O
O
O
H
S
O2N
1.0 PPM
2.0
3.0
4.0
34.8

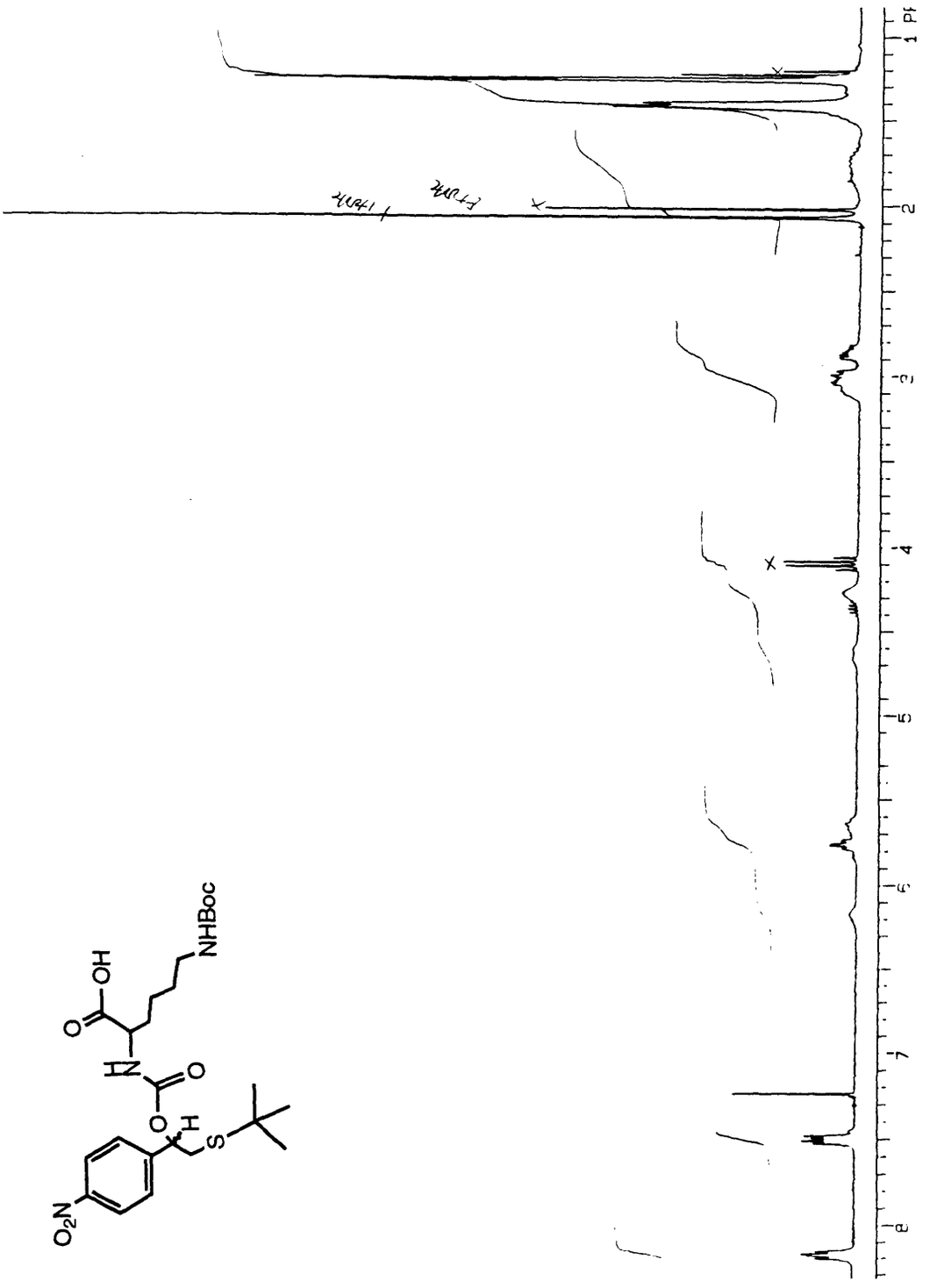
NHBoc
OH
O
HN
O
O
H
S
O2N

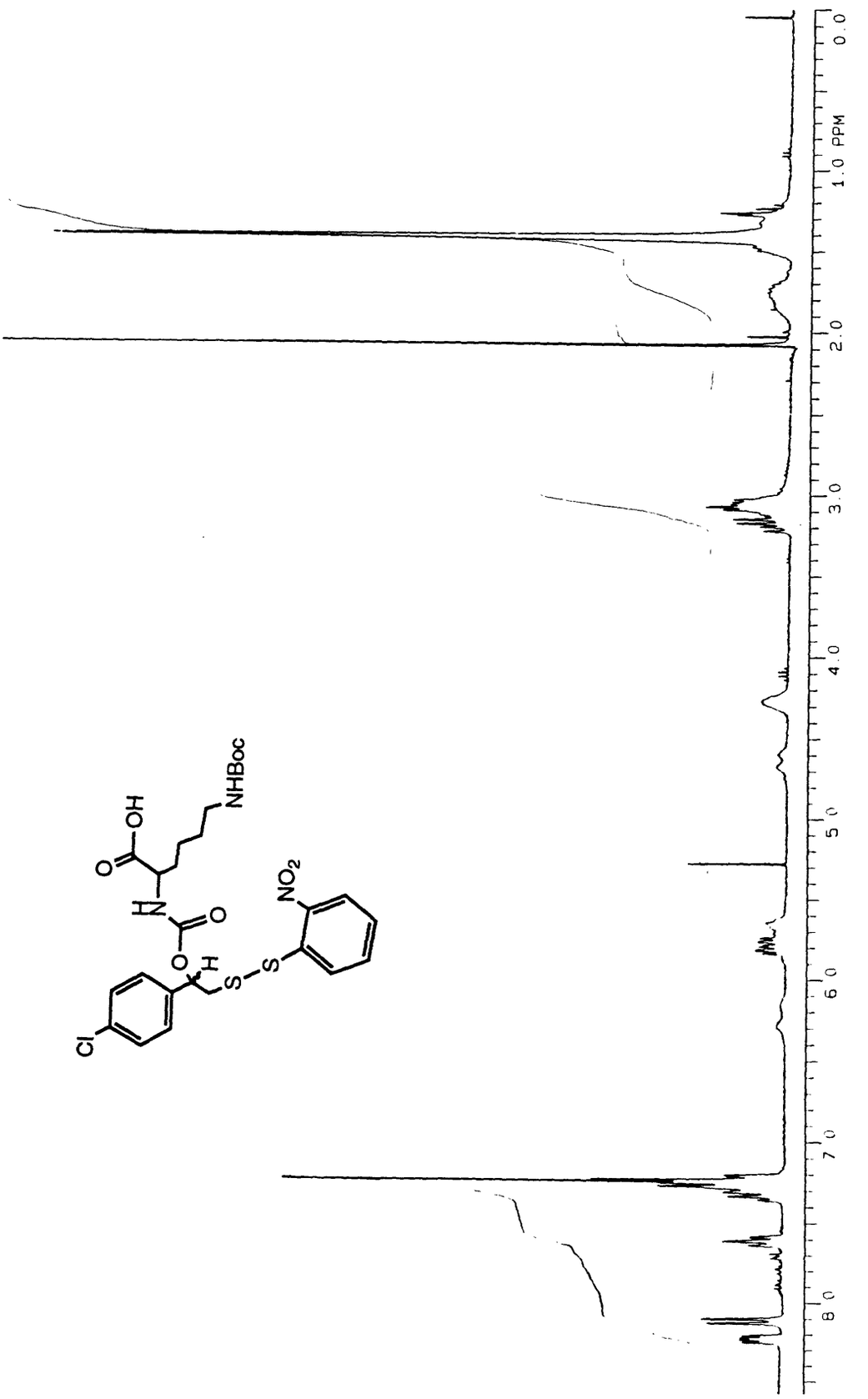
NHBoc
OH
O
N
H
O
O
H
S
S
NO2
Cl
8.0
7.0
6.0
5.0
4.0
3.0
2.0
1.0 PPM
0.0

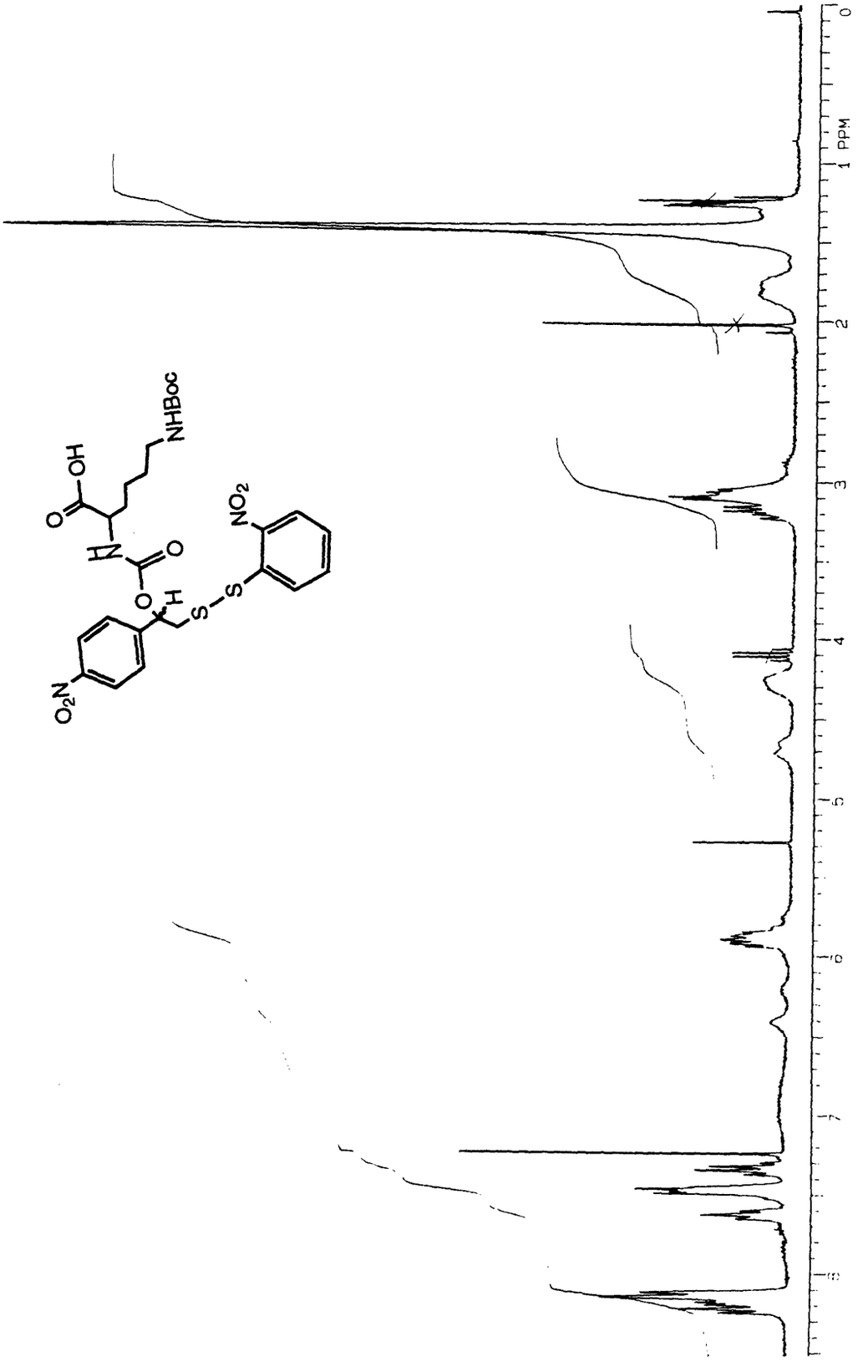
NHBoc
OH
O
N
H
O
O
H
S
S
NO2
O2N
1 PPM